CHALMERS
UNIVERSITY OF TECHNOLOGY

Tunnel inflow, prognosis, and results

Evaluation of inflow to rock tunnels in the Gothenburg region

Master's thesis in Infrastructure and Environmental Engineering

Sofia Løseth

DEPARTMENT OF ARCHITECTURE
AND CIVIL ENGINEERING

CHALMERS UNIVERSITY OF TECHNOLOGY
Gothenburg, Sweden 2020
www.chalmers.se

Master's thesis ACEX30

Tunnel inflow, prognosis, and results

Evaluation of inflow to rock tunnels in the Gothenburg region

SOFIA LØSETH

CHALMERS
UNIVERSITY OF TECHNOLOGY

Department of Architecture and Civil Engineering
Division of Geology and Geotechnics
Chalmers University of Technology
Gothenburg, Sweden 2020

Tunnel inflow, prognosis and results
Evaluation of inflow to rock tunnels in the Gothenburg region
SOFIA LØSETH

Supervisor: Johan Thörn, Bergab and Department of Architecture and Civil Engineering
Examiner: Lars Rosén, Department of Architecture and Civil Engineering

Department of Architecture and Civil Engineering
Division of Geology and Geotechnics
Chalmers University of Technology
SE-412 96 Gothenburg
Telephone +46 31 772 1000

Department of Architecture and Civil Engineering
Gothenburg, Sweden 2020

Tunnel inflow, prognosis and results
Evaluation of inflow to rock tunnels in the Gothenburg region
SOFIA LØSETH
Department of Architecture and Civil Engineering
Chalmers University of Technology

Abstract

Grouting design has been shifted from being based on a rather empirical basis, to having more focus on calculations of fracture apertures and having the design being carried out in accordance with the observational method. In the literature, limited data is available regarding follow-up on prognoses of grouting and tunnel inflow from projects based on either of the two grouting design methods. This thesis therefore aimed at illuminating how the theoretical method used to estimate inflow coincides with the empirical results from four tunneling projects in the Gothenburg region. The aim of the thesis also included to analyse how the parameters used in the inflow equation affected the estimation of inflow, and in particular the choice of skin factor.

Collected data from hydraulic tests performed during the construction of the four tunneling projects, e.g. through probe drillings and preinvestigation boreholes, were used to evaluate the hydraulic conductivity of the rock mass. Since different grouting designs were used, the evaluation of the hydraulic conductivity had to be treated differently depending on the information available. Predictions of the inflow were performed using selected best fit values of the input parameters for the inflow equation based on collected data, which were then compared to the actual measured inflows.

Through a sensitivity analysis, it was found that the main parameters affecting the inflow was the hydraulic conductivity of both the grouted and ungrouted rock mass and the hydraulic head. These three input parameters (K, K_{gr}, and H), also had the largest uncertainties in the estimation of the parameter values. It was also found that the ratio of K and K_{gr} influenced the results to a quite large extent. It was concluded that when a small sealing effect is expected (for example when the rock mass already have a low hydraulic conductivity), more care should be taken when choosing the skin factor.

Generally, the inflow equation overestimated the predicted inflow (approximately with 30%). It was also concluded that the inflow equation worked well in conditions of "normally" fractured rock mass. When the hydraulic conductivity of the rock mass was very low, the equation did not perform as good.

Keywords: grouting, inflow, hydraulic conductivity, water loss measurement, follow-up, prediction, water-proofing, tunnel.

Acknowledgements

Firstly, I would like to give my greatest thanks to my supervisor at Bergab and Chalmers, Johan Thörn, for helping and guiding me through the world of grouting. Without your time and effort invested in helping me get to the finish line of this thesis, I would have been very lost. I would also like to thank my examiner, Lars Rosén, for your help during the work of this thesis.

I also want to thank my colleagues at Bergab, for valuable help and discussions, and for letting me have the opportunity to conduct my master's thesis in collaboration with you. Further, I would like to thank the people at Trafikverket that have helped me complete this thesis. Also, a large thanks to Gryaab and Trafikverket for letting me use the considered tunnels in this thesis as study objects. Without the data, this thesis would not have been possible.

I would also like to give special thanks to Henrik Andersson and Andrea Svensson, and my opponents Linnéa Johansson och Filippa Spånér, for your valuable help and support through these lonely Corona-times.

Sofia Løseth, Gothenburg, June 2020

Contents

Notations

Abbreviations

CDF	Cumulative Distribution Function
GIN	Grouting Intensity Number
IFT	Inflow Test
PFL	Posiva's Flow Log
SGU	Geological Survey of Sweden
TBM	Tunnel Boring Machine
w/c	Water to cement ratio
WLM	Water Loss Measurement

Roman upper case letters

A	Cross-sectional area	$[m^2]$
A_t	Area of tunnel	$[m^2]$
A_w	Area of borehole	$[m^2]$
D	Flow dimension	$[-]$
H	Depth below the groundwater table	$[m]$
I_{max}	Maximum penetration of grout	$[m]$
K	Hydraulic conductivity	[m/s]
K_a	Arithmetic mean of hydraulic conductivity	$[m/s]$
K_D	Mean of hydraulic conductivity based on Matheron's conjecture	$[m/s]$
K_g	Geometric mean of hydraulic conductivity	$[m/s]$
K_h	Harmonic mean of hydraulic conductivity	$[m/s]$
K_i	Intrinsic permeability	[m/s]
K_{3D}	Mean of K based on Matheron's conjecture for 3D flow	$[m/s]$
K_{eff}	Effective hydraulic conductivity	$[m/s]$

K_{gr}	Hydraulic conductivity of grouted zone	$[m/s]$
L	Test length	$[m]$
Lu	Lugeon value	$[l/(min \cdot m \cdot 1MPa)]$
N	Number of samples	$[-]$
Q	Groundwater flow	$[m^3/s]$
R_0	Radius of influence	$[m]$
T	Transmissivity	$[m^2/s]$
T_f	Fracture transmissivity	$[m^2/s]$

Roman lower case letters

b	Hydraulic aperture	$[\mu\text{m}]$
d	Borehole depth	$[m]$
dh/dl	Hydraulic gradient	$[-]$
g	Acceleration of gravity	$[m/s^2]$
q	Inflow	$[m^3/s]$
r_t	Tunnel radius	$[m]$
r_w	Borehole radius	$[m]$
s''/t	Velocity of borehole recovery	$[m/S]$
s_t	Drawdown over the tunnel	$[m]$
t	Thickness of grouted zone	$[m]$

Greek upper case letters

Δh	Difference in hydraulic head	$[m]$
Δp	Excess pressure above the groundwater pressure	$[MPa]$

Greek lower case letters

μ	Dynamic viscosity of a fluid	$[\text{Pa} \cdot \text{s}]$
ρ	Density	$[kg/m^3]$
τ_0	Yield value of grouting material	$[Pa]$
ξ	Skin factor	$[-]$
ζ^2	Variance of hydraulic conductivity	$[m/s]$

1
Introduction

When underground constructions are built below the groundwater level, the groundwater movement changes as the water pressure conditions are altered. A tunnel located below the groundwater table acts as a well, and as long as the water pressure is higher on the outside of the tunnel than on the inside, the water will move towards the tunnel (H. Stille, 2015). In rock, groundwater moves through fractures and open spaces. The volume of water entering a tunnel depend on its depth below the groundwater level and the hydraulic conductivity of the rock mass.

Changes in groundwater movement can cause a decrease in the groundwater level, and thereby contribute to negative impacts on the surroundings. For example, wetlands, peat areas, and surface streams may dry out, changing the conditions for ecosystems (Gustafson, 2012). The quality of groundwater may also be affected negatively if conditions in the soil changes with the new flow directions (H. Stille, 2015). As the groundwater level depletes, groundwater wells in the area may have reduced levels, which will affect the human life conditions (Gustafson, 2012). The population may also suffer from economic losses with regard to agriculture, fishing, farming, and tourism when the water levels are lower (Chiocchini & Castaldi, 2011). Negative societal and economic effects can also occur when the groundwater table declines in clays susceptible of consolidation, which may start to consolidate and thereby affect buildings and infrastructure. Additionally, inflow in tunnels may affect the working conditions in the tunnel, such as the drilling, charging, and rock support, but it may also cause functional problems due to corrosion of equipment (H. Stille, 2015). It can therefore be said that lowering of groundwater tables as a result of inflow in tunnels have several consequences on both humans and ecosystems. Thus, the prevention of inflow in tunnels is crucial.

In order to reduce the negative impacts of a lowered groundwater level when building tunnels, the tunnels are waterproofed. A common approach is to seal the water-bearing fractures in the rock mass using grout, which can be a mixture of cement and, if needed, additives (H. Stille, 2015). The grout is injected under pressure through boreholes and spread through the fractures where it hardens and prevents inflow of groundwater.

1.1 Background

The grouting design has previously been based on experience and a rather empirical basis (H. Stille, 2015). In the more traditional preliminary investigations, the documentation has not been enough to make an appropriate grouting design nor an appropriate choice of grout material (Gustafson, Fransson, Funehag, & Axelsson, 2004). Development in grouting materials and its additives in combination with stricter requirements on inflow in tunnels located in densely populated areas provided a need for new design methods.

In 2004, "Ett nytt angreppssätt för bergbeskrivning och Analysprocess för Injektering" by Gustafson, Fransson, Funehag, and Axelsson (2004) was published, where an alternative way of characterizing the hydrogeologic properties of rock using new research is described. The analytical method is based on calculations of the distribution of transmissivity in fractures, the hydraulic aperture, the distribution of the penetration of grout in fractures and the amount of leakage expected. Since the early 2000's, more focus has thus been given to design by calculations on fracture apertures. Nowadays grouting design is carried out in accordance with the observational method, as specified in Eurocode. Common for the empirical and aperture-based grouting design is that limited data is available in the literature regarding follow-up on prognoses and evaluation of grouting design performance.

In the recent decades, several tunnels has been constructed in the Gothenburg region, for example the Lerum utility tunnel, Chalmers tram tunnel, Göta road tunnel, and the recent Västlänken project. Data sets has been kept of these projects regarding both grouting and hydrogeological properties, such as amount of inflow and results of water loss measurements. As the tunnels are being built, the grouting needs to be sufficient to ensure that the maximum inflow for the different rock tunnel stretches are not exceeded. The amount of leakage is monitored in measurement points, which then needs to be presented for authorities regularly during and after the tunneling project is completed.

The location of the tunnels considered in this thesis can be seen in Figure 1.1. In the figure, the Göta tunnel is orange, the Chalmers tunnel is purple, the Västlänken tunnel is yellow, the Västlänken service tunnels are light green, and the Lerum tunnel is located somewhere in the green oval. The more detailed location of the tunnels located in Gothenburg can be seen in Chapter 3.

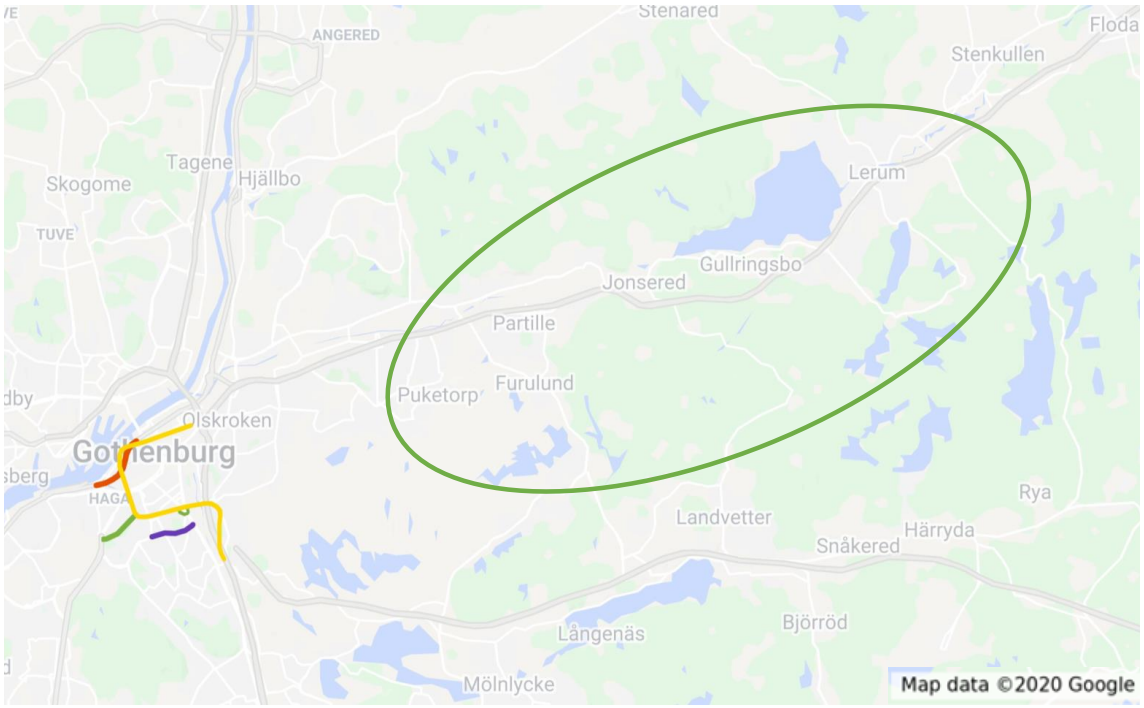

Figure 1.1: The location of the tunnels considered in this thesis.

1.2 Aim and objectives

The aim of the thesis is to construct a method for follow-up on inflow through analyses on existing data from previous tunneling projects in the Gothenburg area. The method is then applied to the ongoing construction of service tunnels in the Västlänken project. The aim also includes to get an increased understanding of the applicability of the inflow equation for different geologic settings when predicting the inflow.

Furthermore, the objective of the thesis is to answer the following questions:

- What are the parameters influencing the inflow into tunnels, and how are they determined?
- How are the different parameters affecting the estimation of inflow (in particular the choice of skin factor)?
- How well are the estimations of tunnel inflow corresponding to the actual inflow?

1.3 Demarcations

In this thesis, tunnels constructed in rock are only considered. In rock, it can be assumed that only fractures are possible paths of groundwater flow. The analyses are limited to the three constructed tunnels mentioned above (the Lerum, Göta and Chalmers tunnel), and the constructed follow-up method based on the inflow equation is only applied to the Västlänken service tunnels that are under construction in 2020.

One of the main objectives of this thesis is to evaluate how well the estimated inflow based on the grouting design corresponds to the actual measured inflow. However, during the construction, deviations from the design might be needed in certain sections. Moreover, only the general grouting design was used in the evaluation for the Västlänken service tunnels. Thus, local variations in the design were not considered in the analyses. The analyses performed were also limited to the data collected during the time frame of the thesis.

A majority of the theoretical references used in this thesis are written by a small research group in Sweden. However, the bedrock in Sweden is crystalline, and most of the exposed rock in rest of the world consists sedimentary rock (Encyclopedia Britannica, n.d.). Since the research group that is mostly cited in this thesis seem to lie in the forefront of the research on grouting in crystalline bedrock, the references used are seen as representative for where the knowledge of the subject is today.

1.4 Outline of the thesis

Firstly, a literature study is performed in Chapter 2 to assess which parameters may influence the estimation of inflow to tunnels. A compilation of information regarding hydrogeologic and geologic conditions and the grouting design from recent tunnel projects in the Gothenburg area are thereafter made in Chapter 3. The projects that are considered in this thesis is the Västlänken service tunnels, Lerum tunnel (utility), Chalmers tunnel (tram) and Göta tunnel (road). Thereafter, the steps used to perform the calculations of the inflow to the tunnels according to modern design methods are described in Chapter 4. The analyses performed on the older tunneling projects are then used to construct a method for the follow-up of the inflow, which then is applied on the Västlänken service tunnels. The results of the calculations are presented in Chapter 5, where analyses regarding the parameter values are performed. The estimated inflow is then compared to the actual, measured inflow. Discussions regarding the results and its uncertainties are performed in Chapter 6. Lastly, the conclusions of the thesis is presented in Chapter 7, and recommendations for further work are given.

2

Theory

In this chapter, the properties of rock and groundwater flow will be described in order to delineate the parameters that affect the prediction of inflow to tunnels. The construction process of tunnels are thereafter described to distinguish how and when grouting and hydrogeological tests are performed. The grouting design process is also described in accordance to the observational method as described in Eurocode. Lastly, the modern equations used to evaluate the inflow to tunnels are described.

2.1 Groundwater in crystalline bedrock

An efficient grouting of a tunnel is achieved when the grouting design is based on the site specific geologic conditions. The water-bearing fracture system has to be characterised in order to estimate the flow conditions around the tunnel considered. Since the mechanical properties of rock is determined by its origin and history, it is of large importance when characterising the rock mass and its fracture system (Gustafson, 2012).

In Sweden, the crystalline bedrock consists of igneous and metamorphic rocks (Banks & Robins, 2002), such as granite and gneiss (SGU, 2017). It is a part of the Fennoscandian Shield, which has, since it was formed, undergone large rotations (Larsson & Tullborg, 1993). These rotational movements created stress regimes, that are represented by for example shear zones and dykes. During the several stress regimes that has occured over more than 2 billion years, fractures and fracture zones has been created with different patterns and extent. In the southwestern part of Sweden, where Gothenburg is located, the bedrock is mainly between 1700 and 1550 million years old and was metamorphosed during the Sveconorwegian orogeny about 1100 - 900 million years ago (SGU, n.d.-a).

Plate movements is the main cause of stress build-up in the earth crust, and when the stresses in the brittle rock exceeds its strength, fractures are formed. Tectonic processes, such as folding, foliation, formation of fractures and faults along fracture planes, create the secondary porosity of the bedrock, which is its flow bearing structures (Olofsson, Jacks, Knutsson, & Thunvik, 2001). The crystalline bedrock is typically hard and fractured, and groundwater flow through the intergranular pore spaces can be seen as negligible since the rock is dense and largely impermeable (Gustafson, 2012). Hence, almost all flow of groundwater takes place in fractures of the rock. Other events that can cause fractures in rock are the rock formation,

orogenesis, unloading, glaciation and erosion of the land surface. Fractures are often sorted into fracture sets, according to e.g. orientation and degree of filling. Granites are often characterized with a regular fracture pattern with two or three dominating fracture sets (Olofsson et al., 2001).

The volume of open spaces of the fractures within in the rock mass depend on the fracture frequency, orientation, width and mineral filling (Olofsson et al., 2001). However, it is quite hard to evaluate the hydraulic properties of fractures since the fractures are normally sensitive to fluid pressure and rock stress (Gudmundsson, 2011). Variation in the mechanical properties of rock layers may also cause a variation in aperture width of a fracture since the local stresses in the layers can change abruptly. For example, a high stress in the rock may squeeze the fracture making it tighter, thereby limiting the flow (Hernqvist, Butrón, Fransson, Gustafson, & Funehag, 2012). Moreover, it has been shown that the fracture aperture is affected already at small changes in stress (Thörn, 2015). The flow through a fracture might also be limited if it is not well connected to the water-bearing fracture network. Fractures that are not well connected and discontinuous will therefore not contribute to the groundwater flow.

In the crystalline bedrock in Sweden, the amount of voids available for flow of groundwater is estimated to be 0.0001-0.1% of the rock mass (Olofsson et al., 2001). Fractures created by shearing can be quite complex as there can be different degrees of crushing and mineral transformation within the fractures. A zone with several parallel shear fractures with crushed rock in between, a fault zone, may however transport large groundwater flows. A fault zone may act as a conduit, barrier or a combined conduit-barrier system depending on the permeability structure of the fault zone and its architecture (Caine, Evans, & Forster, 1996). Fault zones are two-dimensional structures consisting of two components: a fault core with a surrounding damage zone. The damage zone is in turn surrounded by unaffected rock mass. However, both of the components do not have to be present, and the extent of the components may vary from poor to well-developed (Hernqvist, 2009).

Most of the displacement in a fault zone has taken place in the fault core, which consists of a fault gauge (Caine et al., 1996). The fault core may act as a fluid flow barrier because of mineral precipitation and grain-size reduction, which causes a decrease in permeability. Mineral precipitation can result in clay minerals, which in contact with water can be problematic regarding the stability of fractures and rock (Bergab, 2007b). On the contrary, the damage zone may act as a conduit as it can be more intensely fractured than the fault core (Kvartsberg, 2013). The high fracture frequency of deformation zones increases the probability of conductive fractures and that the fracture system is well connected (Gustafson, 2012). Thus, characterization of fracture zones are needed to ensure a good grouting result as groundwater may have several flow paths which has to be sealed.

Figure 2.1 was produced by Fransson and Hernqvist (2010), and is a modification of the scheme for fault-related flow presented by Caine et al. (1996). In the left hand side of the figure, Fransson and Hernqvist (2010) suggest the permeability structures in the host rock that is similar to the fault zone structures. The Type I host rock is characterised by a fracture network which is not well connected, while the Type

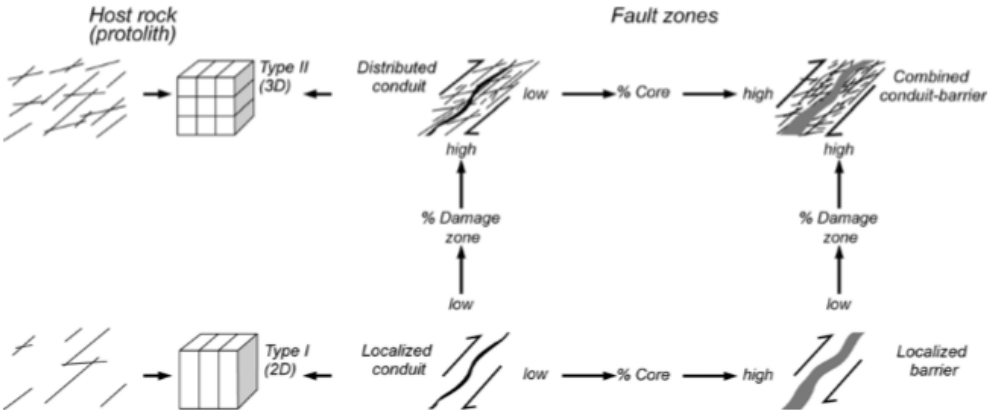

Figure 2.1: Conceptual scheme for fault-related fluid flow (modified from Caine et al. 1996), and the permeability structures in host rock (Fransson and Hernqvist, 2010).

II host rock is characterised with a well-connected fracture network that have more than one conductive fracture set.

2.1.1 Groundwater recharge in rock

When evaluating the impact a tunnel has on the surroundings, the groundwater recharge to the bedrock is of large importance. The recharge can either be direct or indirect (Olofsson et al., 2001). The direct recharge refers to infiltration of precipitation, which is dominating in humid climates, while the indirect recharge refers to the inflow from watercourses and lakes, which is of more importance in arid climates. Gravitation is the dominating factor influencing the recharge, moving water from higher to lower situated areas. Thus, the groundwater recharge is dependent on the topography of the site.

The recharge also depends on the amount of precipitation (Olofsson et al., 2001). The amount of the precipitation that is added to the groundwater is the difference between the total precipitation to an area and the evapotranspiration. In soil, the groundwater recharge depends on, inter alia, the water content of the soil, the grain size distribution (and thereby capillary forces), water uptake by plants, and the hydrogeological year (Gustafson, 2012). In the spring, snow melt contributes to a large amount of moving water in Sweden, resulting in groundwater recharge. The evapotranspiration increases as the temperature does, in combination with the start of vegetation growth. Eventually, the evapotranspiration exceed the precipitation rate during the summer months, and the groundwater recharge decreases. This is also a result of the uptake by plants, which depletes the soil storage. In the autumn, the evapotranspiration decreases again as the vegetation wilt and as the temperature decreases, resulting in increasing groundwater recharge. During the winter, groundwater recharge depends on if the soil freezes, which reduces the recharge, or if mild winters occur where recharge still can take place through the soil.

The groundwater recharge to rock is dependent on if the rock surface is exposed

or if it is overlaid by saturated soil layers (Olofsson et al., 2001). If the rock is exposed, a large part of the precipitation becomes runoff and only a small part can enter through fractures. The amount of water that enters through fractures is very dependent on the presence of fractures, how open the fractures are and the amount of mineral and soil filling.

If the rock is overlaid by soil, groundwater flow can only exist if the permeable soil is in hydraulic contact with the open structures in the bedrock (Olofsson et al., 2001). The probability of the soil being in hydraulic contact with the open structures decreases when the anisotropy of the hydraulic properties of the soil increases. Additionally, the hydraulic conductivity in the soil-rock interface is seldom well known, making the recharge to the bedrock from overlying soil hard to estimate (Rodhe & Bockgård, 2006).

In Sweden, the bedrock is often overlain by till, which can have different grain size distributions, structure, and hydraulic heterogeneity depending on where it was deposited during the last glacial period (Olofsson et al., 2001). In large parts of Sweden, the till is dominated by sand and silt, but it can contain a mixture of all grain sizes (SGU, n.d.-c). The recharge to the bedrock will depend on the thickness of the overlying till layer, and how compact the material is. When the material is compact, the viods are reduced, limiting the flow through the material. Glaciofluvial deposits on the other hand are well sorted, and have good hydraulic properties. If such deposits are located on top of the bedrock, the recharge is mainly dependent on the hydraulic properties of the rock and its fractures (Olofsson et al., 2001).

In urban areas, impermeable areas and stormwater drainage reduces the natural recharge (Sundell, 2018). Thus, a decreased natural recharge can be expected in these areas, which could affect the recovery from groundwater drawdown. Further, it is common that the groundwater recharge increases when groundwater is abstracted or flow into an underground construction (Gustafson, 2012). The inflow to a tunnel might therefore increase the recharge of groundwater to the bedrock. The groundwater supply also affects the possible consequences of drawdown. If unfavorable conditions occur, a relatively small leakage into an underground construction can result in a large groundwater drawdown (Sundell, 2018). Moreover, if favorable hydrogeological conditions occur, e.g. in the presence of an esker with large groundwater recharge, the leakage can be compensated by its high hydraulic conductivity.

2.1.2 Groundwater flow and hydrogeologic properties of fractures

The properties of the fracture system and how it is connected determines how large volumes of groundwater that can pass through different sections of the rock mass. Thus, it is important to get an understanding of how groundwater flows through the rock mass in order to evaluate the tunnel inflow.

The flow of groundwater is assumed to be laminar, meaning that water moves smoothly without any turbulence (Gustafson, 2012). Because of this assumption,

Darcy's Law can be used to describe the groundwater flow, see Equation 2.1.

$$Q = -KA\left(\frac{dh}{dl}\right) \tag{2.1}$$

Darcy's law, which is based on continuum fluid mechanics, states that the flow, Q, through a unit area of porous medium is proportional to the hydraulic gradient, dh/dl, and the cross-sectional area, A (Gustafson, 2012). The hydraulic conductivity, K, is depending on both the properties of the porous medium and the fluid that passes though it (Fetter, 2014). It describes the ability of a material to transmit fluid under an applied hydraulic gradient through pore spaces and fractures. The negative sign of the equation indicates that the flow is going in the direction from higher pressure to lower pressure, i.e. towards decreasing hydraulic gradient. Generally, the hydraulic conductivity decreases with depth in hard rock, as the stresses increase (Olofsson et al., 2001). In natural conditions, the flow is usually laminar. However, a turbulent component may exist in wide fractures that are located close to tunnels or boreholes, which then has to be accounted for (Gustafson, 2012).

The intrinsic permeability can be used as a measure of flow through the porous medium, independent of the properties of the fluid (Fetter, 2014). It is therefore only dependent on the pore structure and the porosity of the medium through which the fluid moves. The relationship between the intrinsic permeability and the hydraulic conductivity can be seen in Equation 2.2.

$$K_i = K\left(\frac{\mu}{\rho g}\right) \tag{2.2}$$

The intrinsic permeability is a function of dynamic viscosity of the fluid, μ, and ρg, which is the driving force of the fluid, and is the product of the density of the fluid, ρ, and the acceleration of gravity, g (Fetter, 2014). The intrinsic permeability of crystalline rocks is primarily the secondary porosity, such as fractures formed after the rock was initially created. Crystalline rocks typically have low porosity and low primary permeability, with few openings within the structure.

When estimating the hydraulic properties of the rock and its fractures for grouting design purposes, the heterogeneity of the rock mass has to be taken into account (Hernqvist, 2009). Thus, an fracture-oriented approach is needed. As the rock is assumed to be impermeable, the groundwater flow is limited to the fracture openings. The hydraulic heterogeneity of hard rock is therefore mainly caused by the variation in fracture frequency, orientation of fractures, fracture length, hydraulic aperture, roughness of fracture surfaces, and filling of minerals (Olofsson et al., 2001). Hence, it is difficult to forecast the groundwater flow and its flow pattern.

The transmissivity, T, can be used to describe the ability of fractures to transmit groundwater. It is the function of the hydraulic conductivity and the thickness of the aquifer, see Equation 2.3. When concerning fractures, the thickness of the aquifer is the fracture aperture.

$$T = b \cdot K \tag{2.3}$$

The transmissivity can be evaluated through performing hydraulic tests *in-situ*. The inflow, Q, and the difference in hydraulic head caused by the test, Δh, is always needed in the evaluation (Hernqvist et al., 2012). According to Åsa Fransson, the transmissivity can be estimated using the specific capacity when performing short-duration tests (Fransson, 2001), see Equation 2.4.

$$T = \frac{Q}{\Delta h} \tag{2.4}$$

In reality, fractures varies in width, direction, and filling, which cannot be measured in the field (Hernqvist, 2009). Thus, the hydraulic properties of a fracture are used to define the hydraulic aperture, see Equation 2.5 (Gustafson, 2012). Equation 2.5 assumes laminar flow and that the fracture consists of two flat parallel planes, which is not the case in nature. Thus, the hydraulic aperture represent the width of the fracture transporting groundwater if it would have had parallel, plane walls. In the equation, it can be seen that only a small change in aperture width, b, can cause a quite large change in the transmissivity of the fracture, T_f. Usually, only a few larger fractures account for the larger part of the groundwater flow, which can be explained through the cubic law (H. Stille, 2015).

$$b = \sqrt[3]{\frac{12\mu T_f}{\rho g}} \tag{2.5}$$

The cubic law is a reasonably accurate representation of the real fracture aperture for fractures larger than approximately 100 μm, which roughly corresponds to groutable fractures (Thörn, 2015). Gustafson et al. (2004) found that the same flow paths were used by both water and grout. Further, the hydraulic aperture has also been proven to be appropriate when estimating the penetration of grout. More on the properties and penetration of grout can be read in section 2.4.

The flow of groundwater through fractures can have different dimensions depending on the fracture geometry and network. Mainly, fractures are 2D and enable a radial spread (Gustafson, 2012). The flow can also be 1D and channeled since the fracture aperture varies within fractures, or 3D in heavily fractured deformation zones. When fractures have large open areas, the flow is generally 2D and radial, while thin fractures with large contact areas generally have channeled 1D flow (Hernqvist et al., 2012). Further, the hydraulic conductivity is larger with larger flow dimension. The possibility of intersecting a 2D or 3D fracture system when performing site characterization is high, whereas it is harder to intersect 1D fracture systems (Butron, Gustafson, & Funehag, 2008). The flow dimension of fractures in rock mass affects its permeability and groutability (Hernqvist et al., 2012). Additionally, the inflow prediction equations described in section 2.5 are based on the assumption of 2D (radial) flow towards the tunnel, making the flow dimension important to take into consideration.

2.1.3 Statistical representation of hydrogeological properties

Measurements from hydraulic tests in crystalline bedrock often show that hydrogeological values are close to log-normal distributed (Olofsson et al., 2001). Fransson and Gustafson (2006) has also shown that the transmissivity distribution of fractures can be assessed using Pareto distribution. The Pareto distribution applies for populations where there are a majority of small values and a few large ones, which is typical for fracture transmissivities in crystalline rock (Hernqvist, 2009).

The groutability of rock mass can be evaluated with a method based on fitting a Pareto distribution on measured transmissivities, through which fracture aperture distributions can be assessed (Gustafson et al., 2004). The number of fractures per section and the section transmissivity data is needed in the evaluation, where it is assumed that the transmissivity of the tested section is the sum of the fracture transmissivities (Gustafson & Fransson, 2006). The result is a distribution parameter k, from which it is possible to evaluate the transmissivity of the most conductive fracture, T_{max}. These parameters can then be used to assess the fracture aperture distributions based on the cubic law (Equation 2.5).

In order to be able to describe a larger section of rock mass using measurements performed in a smaller scale, scale effects has to be taken into account. As the rock is heterogeneous with fractures of finite extent, the properties of the rock mass will change depending on which scale is examined (Gustafson, 2012). In the large scale, an assumption can be made that the rock is seen as a continuum with conductivities that are log-normally distributed. Typically, when using a larger measurement scale larger volumes becomes affected by the measurement, and a better fit to the log-normal distribution can be achieved. The arithmetic mean can be used in the evaluation on large scales, as the rock mass is, sometimes, seen as a homogeneous porous medium. However, on the small scale, individual fractures are considered and used to estimate the transmissivity distribution. On the mid-scale, which is the scale considered when performing hydraulic tests in boreholes, the test section is intersected by several fractures. The fractures is thus not completely independent, and the hydraulic properties can then be represented by interval transmissivities.

The effective hydraulic conductivity, K_{eff}, can be used for a heterogeneous medium to describe a representative value of the flow (H. Stille, 2015), and it is dependent on the statistical distribution of the hydraulic conductivity and the flow regime (B. Stille, 2016). The heterogeneous rock mass can be divided into domains with similar properties, where K_n is independent of the other domains. 1D flow through domains in series will be governed by the harmonic mean value, see Equation 2.6, while a 1D flow through domains in parallel will be governed by the arithmetic mean, see Equation 2.7.

$$K_h = \frac{N}{\sum_{n=1}^{N} 1/K_n} \tag{2.6}$$

$$K_a = \frac{1}{N} \cdot \sum_{n=1}^{N} K_n \tag{2.7}$$

Further, a 2D flow is dependent on the geometric mean, see Equation 2.8, while a 3D flow is dependent on the geometrical mean, K_g, and the variance of $ln(K_i)$, ζ^2, and can be described using Matheron's conjecture, see Equation 2.9 (H. Stille, 2015). For a log-normal distribution, the geometric mean is equal to the median.

$$K_g = \sqrt[N]{\prod_{n=1}^{N} K_n} \tag{2.8}$$

$$K_{3D} = K_g \cdot \exp\left(\zeta^2/6\right) \tag{2.9}$$

Matheron's conjecture uses the flow dimension in the estimation of the mean according to Equation 2.10. As can be seen, for a 2D flow, K_{2D} is equal to the geometric mean, K_g, as the exponent becomes zero (Hernqvist, 2009).

$$K_D = K_g \cdot \exp\left[\zeta^2 \left(\frac{1}{2} - \frac{1}{D}\right)\right] \tag{2.10}$$

When doing analyses of data sets from hydrogeological tests, it is important to chose the most appropriate representative value of this data set. According to Gustafson (2012), the arithmetic mean usually is one order of magnitude greater than the geometric mean. Further, it have been shown that the effective hydraulic conductivity for a larger scale is represented well by Matheron's conjecture. The different mean values can also be used to form an upper and lower boundary of the hydraulic conductivity (B. Stille, 2016).

It should be noted that preliminary investigations are mainly based on vertically oriented boreholes, whilst pilot holes in the tunnel front are horizontal (Gustafson, 2012). Thus, the prediction of hydraulic conductivity might be affected by the orientation of boreholes and fractures in the rock mass. Further, the investigations are often performed from the ground surface where the fracture frequency is higher, the overburden smaller and the possibility of hitting sheeting planes is higher, resulting in a higher hydraulic conductivity. Because of this, the calculated inflow, see section 2.5, can be overestimated. The type of flow should also be considered, as, among other, the geometry, the rock quality, and the flow path usually changes as the rock mass is heterogeneous, which further will determine the statistical mean that proves to fit the best (B. Stille, 2016).

Gustafson (2012) illustrated the scale dependence between the arithmetic, geometric and the value according to Matheron's conjecture, see Figure 2.2. In his graph, the arithmetic mean decreases with scale, while both the values calculated with Matheron's conjecture and the geometric mean will increase as the scale increases. Eventually, the three mean values will approach each other as the scale grows larger. Thus, on a small to a mid-scale, the choice of representative mean value will give

larger affects in the evaluation.

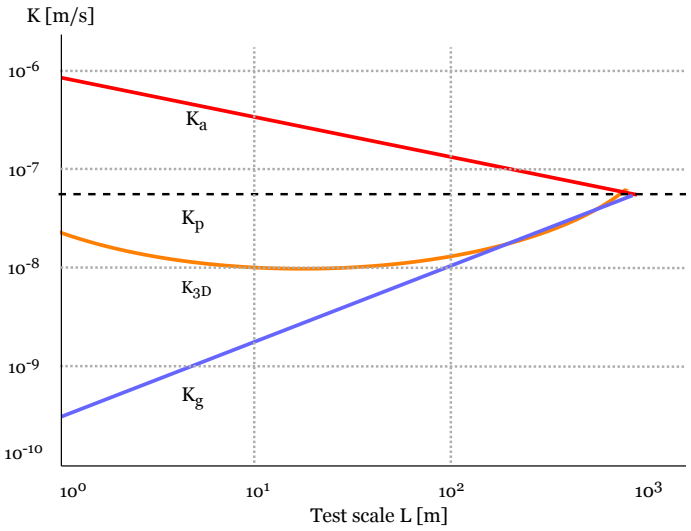

Figure 2.2: Comparison between means of hydraulic conductivity. The dotted line, K_p, is the effective value that can be derived from measurements in long boreholes on a large scale. Modified from Gustafson (2012).

2.2 Hydrogeological tests

The most important parameters used to describe the hydrogeologic properties of the rock mass is the hydraulic conductivity or the transmissivity. These parameters often have large variations over short distances (Gustafson, 2012). Thus, the order of magnitude of the hydraulic conductivity need to be estimated in order to get a representative evaluation of the groundwater flow through the rock mass.

The hydrogeologic conditions around a tunnel has a depth dependence, and the hydraulic conductivity generally decreases as the depth increases (Gustafson, 2012). If the hydrogeological test is a part of the site characterisation, it therefore has to be carried out so that it describes the conditions where the tunnel will be located. Additionally, the appropriate investigation methods have to be chosen with regard to the specific site conditions and demands of the tunnel project (Hernqvist et al., 2012). Other investigations, such as geophysical methods and geological mapping of boreholes, are also often performed when characterizing the hydrogeological properties of the rock mass (Kvartsberg, 2013).

The hydrogeological tests are carried out during the site characterization in order to perform the preliminary grouting design (Kvartsberg, 2013). The tests are also performed during construction to ensure that the hydraulic conductivity of the fractures in the rock mass is reduced, and that the inflow lies within the set requirements for the project.

2.2.1 Short-duration tests

A common way of determining the hydraulic conductivity of rock is by performing Water Loss Measurement Tests (WLM test) (Gustafson, 2012). During the test, water is injected into a borehole section under constant pressure, and the outflow is measured under stationary conditions. The borehole is often sectioned off using two packers, and common section lengths are 3 and 5 meters (Thörn, Kvartsberg, Runslätt, Almfeldt, & Fransson, 2015). The test can begin close to the rock surface, and the packers are then moved further down into the borehole, testing the rock sectionwise. The test can also be performed using only one packer, where the test section is defined from the packer to the bottom of the borehole. Figure 2.3 illustrates the WLM test when using both one and two packers.

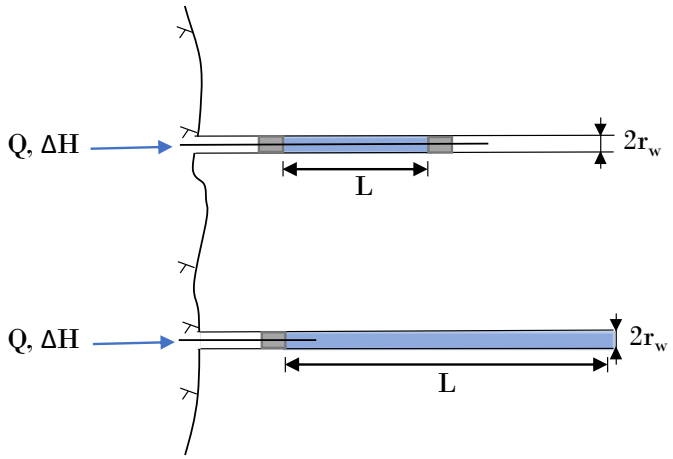

Figure 2.3: A basic sketch of an WLM test using two packers is illustrated in the top borehole, while an WLM test using one packer is illustrated in the bottom borehole. Modified from Thörn et al. (2015).

When the test is performed using one packer, it is not possible to distinguish sections with smaller transmissivity when a more water-bearing section is crossed (Thörn et al., 2015). However, when using only one packer, leakages around the packer will be smaller than when using two. Ten to thirty minutes are generally needed to achieve stationary conditions during the test. The overpressure is controlled by a gauge that is attached to a water hose at the borehole opening, and the flow of water is measured using a flow meter (H. Stille, 2015).

The WLM test is also called Lugeon test, injection test, or water pressure test, and the result is traditionally given using the Lugeon value, see Equation 2.11, where Q is the flow, L is the test length, and Δp is the excess pressure (H. Stille, 2015). The unit of one Lugeon is the loss of water in liters per minute and per meter borehole at an overpressure of 1 MPa.

$$Lu = \frac{Q}{L \cdot \Delta p} \tag{2.11}$$

Inflow tests (IFT) can be used when evaluating the transmissivity of boreholes in

a tunnel (Thörn et al., 2015). The IFT is performed by installing a packer in the borehole, and then measuring the amount of water that is running out. A common way is to use a bucket and watch, measuring the volume that flows over a certain time. It can be performed in the whole borehole or in sections, similar to the WLM test as is described in Figure 2.3. The accuracy of the measurement is limited to the choice of an adequate measurement vessel. The WLM test gives information about the transmissivity of all open fractures that crosses the borehole, while the IFT only results in information about the transmissivity of open, connected fractures. Hence, the WLM test is more appropriate when the purpose of the investigation is to evaluate the fractures that can be grouted.

Moye's formula can be used to evaluate short duration tests, such as WLM tests and IFTs, performed in sections (Hernqvist et al., 2012), see Equation 2.12 (Gustafson, 2012). Q is the flow in m^3/s, g is the gravitational acceleration in m/s^2 , ρ is the density of water in kg/m^3, L is the length of the tested borehole section in meters, Δp is the overpressure above the groundwater pressure in Pascal, and r_w is the radius of the borehole in meters.

$$K = \frac{Q \cdot g \cdot \rho}{2\pi \cdot L \cdot \Delta p} \cdot \left[1 + ln\left(\frac{L}{2r_w}\right)\right] \tag{2.12}$$

Ylinen (1994) has made a modified version of Moye's formula, which performs more accurate results of the hydraulic conductivity when the length of the borehole is larger than 30 times the radius of the borehole, see Equation 2.13 (Hämäläinen & Hurmerinta, 2013; Ylinen, 1994). When using a double packer in a borehole with small diameter, the hole can be considered as a linear source. If Moye's formula is used to evaluate linear sources, the hydraulic conductivity is overestimated since it best applies to radial and point sources.

$$K = \frac{Q \cdot g \cdot \rho}{2\pi \cdot L \cdot \Delta p} \cdot \left[ln\left(\frac{L}{2r_w}\right)\right] \tag{2.13}$$

Additionally, Equation 2.4 can be used to evaluate short duration tests. When evaluating water pressure tests, the change in hydraulic head can be calculated by dividing the overpressure by the density of water and the gravitational acceleration (Hernqvist, Gustafson, Fransson, & Norberg, 2013). If an IFT is used, the change in hydraulic head is the groundwater head.

The Posiva's Flow Log (PFL) is an alternative to the WLM test, where the hydraulic conductivity of individual fractures can be estimated as the measured section can be made quite short (Gustafson, 2012). The device can be moved stepwise along the whole borehole, locating the water-bearing fractures and thereby create a detailed hydrogeological characterization of the fracture network (Hernqvist, 2009). As the testing time is longer for PFL than for WLM tests, the hydrogeologic properties of the rock mass at a larger distance can be evaluated.

By testing several boreholes simultaneously through a interference test, it is possible to see if the boreholes are connected by the fracture network (Hernqvist, 2009).

A disturbance is applied in one borehole, and the response is observed in the surrounding boreholes. The disturbance can be created by injecting water, pumping out water or allowing water to flow out of the borehole.

Generally, boreholes are used to estimate the hydraulic conductivity of the rock mass during the preliminary investigations. When percussion boreholes are drilled, the specific capacity of the borehole can be estimated with the same equipment used during drilling (Ryd, 2017). During the capacity test, water is lifted from the borehole using compressed air, and the flow is measured, see Figure 2.4. The specific capacity can then be estimated by dividing the pumping rate with the drawdown for a specified time during the test. When the boreholes have a high capacity, the result may be misrepresented as the compressed air is not able to empty the borehole on water (Gustafson, 2012). If the drawdown, s_w, during the test is not known, it can be assumed to be the well/borehole depth, d: $s_w \leqslant d$. The transmissivity for crystalline bedrock can then be calculated using Equation 2.14

$$T \approx \frac{Q}{s_w} \leqslant \frac{Q}{d} \tag{2.14}$$

The capacity test is a short-duration test, and only takes a few hours to perform (Ryd, 2017). The capacity can be estimated performing test pumpings or by measuring the recovery of the groundwater in the borehole after the boreholes is emptied during the capacity test. When the recovery of the groundwater is measured, Equation 2.15 can be used to estimate the capacity, where A_w is the area of the borehole, and s''/t is the velocity of the recovery of the groundwater (Gustafson, 1986). The data received through these capacity tests are not very precise, but it is an easy, accessible test that gives an indication of the permeability of the rock mass.

$$Q = A_w \cdot \frac{s''}{t} \tag{2.15}$$

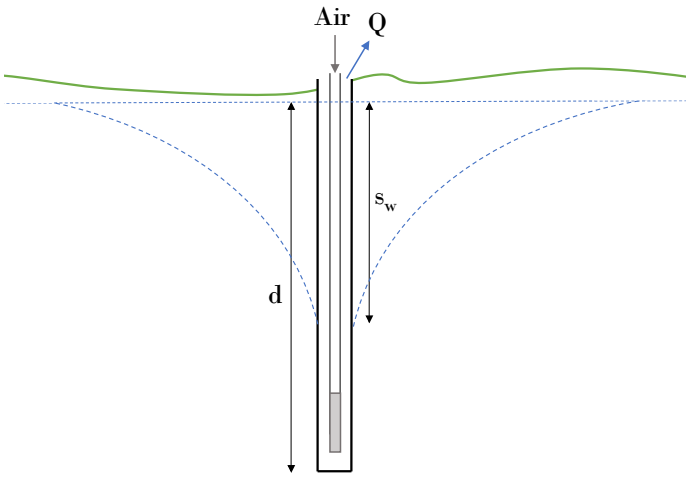

Figure 2.4: Basic sketch illustrating the specific capacity test in a drilled borehole. Modified from Gustafson, 2012.

2.2.2 Long-duration test

When performing short-duration tests, only the conditions of the rock mass closest to the borehole is determined (Hernqvist, 2009). However, if properties of the fracture network further away from the borehole is wanted, long-duration, transient tests such as pressure build-up tests are needed. This is since a pressure disturbance from a hydraulic test take some time to spread through the rock mass, and a longer time is needed to see the effects at a larger distance. The pressure build-up test consists of two periods, a flow period which is followed by a recovery period. During the flow period, the flow Q is measured as the borehole is kept open. Thereafter, the borehole is closed and the recovery period starts, where the pressure is measured as it builds up. The time of the two periods, the flow and the pressure increase during the test is thereafter used to estimate the transmissivity. The pressure build-up test can also be used to evaluate the skin factor.

2.2.3 Measurement weirs

During tunnel construction, weirs are used to collect the inflow from the tunnel from certain tunnel sections. The volume of water that has entered the weir are measured after a specified time when there is a production stop in the construction of the tunnel. This to ensure that only inflowing groundwater is measured, and no process water are added to the measurement. The measurement then represent the total inflow from that tunnel section. Thereafter, the volume can be recalculated to the unit l/min·100m, or l/min for a specified tunnel stretch, in order to be compared to the inflow requirements set for the different tunnel sections. The flow of the leakage to the tunnel can be estimated by flowmeters, or by pumping the water that has been collected in the tunnel front during a production stop, and then timing how long time it takes to fill a known volume in a bucket.

2.2.4 Uncertainties of hydrogeological tests

There are several uncertainties related to the values received through hydrogeologic tests in rock mass. For example, the location of the boreholes used in the test and the amount and width of the fractures intersected by the borehole is relatively random since the rock mass is heterogeneous. Additionally, interference between the boreholes in the test can occur, which will influence the result (Eriksson & Stille, 2005). As described earlier, the scale effect may also influence the evaluation when using tests performed in boreholes to represent a larger tunnel stretch. More uncertainties related to the hydrogeological tests used in the evaluation of the considered tunnels in this thesis are later described in section 4.1 and section 6.1.

2.3 Tunnel construction

As mentioned in section 2.1, the crystalline bedrock in Sweden mostly consist of igneous and metamorphic rocks. These rocks, such as granite and gneiss, often have good strength, and thus have favorable properties for tunnel driving. However, when the rock mass have intersecting fracture planes, stability problems may occur as rock blocks can start to move and fall into the tunnel (Lindblom, 2010).

Before a tunnel is constructed, prognoses are made of the rock to characterise its properties. The prognoses are based on investigations in field through aerial photos, seismic measurements, core drillings, and percussion drillings, but also archive studies (Lindblom, 2010). When performing core drillings, a rock core is obtained which can be used to find fracture patterns and the mineral composition of the rock mass. The cores can also be used to perform laboratory tests. Core drilling is the best method to characterise the rock mass, but it is expensive. Percussion drillings are less expensive, and are performed by lifting and dropping a heavy hammering bit (Patel, 2019). Several parameters are logged during the drilling, which are then used during the analyses of the rock quality (Lindblom, 2010).

Several rock classification systems are used in the field to assess the rock, such as the Rock Quality Designation (RQD), Rock Mass Rating (RMR), and the Rock Tunnelling Quality Index (Q-method) (Heiniö, 1999). A quality value is achieved through these different systems, which then can be used to design the reinforcement needed in the tunnel.

The rock prognoses are then used to design the execution of the blasting, reinforcement and grouting (Lindblom, 2010). There are mainly two different ways to construct a tunnel; drill and blast or by using a tunnel boring machine (TBM). When using TBMs, the cross-section of the tunnel becomes circular, while when using the drill and blast method, the cross-section can be modified into several different geometries (Heiniö, 1999). Examples off different tunnel cross-sections can be seen in Figure 2.5, where the first is a tunnel with vertical walls and arched roof, the second is a horseshoe tunnel, and the third is a circular tunnel. As can be seen in Figure 2.5, the uppermost part of the tunnel is called crown, the floor of the tunnel is called invert and the point where the tunnel wall starts to slope inward towards the crown is called springline. As the drill and blast method is used in the case studies considered in this thesis, this method will be described further below.

When constructing the tunnel, the blasting is performed in blasting rounds (Lindblom, 2010). Each blasting round consists of several boreholes that are drilled according to a predetermined design in the tunnel face, and are usually between 3-5 meters long. Thus, the tunnel advance is between 3-5 meters during each blasting round. The boreholes that are drilled in the invert of the tunnel are usually more heavily blasted in order to facilitate the unloading of the rock masses. Hence, damage of the rock can occur which will lead to an increased groundwater flow in the invert. Gentle blasting can be performed to minimize the damage zone around the tunnel. This can be performed by drilling more boreholes in the tunnel contour, and by using a weaker explosive.

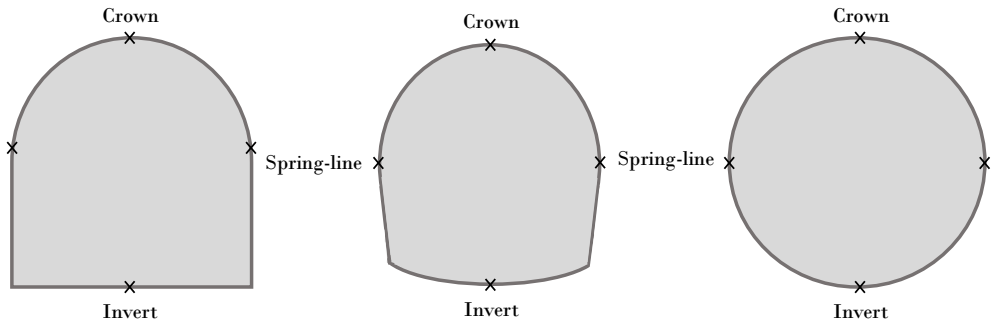

Figure 2.5: Examples of tunnel cross-sections that are used.

After the tunnel is blasted, scaling is performed to remove loose blocks (Lindblom, 2010). Thereafter, the blasted rock masses are removed. Usually, when a tunnel is blasted, shotcrete is used as a fast reinforcement to ensure that no blocks will fall down into the tunnel. The blocks are thereafter fully reinforced using rock bolts or shotcrete that can be enhanced by using fibers or reinforcement. Linings of concrete can also be used as a permanent reinforcement, which may be used where the rock is of bad quality.

To summarize, the process used when constructing a tunnel using the drill and blast method with continuous pregrouting can be initiated with drilling probe holes, which are used to check the rock quality of the upcoming tunnel section. Thereafter, boreholes are drilled which are then pregrouted in order to decrease the groundwater inflow to the tunnel. Control holes can be drilled in order to evaluate if the grouting is sufficient. Boreholes that will be used for blasting are then drilled in the pregrouted rock mass, which are then loaded with explosives and blasted according to the predetermined blasting design. The blasted rock masses are then transported out of the tunnel, and scaling is performed in the roof and on the walls to remove loose rock blocks. Thereafter, the tunnel is reinforced using for example rock bolts and shotcrete. If post grouting is needed, this is performed last.

2.4 Grouting of tunnels

Generally, systematic pregrouting is used when there is a need of prohibiting tunnel inflow. The principle of pregrouting is to create a low permeable zone around the tunnel by forcing grout out in the fractures (Gustafson et al., 2004). When using pregrouting, a fan of grouting boreholes are drilled around the tunnel contour which are directed in front of the tunnel (Gustafson, Claesson, & Fransson, 2013), see an example in Figure 2.6. In order to get grout into the fractures, the grouting boreholes should be oriented at an angle with high probability of intersecting the fractures in the rock mass (Hernqvist et al., 2012). Thereafter, grout is injected into the boreholes, usually one at a time, with a chosen grout mix, and then the tunnel is excavated using the drill and blast method in the grouted rock mass (Gustafson et al., 2013). Grouting boreholes are often long enough to cover around 3-4 blasting

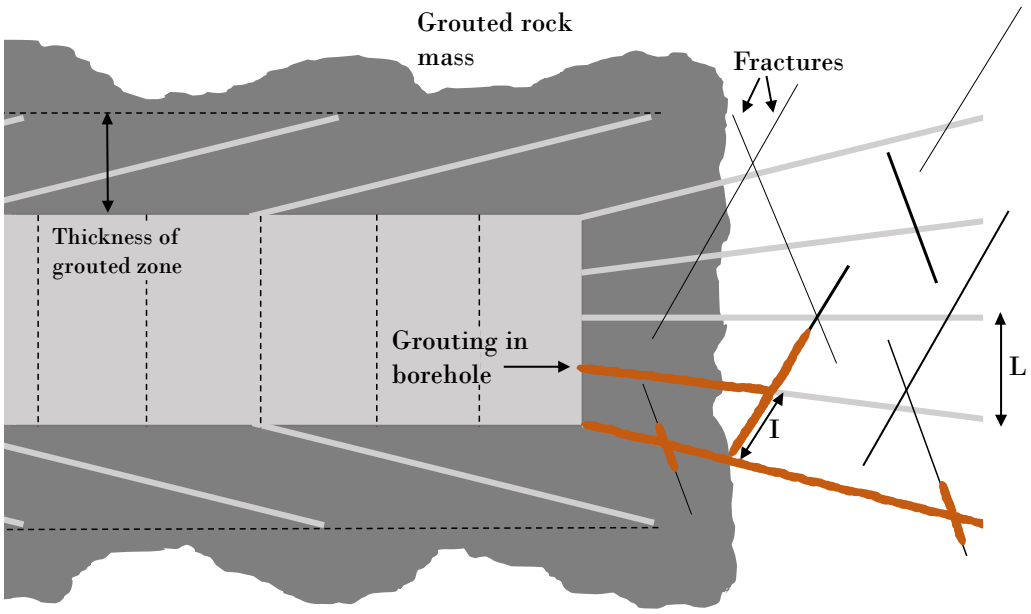

Figure 2.6: A grouting fan and the grout spread during grouting. Modified from Gustafson (2012) and Stille (2016).

rounds.

The grout spreads through the fractures from the borehole as it is injected, and the appropriate pressure and properties of the grout has to be chosen so that the distance the grout penetrates, I, will cover the whole distance, L, between the boreholes (Gustafson et al., 2004), see Figure 2.6. Hence, at least half the distance between the boreholes has to be filled with grout from one borehole. The penetrated distance, I, is individual for each fracture, and is dependent on the fracture aperture, properties of the grouting material and the grouting technique (Gustafson et al., 2013; H. Stille, 2015). The grout will penetrate longer into a fracture with wider aperture compared to a fracture with a smaller aperture, if the conditions during grouting is held constant (Hernqvist, 2009).

There are several reasons why it is difficult to achieve a satisfactory result of the grouting. For example, some fractures have too small openings for the grout to enter, and the grout may not penetrate far enough to get an overlap of the grouting (Gustafson et al., 2004). The grout usually consist of cement grains with a specific grain size distribution, whose diameter may be larger than the aperture of the fracture. A rule of thumb is to choose a grout where the largest particle size of the grout is one third of the smallest fracture aperture that has to be sealed (Trafikverket, 2016c). The penetration length of the grouting may also be underestimated since the fractures are more tortuous than the distance between the boreholes (Gustafson et al., 2004). Furthermore, there might be fractures that the grouting boreholes did

not manage to hit, which are then left ungrouted. The probability of this is higher when the flow dimension in the rock mass is lower.

Thus, the aperture of the fractures that need to be sealed should be taken into account when choosing the type of grout, as different grouts has different abilities to penetrate into fractures (Hernqvist et al., 2012). The smallest hydraulic aperture is dimensioning as it determines the length of the penetration of grout, and hence also the penetration length needed to ensure that the inflow requirements are not exceed (Funehag, 2011). The penetration length of the grout in the smallest fracture thus need to be long enough to cover the length between boreholes, including an overlap (Fransson, 2008). Further, it should be assessed if the penetration in the largest aperture is acceptable, or if it will take a too large grout volume. These factors are included when determining the fan geometry; the distance between the boreholes and the penetration length are adjusted to ensure that an theoretical overlap is achieved and thus also an grouted zone with reduced hydraulic conductivity around the tunnel.

The cement-based grouts are mostly used, but the practical limit of the fracture aperture that these grouts can penetrate is often given as approximately 100 µm (Gustafson, 2012). Furthermore, Fransson (2008) stated that fractures with an hydraulic aperture below 50 µm-100 µm is likely not groutable with cement-based grout.

The cement-based grouts can be described as Bingham-fluids, which means that in order for the fluid to flow, the shear stresses in the fluid must exceed a yield value (H. Stille, 2015). The grains of the cement grouts typically have a d_{95} (95% of the particles are smaller than this diameter) that ranges between 16 µm-30 µm (Hernqvist, 2009). The shear stress acting on the fluid is dependent on the viscosity of the fluid (H. Stille, 2015). These properties can change with time, and must therefore be monitored during grouting to ensure that the properties are satisfactory (Fransson, 2008).

As mentioned in section 2.1.2, Gustafson et.al. (2004) found that water and grout follow almost the same paths through the fracture network. Thus, Equation 2.5 can be used to estimate the hydraulic aperture of a fracture. However, the actual fracture apertures vary in width and can have different kinds of fracture fillings, such as fragments of rock or clays formed by chemically weathered rock. Because of the variation in fracture width, cement particles might not be able to penetrate all fractures. Equation 2.16 can be used to estimate the maximal penetration of grout in fractures that have apertures that is ideally large enough for the cement particles to enter. Δp is the grouting overpressure and can be described as the difference between the grouting pressure and the water pressure, $p_g - p_w$, and τ_0 is the grouts yield value. The yield stress of the grout has to be exceeded in order to initiate flow.

$$I_{max} = \left(\frac{\Delta p}{2\tau_0}\right) \cdot b \tag{2.16}$$

Several grouting materials exist on the market that can be used to grout fractures with small apertures. One example is silical sol, which is made from raw glass

and has a particle diameter that ranges between 5 nm-100 nm (Funehag, 2007). When salt is added to the silica sol, the particles start to aggregate and forms a strong gel. Silica sol can be described as an Newtonian fluid, which flows directly proportional to a pressure gradient. The penetration length of silica sol depends on the overpressure, aperture, gel induction time, and viscosity. However, when calculating the penetration length, the properties of the silica sol is distinguished between when it is non-gelling and gelling, making the expression more complex.

There are several different grouting techniques that are used in the field. Grouting can be performed either by changing the pressure to achieve a constant flow of the grout, or by changing the flow of the grout to achieve a constant pressure (H. Stille, 2015). Further, the choice of grouting pressure used during grouting can be either moderate or high, where a high pressure may increase the grout spread, but it may also increase the rick of jacking of fractures (Hernqvist, 2009).

One technique that is used during grouting is called split-spacing, which is based on a different borehole layout. Firstly, one fan of boreholes with fairly large spacing is grouted (Hernqvist, 2009). Thereafter, additional boreholes are drilled in between the old ones, which are then hydraulically tested and grouted. This method was used in the grouting of the Chalmers tunnel for the grouting class designed for the most water-bearing sections along the tunnel stretch, see Figure 3.2.

Stop criteria has to be chosen, which defines when to end the grouting round. The chosen stop criteria should ensure that fractures are grouted to a certain distance from the borehole (H. Stille, 2015). One stop criterion is to finish grouting when the borehole is filled after using a specified pressure (Hernqvist, 2009). It can also be based on a maximum volume of grout injected, or a maximum grouting time. Stille (2015) has compiled some of the results of the current research on grout spread, and it is shown that the grout spread to a certain distance from the borehole will not be reached at the same time nor at the same flow depending on the pressure used, flow properties, and fracture aperture. Because of the spread differences in fractures, it is hard to estimate the thickness of the grouted zone, which is later used when estimating the inflow to a tunnel after grouting.

The GIN method, which uses an active stop criteria, is described below. It was used in the construction of the Göta tunnel, which is considered in this thesis.

2.4.1 GIN method

The Grouting Intensity Number (GIN) method was developed by Lombardi and Deere (1993), which uses active stop criteria on pressure and volume to control the grouting (H. Stille, 2015). Primarily, the GIN method was developed for grouting of dams, but has been further developed for grouting of tunnels (Hernqvist, 2009).

The product of the final grouting pressure p and the volume of grout injected V is called the Grouting Intensity Number, and generally has the unit bar·liters/m (Lombardi & Deere, 1993). When performing the grouting design, a GIN value is chosen that will be kept constant during the whole grouting process. When using a constant GIN value, Lombardi and Deere state that a nearly constant reach of

the grout is obtained, and that the heave-jacking of the fractures are limited. The constant GIN value is plotted on a pressure versus volume curve, which results in the limiting envelope of the grouting, an example can be seen in Figure 2.7. Thus, the grouting is stopped when the pressure and volume of grout reaches the predetermined GIN curve. Lombardi and Deere produced five different GIN values and curves with different intensities that could be used when grouting, and recommended to use the middle curve initially which then could be changed when the grouting result had been evaluated (H. Stille, 2015). The geological conditions, the results of WLM tests, and the uplift pressure are factors that need to be considered when choosing an appropriate GIN value (Lombardi & Deere, 1993). Hence, when using the GIN method, the pressure is adjusted to the properties of the rock and the injected volume of grout (H. Stille, 2015).

One of the main objectives with the method is that, as far as possible, only a single mix of grout could be used for the whole grouting design (Lombardi & Deere, 1993). Further, the constant GIN value limits the volume of grout injected into large open fractures and allows a pressure increase in zones with smaller and less groutable fractures.

Figure 2.7 illustrates an example of a grouting path, which crosses the GIN curve in point A. When the GIN curve is crossed, the grouting is stopped with a final pressure of p_A and a total volume of injected grout per unit length V_A.

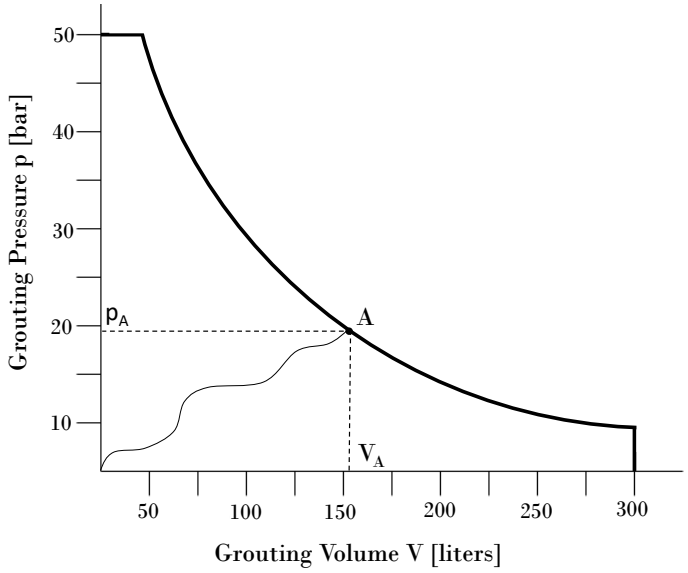

Figure 2.7: An example of a GIN-curve designed from a GIN value of 2500, which is used for grouting of very high intensity, and a grouting path. Modified from Lombardi and Deere (1993).

2.4.2 Grouting design based on the observational method

In the beginning of projects, a lot of uncertainties are related to the properties of the sub-surface . The characterisation of rock mass in the preliminary investigations

are, among other, consisting of hydraulic tests in boreholes, which are relatively expensive and time consuming. The characterisation of the rock mass is therefore mainly based on the locations of the boreholes, leaving large volumes of rock mass not being characterised in detail. Thus, during construction, the prevailing conditions are not always what were predicted in the preliminary investigations as local variations always will occur. In *Eurocoode 7: Geotechnical design*, it is stated that the observational method can be used when the it is difficult to perform predictions of the geotechnical behaviour (Holmberg & Stille, 2007). *Eurocoode 7* is one of the European standards that is used as a general basis when designing geotechnical structures.

The observational method is designed to take into account the uncertainties related to the lack of detailed information by monitoring specified parameters that govern the design during construction (Holmberg & Stille, 2007). A preliminary design is constructed based on the most likely conditions, with several contingency actions for when the conditions start to change during construction. The choice of the predetermined alternative design when the conditions change is based on the observations that are performed during construction on the selected parameters that will govern the design. By using this method, the uncertainties related to the preliminary investigations are decreased as the construction progresses. The observational method was formulated by Peck (1969), who stated that the method should only be applied when an alternative design for each unfavorable condition that might be encountered was created. It is also important that the parameters chosen to be monitored are relevant for verifying the design prerequisites (B. Stille, 2016). Further, Peck stated that savings in both time and costs can be achieved when the method is applied correctly (Peck, 1969).

When concerning grouting purposes, the preliminary grouting based on the expected conditions can be adapted with regard to, for example, the grouting mix, the grouting pressure, the borehole pattern or the stop criterion (H. Stille, 2015). One example of the application of the observational method on the tunneling projects considered in this thesis are the three predefined project specific grouting classes produced for each tunnel. In the older projects, the choice of grouting class was based on water loss measurements performed in probe holes, and a predetermined stop pressure had to be reached in order to terminate the grouting. For the Västlänken service tunnels, the choice of grouting class is based on the hydraulic conductivity of the ungrouted rock mass and requirements of the surroundings (Trafikverket, 2016c). A design pressure is used, which is adapted depending on the rock cover of the considered tunnel section. Further, the general design includes limits on design validity as well as possible actions for conditions where the design is not valid.

2.5 Tunnel inflow

As an unsealed tunnel is constructed, groundwater will flow in from all sides, see Figure 2.8, causing drawdown in the surroundings (Gustafson, 2012). As the floor of the tunnel is located at a larger distance from the groundwater table than the crown of the tunnel, the inflow is generally larger further down in the tunnel towards the tunnel invert.

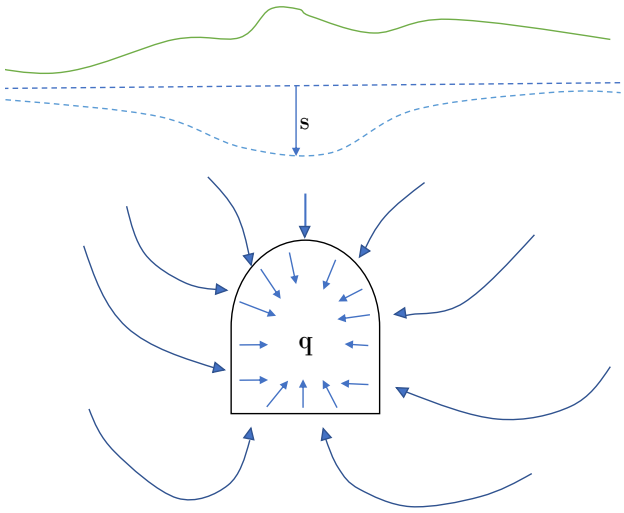

Figure 2.8: Basic sketch illustrating how groundwater flows around a tunnel. Modified from Gustafson (2012).

The equations used to evaluate the inflow of water to a tunnel can either be based on a continuum approach, where the average hydraulic properties over a specific tunnel stretch is represented by a hydraulic conductivity, or a discrete analysis, which is based on a characterization of the existing fracture network (Eriksson & Stille, 2005). The discrete analysis use calculations of flow through individual fractures, which can be performed using Equation 2.5 and Equation 2.17, where H is the depth below the groundwater table and r_t the tunnel radius. These calculations are often performed using computer models with finite element methods. However, the discrete analysis will not be further discussed in this thesis, and the continuum approach will be used in the following calculations.

$$Q = \frac{2\pi T_f H}{ln\frac{2H}{r_t}} \tag{2.17}$$

A first approximation of the tunnel inflow can be performed using Equation 2.19, which is based on Thiem's well equation (Gustafson, 2012), see Equation 2.18. Equation 2.19 assumes that the tunnel is a horizontal well, which is located at depth H below an undisturbed groundwater level. Further, it assumes that the groundwater table is close to the ground surface and that the mean hydraulic conductivity can be calculated by dividing the sum of the transmissivity for all fractures that the tunnel crosses by the length that the inflow will be calculated for (see Equation 2.3). The

later assumption implies that the fracture transmissivities are independent of each other, and that they do not intersect, thus applying a 2D assumption (Hernqvist, 2009). In reality the fractures do intersect, meaning that the total transmissivity of a section can be overestimated.

In both equations, the hydraulic conductivity is denoted $\overline{K}$, the tunnel radius r_t, and the skin factor ξ. In the Thiem equation, s_t is the drawdown at the tunnel and R_0 is the radius of influence.

$$s_t = \frac{q}{2\pi\overline{K}} \cdot ln(\frac{R_0}{r_t}) \tag{2.18}$$

$$q = \frac{2\pi\overline{K}H}{ln(2H/r_t) + \xi} \tag{2.19}$$

The skin factor ξ describes how well the water-bearing fracture system is in hydraulic contact with the tunnel considered (Gustafson, 2012). It takes into account several factors that could influence the inflow to the tunnel, such as the effect of clogged fractures near the tunnel, which will reduce the inflow, and the increased flow resistance caused by the partially saturated rock mass close to the tunnel (Gustafson, 2012; Eriksson & Stille, 2005). Additionally, stress concentrations around the tunnel and the release of chemical precipitation and dissolved gases can reduce the inflow as the fractures around the tunnel are squeezed respectively blocked. According to Eriksson and Stille (2005), a guideline for choosing the skin factor is to use a value between 2-5. Based on experience, the skin factor is larger in low-permeable rock mass (Gustafson, 2012).

Often, tunnels that are constructed using the drill and blast technique have a horse shoe shaped cross-section, i.e. a cross-section similar to the one in Figure 2.8. Hence, the area of the tunnel has to be recalculated to an representative radius which corresponds to a circular cross-section. This can be performed using Equation 2.20, where A_t is the area of the tunnel, see Figure 2.9.

$$r_t \approx \sqrt{A_t/\pi} \tag{2.20}$$

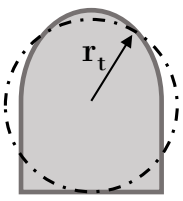

Figure 2.9: The approximate radius of a tunnel with a non-circular cross-section.

In Sweden, the Geological Survey of Sweden, SGU, collects data from wells found all over the country in the so-called Wells archive (SGU, n.d.-b). Data, such as the well capacity, well depth, soil depth, and groundwater level are stored and free to use. The well capacity is generally evaluated using short duration pumping tests.

Thus, the information from the well archive (and other short duration tests) can be used to evaluate the inflow of groundwater to a tunnel using Equation 2.21, which also is based on the Thiem's well equation, Equation 2.18 (Gustafson, 2012).

$$q \approx \frac{H}{2R_0} \cdot (Q/d)_{50} \cdot ln(\frac{R_0}{r_w}) \tag{2.21}$$

In Equation 2.21, H is the groundwater head, Q_{50} is the median well capacity, d_{50} the median well depth, and r_w is the well radius. Generally, the radius of influence is estimated as $5 \cdot$ H (Gustafson, 2012).

Decreased pressure levels will be seen in the water bearing fracture system in the bedrock, even though the tunnel is grouted, as groundwater leaks into the tunnel (Bergab, 2007b). The groundwater level in soil may also get decreased levels if the water bearing soil layers are in hydraulic contact with the fractures. The equation above assumes that the groundwater head is unaffected. Thus, when groundwater flows into underground constructions, the estimated inflow will decrease as the groundwater head decreases. With time, drawdown will spread in the area of influence, where the largest groundwater lowering will occur closest to the tunnel, see example in Figure 2.8.

In tunneling projects, requirements are often set on how much inflow that are allowed to enter to the entire tunnel, or divided into requirements for specific tunnel stretches. The maximum permitted inflow can be given as volume of inflow per time unit and tunnel stretch, and are generally given for the construction and operation phase separately (Merisalu & Rosén, 2020). Merisalu and Rosén (2020) stated that a majority of the projects considered in their study had requirements that were linked to both inflow, groundwater levels and harmful effects on the surroundings. It was also stated that the strictness of the requirements should be linked to the risk of harmful effects on the surroundings, in order to avoid disproportionate sealing costs.

In order to estimate the amount of inflow that can be expected to a tunnel, Equation 2.22 can be used to perform an inflow prognosis (Gustafson et al., 2004; Hawkins, 1956). The driving force of the groundwater flow is dependent on the pressure difference and the length of the flow path (B. Stille, 2016). Generally, it is assumed that the driving force, the gradient, is acting over the thickness of the grouted zone.

$$q = \frac{2\pi \overline{K} H}{ln(2H/r_t) + (\overline{K}/\overline{K}_{gr} - 1) \cdot ln(1 + t/r_t) + \xi} \tag{2.22}$$

The inflow to the tunnel, q, is estimated using the hydraulic conductivity of the ungrouted rock mass, $\overline{K}$, the groundwater head from the center of the tunnel, H, the tunnel radius, r_t, the hydraulic conductivity of the grouted zone around the tunnel, $\overline{K}_{gr}$, the mean thickness of the grouted zone, t, and the skin factor, ξ (H. Stille, 2015). $\overline{K}_{gr}$ can also be described as the residual hydraulic conductivity of the fractures that did not get sealed during the grouting (Fransson & Hernqvist, 2010). Figure 2.10 is illustrating an ungrouted and a grouted tunnel, and the parameters needed in the evaluation. The evaluated parameters has to correspond to the length

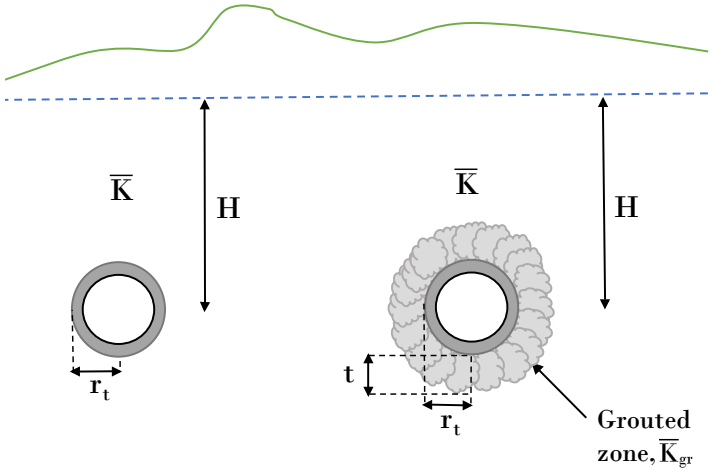

Figure 2.10: The figure to the left is illustrating an ungrouted tunnel, while the figure to the right is illustrating a grouted tunnel. Modified from Gustafson, 2012.

of the tunnel section considered in order for the results to be representative. For example, the boreholes through which the hydraulic conductivities are evaluated has to have a length that corresponds to the length of the tunnel section that is considered (Hernqvist et al., 2013).

Equation 2.22 can be used after grouting, where a prediction of the inflow can be achieved through the actual transmissivity of the grouted zone (Hernqvist et al., 2013). It can also be used in the preliminary investigations to evaluate the needed transmissivity of the grouted zone by inserting the inflow requirement. The resulting K_{gr} can then be used to evaluate the smallest aperture that needs to be sealed in order to meet the inflow requirements. This aperture can then be used to evaluate if cement grout will be sufficient, or if a solution grout will be needed (Hernqvist, 2009).

By rearranging Equation 2.22, the hydraulic conductivity of the grouted zone can be calculated, see Equation 2.23.

$$K_{gr} = \frac{\overline{K}}{1 + \left(\frac{2\pi\overline{K}H}{q_{gr}} - \xi - ln(\frac{2H}{r_t})\right) \cdot \frac{1}{ln(1+\frac{t}{r_t})}} \tag{2.23}$$

Further, Equation 2.19 can be simplified to Equation 2.24, and Equation 2.22 can be simplified to Equation 2.25, when the tunnel is located at a reasonable depth (Gustafson, 2012).

$$q \approx \overline{K} \cdot H \tag{2.24}$$

$$q \approx 2\pi\overline{K}_{gr} \cdot H \tag{2.25}$$

When a tunnel is ungrouted, the ratio of the mean hydraulic conductivity of the

ungrouted rock mass and the grouted rock mass is equal to 1, see Equation 2.26. In an example described in Gustafson (2004), the ratio was equal to 60 when using cement grout, and equal to 208 if microcement and additives was used to seal fractures down to 50 µm.

$$\frac{\overline{K}}{\overline{K}_{gr}} = 1 \tag{2.26}$$

In literature, several variations of Equation 2.22 can be found. For example, Equation 2.27 is described in Eriksson and Stille (2005), Equation 2.28 was used in the calculation of inflow in the Lerum tunnel (Bergab, 2002) (see section 3.3.2), and Equation 2.29 is described in Stille (2016). Equation 2.28 was also used in a sensitivity analysis of the inflow performed in internal documents for the Chalmers tunnel. In these equations, the grouted zone is treated differently than in Equation 2.22.

$$q = \frac{2\pi\overline{K}H}{ln\left(\frac{r_t+t}{r_t}\right) + \frac{K_{gr}}{\overline{K}} \cdot ln\left(\frac{2H}{r_t+t}\right) + \frac{K_{gr}}{\overline{K}} \cdot \xi} \tag{2.27}$$

$$q = \frac{2\pi K_{gr}H}{ln\frac{r_t+t}{r_t} + \frac{K_{gr}}{K} \cdot ln\frac{2H}{r_t+t} + \xi} \tag{2.28}$$

$$q = \frac{2\pi K_{gr}H}{\left(1 - \frac{K_{gr}}{K_{eff}}\right) \cdot ln\left(\frac{r_t+t}{r_t}\right) + \frac{K_{gr}}{K_{eff}}\left[ln(\frac{2H}{r_t}) + \xi\right]} \tag{2.29}$$

In Equation 2.22, the grouted zone is seen as homogeneous (B. Stille, 2016). However, the penetration of grout is dependent on the grout mix, the fracture aperture, and the grouting pressure. A further development of Equation 2.29 was therefore performed by Stille (2016), where the residual transmissivity was assumed to consist of ungrouted fractures, whose hydraulic conductivity can be calculated by dividing the mean of the transmissivities, μ_{Tgr}, with the interval length, L, see Equation 2.30. Since the fractures are assumed to be ungrouted, the equation could be simplified to the equation for an ungrouted rock mass, see Equation 2.31.

$$q_{gr} = \frac{2\pi(\mu_{Tgr}/L) \cdot H}{ln\left(\frac{2H}{r_t}\right) + \xi} \tag{2.30}$$

For ungrouted tunnels located at small depths, Equation 2.31 can be used (Eriksson & Stille, 2005). In this equation, the groundwater pressure is reduced with the radius of the tunnel. For an ungrouted tunnel located at large depths, the correction of the groundwater pressure is not used and the term H-r_t is replaced by H.

$$q = \frac{2\pi\overline{K}(H - r_t)}{ln\left(\frac{2H}{r_t}\right) + \xi} \tag{2.31}$$

3

Study objects

In the following chapter, the four tunneling projects considered in this study is presented. The tunnels are described in chronological order according to the completion of the construction.

3.1 Chalmers tunnel

The Chalmers tunnel is an approximately 1.1 km long tram tunnel located between Aschbergsgatan, where Chalmers University of Technology is situated, and Södra Vägen (Bergab, 1999c), see Figure 3.1. It was a part of the public transportation project Kringen, whose goal was to make the tramway in Gothenburg more effective. The construction of the tunnel started in the year 2000, and was open for the public transport on February 10, 2002. The tunnel consists of two parallel tunnels, which are linked each 250-300 meters by, in total, 8 connection tunnels. During construction, the tunnel was blasted in four tunnel fronts; Chalmers south, Chalmers north, Södra vägen south, and Södra vägen north. The cross-sectional area of one tunnel tube is approximately 38 m^2.

The Chalmers tunnel is located in the central parts of Gothenburg, and are passing under both residential areas, the Carlanderska hospital and parts of Chalmers University of Technology. As the tunnel was constructed below the groundwater table, drawdown and changed flow directions could occur as a result of the construction (Bergab, 1999b). Hence, the groundwater lowering had to be limited in order to avoid damage caused by subsidence.

3.1.1 Geologic conditions

During the preliminary investigation, four valleys with larger clay layers were found that may be subjected to harmful groundwater lowering along the tunnel stretch (Bergab, 1999c). One of the valleys follows Gibraltargatan, and are crossing the tunnel approximately in section 5/350 and 7/350. These sections are located in the part of the tunnel stretch that is chosen to be evaluated in this study. The valley mainly consists of clay with some elements of silt, and a layer of frictional material located below the clay. Where the groundwater in soil is in hydraulic contact with the fracture network crossed by the tunnel, drawdown could occur. Since the clay in the valleys are sensitive for consolidation, groundwater lowering in the lower layer of frictional material could result in large time dependent settlements.

Figure 3.1: Tunnel stretch of the Chalmers tunnel. The red line represents the southern tunnel tube, and the black line represents the northern tunnel tube.

The bedrock mainly consists of gneiss, with a section of norite (a magmatic plutonic rock which is comparable to gabbro (SLU, n.d.)) at the tunnel opening towards Chalmers (Bergab, 1999c). In the contact area between the gneiss and norite, a fracture zone was expected. The bedrock is distinctly foliated, and the dominating fracture set follow the direction of the foliation. Further, the tunnel is crossing the fractures in a favorable angle.

3.1.2 Hydrogeologic conditions

The bedrock where the Chalmers tunnel is located is largely heterogeneous regarding hydrogeological properties, as the top of the bedrock have a higher fracture frequency than the deeper parts of the bedrock (Bergab, 1999c). The soil is often in hydraulic contact with the upper parts of the bedrock because of the higher fracture frequency.

In the preliminary investigation, the transmissivity of the soil and rock was estimated through hydraulic tests in percussion boreholes and core drilled holes (Bergab, 1999c). The hydrogeological tests consisted of slug tests and infiltration tests in wells, and WLMs in the percussion boreholes. The evaluation of the transmissivity in rock through the percussion and core drilled boreholes gave values ranging between $<1 \cdot 10^{-8}$ and $2 \cdot 10^{-5}$ m^2/s (Bergab, 1999b). Generally, the higher areas located between the valleys had low to moderate water bearing ability.

3.1.3 Inflow requirements

The following is a translation of the Environmental ruling from the Environmental Court for the Chalmers tunnel (Vänersborgs district court, case number M147-99, verdict 2000-03-10), where the following is stated about the requirements for the rock tunnel:

During the construction phase, groundwater is allowed to be led away:

- *in the main tunnels and the working tunnel with openings and rock chambers, the inflow of groundwater can be 120 l/min in average per week, though 180 l/min in maximum.*

During the operating phase, groundwater is allowed to be led away:

- *in the main tunnels and the working tunnel with openings and rock facilities, the inflow of groundwater can be 42 l/min in average per week, though 66 l/min in maximum corresponding to 22 100 m^3 per year.*

The above specified numbers regarding inflowing groundwater applies to the entire tunnel and corresponds to a inflow of 2 l/min·100m in average per week, and 3 l/min·100m in maximum.

In the preliminary investigations, the inflow requirements were calculated in a conservative way, meaning that the actual inflow most probably were smaller than the prognosis showed (Bergab, 1999c). The inflow requirements were calculated for specified stretches, and ranged between 1-5 l/min·100m. The considered tunnel stretches in this thesis, 5/288-5/392 and 7/285-7/372 in the northern respectively southern tunnel tube, had the requirement set to 1.0 l/min·100m. However, it was found in internal documents that the requirement might be set to strict for these two tunnel sections in the Chalmers tunnel, but no decision on the matter was found.

3.1.4 Grouting design

The grouting of the Chalmers tunnel was primarily based on continuous pregrouting using cement grout (Bergab, 1999a). Where the requirements on sealing of the tunnel was not met, continuous postgrouting was used.

The location and pattern of the boreholes used for grouting was adapted to the prevailing geologic settings (Bergab, 1999a). Further, the properties of the cement grout, such as the initial w/c ratio, was adapted according to the hydrogeologic conditions. The length of the fan was adapted to include a section of rock mass with the same hydrogeologic properties. For example, when crossing larger fracture zones, the fan length was adapted so that it covered the length of the zone. Likewise, an adapted fan was used when the overburden was smaller. Generally, a shortened fan was used for water-bearing zones, while the fan of normal length (20 meters) was used for the less water-bearing rock mass in between.

In order to determine the design of the grouting fan, the probe wholes that were included in the first grouting round were drilled and cleaned, and WLMs were performed (Bergab, 1999a). According to the results of the WLMs, the proper grouting class was chosen with the appropriate fan length.

The WLMs were performed with an overpressure of 0.5 MPa over the groundwater pressure. Furthermore, the tests were performed in the entire borehole, with a packer placed at least 1 meter into the borehole. During the test, the overpressure had to be held for at least 2 minutes after stationary conditions was obtained. If there were boreholes that were in hydraulic contact with each other, packers were installed

during the measurement. When a WLM gave results above the given requirements, additional grouting holes were drilled around this borehole.

The grouting was performed until a stop-pressure was reached (Bergab, 1999a). Generally, a stop-pressure of 2.5 MPa over the groundwater pressure was used, but it was adapted to the prevailing geologic conditions. The grouting was stopped when the stop-pressure was reached, and the flow of grout had been smaller than 2 l/min during 5 minutes. Additionally, a maximum amount of injected grout was given to ensure that an undesirable spread of grout did not occur. If a section of, for example, high fracture frequency occured, accelerator additives could then be added to ensure that the maximum volume was not reached.

Three different grouting classes were designed for the different geologic and hydrogeologic settings that could occur along the tunnel stretch. The work and design process is described below in Table 3.1 (Bergab, 1999a), and the grouting design is illustrated in Figure 3.2, and Figure A.1 in Appendix A. The number of probe, grouting and control holes included in the normal fan for each grouting class is illustrated in Figure 3.2. The distance from the tunnel to the tip of the boreholes was 4 meters for grouting class 1, and 4 meters in the crown and walls respectively 5 meters in the invert of the tunnel for grouting class 2 and 3. The following is a description on when the respective grouting class were used (Bergab, 1999a), and the work process is given in Table 3.1.

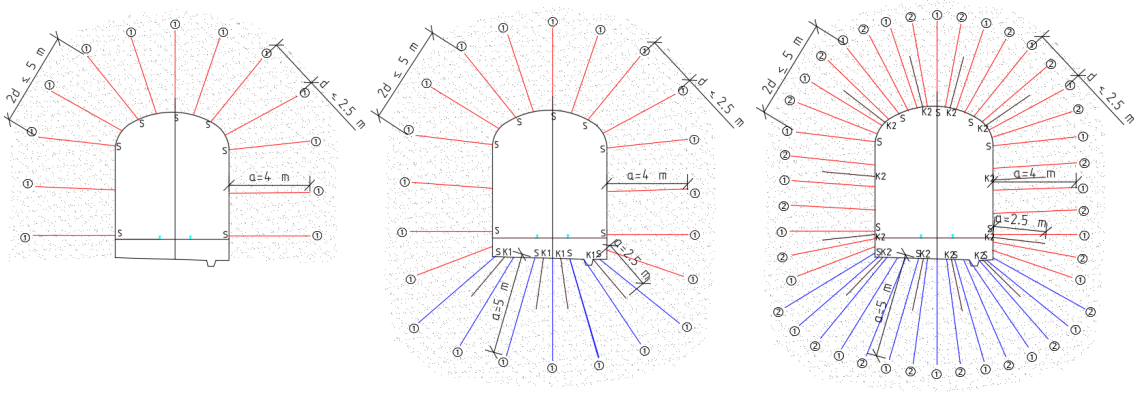

Figure 3.2: Grouting design of the Chalmers tunnel, illustrating the three grouting classes (Technical drawing 620/98-9950).

- **Grouting class 1**: was used in sections where the rock mass was of good quality, and where the inflow into the tunnel was not expected to cause harmful effects on the surroundings.
- **Grouting class 2**: was used where the permissible value on inflow was larger than in sections where grouting class 3 were used.
- **Grouting class 3**: was used in areas where a groundwater drawdown could case harmful effects on the surroundings.

Table 3.1: Grouting process for the three grouting classes in the Chalmers tunnel (Bergab, 1999a). Each grouting class is denoted IK.

Work process IK1 and IK2	**Work process IK3**
Probe holes with WLMs	Probe holes with WLMs
IK1, if WLM probe >0.3 Lu, additional grouting holes	Grouting holes drilled
Grouting holes drilled	Grouting round 1
Grouting round 1	Grouting holes drilled
IK1: control holes with WLMs if borehole take 50kg grout IK2: control holes K1 with WLMs	Grouting round 2
Both: if WLM control >0.3 Lu, additional grouting holes	Control holes K2 with WLMs
	If >0.15 Lu, additional grouting holes

Measurements of inflow to the tunnel were performed every week in measurement weirs (Bergab, 1999a). The measurements had to be performed after the production stop that occurred during the weekend, before the work was resumed. Additionally, measurements on inflow were performed at the tunnel front with the same time interval and requirement of production stop.

3.2 Göta tunnel

The Göta tunnel is a 1.6 km long road tunnel between Järntorget and Lilla Bommen in the central parts of Gothenburg. The construction of the tunnel began in the year 2000, and the whole tunnel was finished in 2006. The purpose of the tunnel was to improve the environment and the traffic safety by redirecting the through traffic under ground.

The tunnel consists of two excavated concrete tunnels that leads down to the 1 km long blasted rock tunnel, whose invert is situated at a maximum depth of 33 meters below the groundwater table (VBB Viak AB, 1997). The tunnel has two 14 m wide tubes, each with the cross-sectional area of approximately 120 m^2, which are separated by a 10 m pillar (Lindblom, Ludvig, & Axelsson, 2005). The tunnel stretch can be seen in Figure 3.3, and the cross-section of one of the tunnel tubes can be seen in Figure 3.4, which illustrates the grouting design.

Along the tunnel stretch, several existing underground facilities are located close by (Petro Bloc AB, 1991). If the inflow to the tunnel was not prevented by using grouting, the groundwater lowering would most probably damage the buildings situated close to the tunnel stretch, as well as existing wells and conduits in the ground (VBB Viak AB, 1997). Further, as the fracture system and frictional soil form a relatively closed aquifer with no open groundwater table because of the overlying clay, small leakages into the tunnel can result in quite large settlements. Therefore,

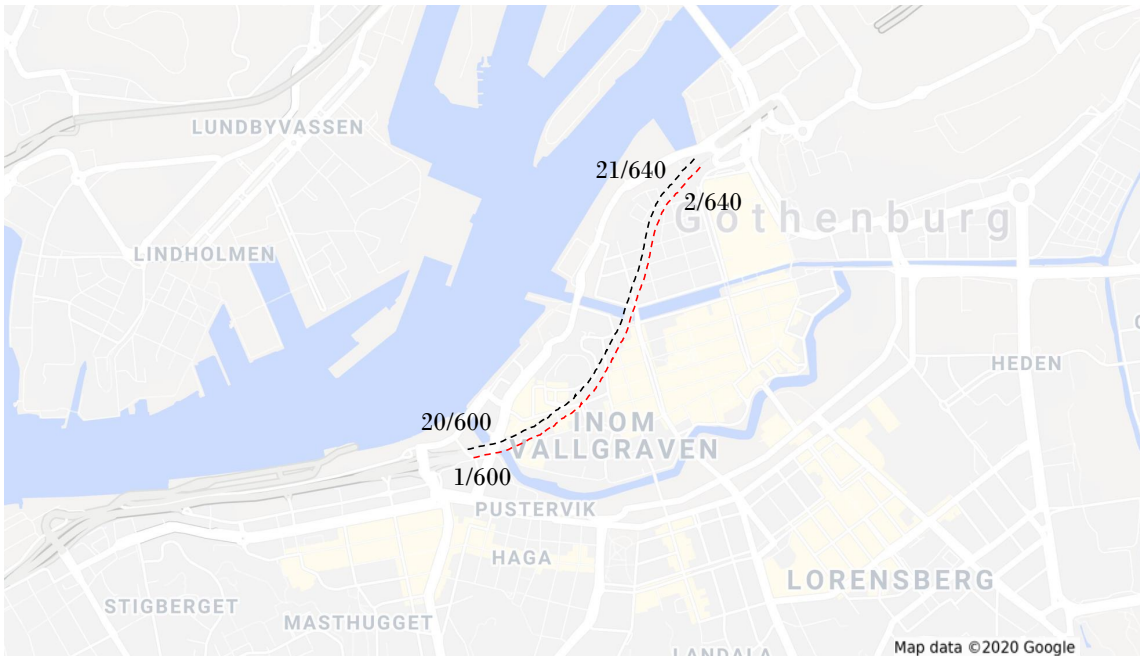

Figure 3.3: Tunnel stretch of the Göta tunnel. The red line represents the southern tunnel, and the black line represents the northern tunnel.

the system is sensitive to changes in groundwater pressure, and thus a successful grouting is needed to avoid damage.

The rock tunnel starts in section 1/615 at Rosenlund and ends in section 2/635 at Lilla bommen (Environmental Court, case number M86-99, verdict 2000-10-25). The construction of the tunnel began with two working tunnels, which connects to the main tunnel.

3.2.1 Geologic conditions

In the area considered, a rock ridge is located between Carolus Rex in the south and Kvarnberget in the north (Petro Bloc AB, 1991). The rock ridge is partly situated below ground level. However, exposed bedrock can be seen in the southern part at Kungshöjd and in the northern part at Kvarnberget. The tunnel stretch of the Göta tunnel is parallel to the bedrocks foliation, and the dominating fracture set follows the direction of the foliation.

The bedrock is in most parts covered with soil, with a soil depth varying between 0 to 20 meters (VBB Viak AB, 1997). The soil mostly consist of clay, which is often overlaid by organic soils. In most parts of the investigated area, a layer of frictional material was located between the bedrock and the clay. At Kungsgatan and Stora Hamnkanalen, the thickness of the frictional layer was larger, and thus a larger groundwater storage can be expected there. Parts of the investigated area were filled marshlands, which could result in variations in settlements.

The bedrock consists of intermediate banded gneiss with elements of greenstone, which have advantageous properties for tunnel driving (VBB Viak AB, 1997). Only

approximately 30% of the bedrock investigated in the preliminary investigations were evaluated to be of bad quality (Petro Bloc AB, 1991), and fewer than 10 larger fracture zones and 100 smaller fracture zones were estimated to be located along the tunnel stretch (VBB Viak AB, 1997). In the zones with highly fractured rock mass, clay resulting from chemically weathering was expected (Petro Bloc AB, 1991). This clay may have swelling properties, which in contact with water can result in an additional pressure on the surrounding rock.

3.2.2 Hydrogeologic conditions

The groundwater level follows the topography, and is disturbed by the already existing underground constructions and infiltration facilities situated in the area (VBB Viak AB, 1997). The permeability of the rock mass was evaluated to be relatively low, and inflow to the tunnel was expected to take place both diffusely through individual fractures and with higher flows through the fracture zones.

Fifteen percussion boreholes and nine core drilled boreholes were drilled in order to evaluate the hydrogeologic properties of the bedrock (VBB Viak AB, 1997). Out of 764 meters of the investigated core drilled boreholes, 520 meters had a hydraulic conductivity that is lower than 10^{-9} m/s. The compiled results of the hydrogeologic tests in the core drilled boreholes can be seen in Table 3.2. The WLMs performed in the core drilled boreholes used a test length of three meters, an overpressure of both 0.2 and 0.4 MPa, and a test time of five minutes (Petro Bloc AB, 1995).

The percussion boreholes were used to evaluate the capacity of the rock mass (VBB Viak AB, 1997). The test method using compressed air was performed, see section 2.2, where the time of recovery was considered in the evaluation of the capacity. The capacity and the borehole lengths were then used to evaluate an approximate permeability, see Table 3.2.

Table 3.2: Compilation of results from measurements in core drilled boreholes and percussion boreholes for the Göta tunnel (VBB Viak AB, 1997).

Variable	**Core drilled borehole**	**Result**	**Percussion borehole**	**Result**
Number	Tests	137	Boreholes	15
Median	K [m/s]	$1.3 \cdot 10^{-8}$	Capacity	0.6 l/h
Lowest	K [m/s]	$1.0 \cdot 10^{-9}$	Capacity	0.002 l/h
Highest	K [m/s]	$1.1 \cdot 10^{-6}$	Capacity	180 l/h
			Estimated median K [m/s]	$0.8 \cdot 10^{-9}$ m/s
Median	Scale	3 meter	Scale	25.9 meters

In the preliminary investigations, the hydraulic conductivity was evaluated to lie between the evaluated values from the core drilled boreholes and the percussion boreholes, i.e. 0.8 - 130 $\cdot 10^{-9}$ m/s, and the chosen mean hydraulic conductivity of the rock mass was 5 $\cdot 10^{-8}$ m/s. Further, the highest expected hydraulic conductivity

was 10^{-5} m/s. A short pumping test was also performed in a borehole, which resulted in a transmissivity of $3 \cdot 10^{-6}$ m^2/s in the rock mass.

3.2.3 Inflow requirements

The prognosis of the inflow to the tunnel was performed using the hydraulic tests that were executed in the percussion and core drilled boreholes (VBB Viak AB, 1997). Approximately 700 out of total 1000 meters were estimated to be relatively dry with low fracture frequency (VBB Viak AB, 1997).

The following text is a translation of the Environmental ruling from the Environmental Court for the Göta tunnel (Vänersborgs district court, case number M86-99, verdict 2000-10-25) where the following is stated about the requirements for the rock tunnel:

The Environmental Court grants the Swedish Road Administration permission to carry out the following measures and facilities for the execution of the Göta tunnel to the stretch stipulated in the work plan.

- *Discharge of inflowing groundwater in the rock tunnel and the working tunnels, provided that the groundwater level in the lower groundwater reservoir at the roof of the tunnel tube may be permanently submerged at a maximum of one (1) meter below the lowest naturally occurring groundwater level with a mean return period of 50 years; a larger lowering than one meter may only occur in exceptional cases.*

According to the preliminary investigations, the requirement of a maximum drawdown of 1 meter when stationary conditions prevail in the frictional soil corresponds to a inflow of 20 l/min when the tunnel is sealed using pregrouting (VBB Viak AB, 1997). The expected maximum leakage if no sealing would be performed in the tunnel was between 50-100 l/min per fracture zone, but a typical water-bearing zone was expected to give an inflow of 3-30 l/min. The requirement of the drawdown given in the court ruling corresponded to a sealing requirement of 0.7 l/min·100m for the entire tunnel stretch (Lindblom et al., 2005).

3.2.4 Grouting design

The grouting design consisted of a fixed pregrouting cycle, where only one grouting fan was used that could handle all expected geologic conditions (Lindblom et al., 2005). By doing a large first grouting round, the need of several rounds with measurements in between could be avoided. Probe holes were drilled as a part of the fan to verify the rock quality for the upcoming section. WLMs were performed in the probe holes at an overpressure of 0.5 MPa for 5 minutes after stationary conditions was obtained (Internal document, Vägverket, 2002-08-29). If the inflow was assessed to be higher than the prognosis, the fan was expanded with more and longer holes in the tunnel invert (Lindblom et al., 2005). All fractures, except the ones smaller than 0.2 mm were expected to be sealed with cement grout. The grouting fan included 77 drill holes, each hole being 19 m long.

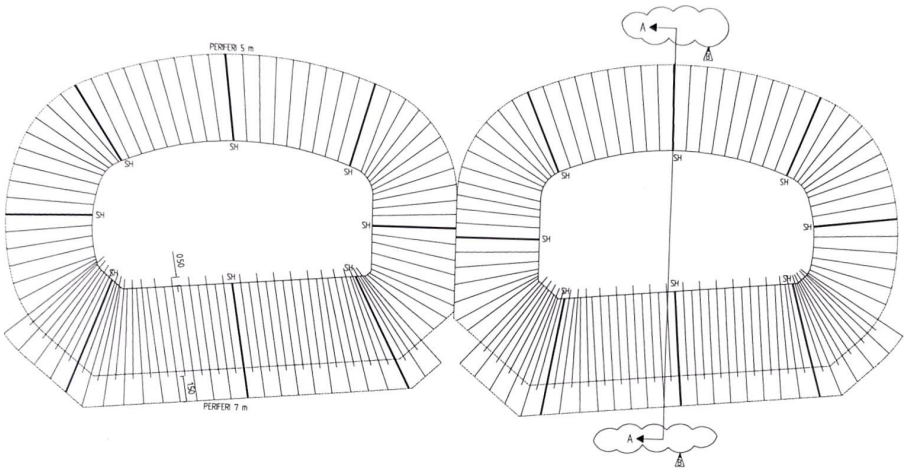

Figure 3.4: The grouting design used for the main tunnel tubes for the Göta tunnel (Technical drawing 200B2442).

The Grouting Intensity Number (GIN) method was used to steer the grouting with active stop criteria on pressure and volume. As the pressure and flow were reaching a predetermined GIN-curve, the grouting was stopped (Eriksson & Stille, 2005). The limits of 3 MPa in pressure or 20 liter grout per meter hole were used (Lindblom et al., 2005) The grouting was stopped when a GIN-value of 30 MPa ·l/m borehole was achieved, and the pressure had been held during 5 minutes after stationary conditions was obtained (Internal document, Vägverket, 2002-08-29).

The grouting design for the Göta tunnel is illustrated in Figure 3.4 and Figure A.2. In Figure 3.4, the thicker lines represent the probe holes, which were used to perform WLMs and to evaluate the quality of the upcoming rock mass. If the prognosis indicated that there would be high inflow of groundwater, the double rows of grouting holes were used in the tunnel invert (Lindblom et al., 2005), as can be seen in Figure A.2.

The goal of the grouting was to ensure that the restriction of a drawdown of maximum 1 meter in soils prone to consolidation were not exceeded (Lindblom et al., 2005), as mentioned above in the court ruling from the Land and Environmental Court for the Göta tunnel. After the completion of the tunnel, the inflow was lower than the calculated critical level. However, infiltration is needed at some locations along the tunnel to ensure that the groundwater level in some local aquifers are kept high enough.

3.3 Lerum tunnel

The Lerum utility tunnel is located in Gothenburg with suburbs, and was constructed between 2007 and 2012. The tunnel is 8 km long and connects Lerum to Gryaabs existing wastewater tunnels, which transports sewage to the wastewater treatment plant Ryaverket at Hisingen in Gothenburg (Bergab, 2007a). The cross-sectional area of the tunnel is approximately 10.5 m^2. The construction of the main tunnel began from a working tunnel that is located at the mid point of the

tunnel stretch, and was performed simultaneously in each direction from that point (Bergab, 2012).

The area around the tunnel mainly consists of undeveloped mountain areas covered with coniferous and mixed forest. Some buildings are located nearby, which mainly are founded on rock and firm soils, and are therefore not as sensitive for groundwater lowering (Bergab, 2007b).

3.3.1 Geologic conditions

The stratigraphy mainly consists of a thin layer of till on top of the hillsides and a thicker layer of clay and silt material in the adjacent valleys (Bergab, 2007b). The tunnel passes several peat lands and smaller streams which may be affected negatively if the groundwater level decreases as an effect of the construction of the tunnel. Additional protection values that may be affected by the tunnel are private wells, geothermal wells and buildings founded on soil sensitive for consolidation.

The bedrock mainly consists of gray, granodioritic to tonalitic gneiss (Bergab, 2007a). A system of larger zones of weakness is found parallel to the gneiss's foliation, and the dominating fracture set coincides with the foliation of the rock. The rock cover varies between 20 m and 100 m along the tunnel stretch.

The properties of the rock is evaluated to be favorable for tunneling over a larger part of the tunnel stretch (Bergab, 2007a). Exceptions are the fracture zones, which predominantly cut the tunnel in a obtuse angle and have a varying degree of chemical weathering and flow of water. The chemical weathering may lead to clay minerals forming in the fracture zones, which can reduce its stability (Bergab, 2007a). In between the fracture zones more intact rock is located, with low to moderate fracture frequency. In these zones the flow of water is more bound to the individual fractures.

3.3.2 Hydrogeologic conditions

In the bedrock, the groundwater is mainly found in the fracture zones which may have large groundwater flows (Bergab, 2007b). The groundwater flow is estimated to be moderate in the areas where both fracturing and the presence of clay minerals are high (Bergab, 2007a). Groundwater in soil is mainly found in the larger till layers. Along the tunnel stretch, the groundwater level in bedrock varies between 1 to 30 meters below ground level over. During the preliminary investigation, percussion boreholes were drilled to evaluate the transmissivity of different sections along the tunnel stretch.

In the preliminary investigation, estimations of inflow were calculated both numerically and analytically (Bergab, 2002). In the analytical evaluation, the maximum water pressure was used in the estimation of inflow, i.e. no drawdown has yet occured. This gave an conservative result, as some drawdown is inevitable. In the calculations, the rock mass was seen as a homogeneous water bearing medium, meaning that the prognosis will give overestimations in some sections and underestimations in others. Equation 2.28 was used for the inflow prognosis. The parameters used in the estimation can be seen in Table 3.3.

Table 3.3: Parameters used in the analytical calculation of the inflow to the considered tunnel stretch in the Lerum tunnel (Bergab, 2002).

Parameter	**1/900 - 4/000**	**4/000 - 4/600**	**4/600 - 5/750**
H [m]	75	70	70
K [m/s]	$5*10^{-8}$	$1*10^{-7}$	$5*10^{-8}$
K_{gr} [m/s]	$2.0*10^{-8}$	$1.5*10^{-8}$	$2.0*10^{-8}$
Skin [-]	5	5	5
r_t [m]	2	2	2
t [m]	3	3	3
q [l/min·100m]	7.8	6.2	7.3

The total inflow to the tunnel is estimated to be 503 l/min or 8.4 l/s (Bergab, 2002). If the tunnel would have been unsealed, the total inflow would amount to 1800 l/min.

In summary, large local groundwater flows were expected during the tunnel driving, but in between these zones low groundwater flows were foreseen (Bergab, internal document, 2012-05-23). As the overburden was quite large along the majority of the tunnel stretch, large water pressures were also expected (Gryaab, 2007). The deeper below the groundwater level, the larger inflow was expected.

3.3.3 Inflow requirements

The following is a translation of the Environmental ruling from the Environmental Court for the Lerum utility tunnel (Vänersborgs district court, case number M274-02, verdict 2004-05-17), where the following is stated:

- *The guide value for discharge of groundwater is maximum 9 l/s during both the construction and the operating phase for the whole tunnel stretch and its openings. This equals a maximum volume of 23700 m^3 per month.*

The inflow requirements were based on the numbers given in the Environmental ruling, as well as on the geologic and hydrogeologic conditions and the protection values that are situated in the area (Bergab, 2007b). In Table 3.4, only the requirements for the tunnel stretch considered in this thesis is given. The requirements set for the different tunnel sections along the entire tunnel stretch ranged between 3.5-7.0 l/min·100m.

Table 3.4: Inflow requirements for the considered tunnel stretch in the Lerum utility tunnel (Bergab, 2007b).

Tunnel section	**Inflow requirement [l/min·100m]**
1/900 - 4/000	7.0
4/000 - 5/750	6.0

Measurements on the inflow were performed in the front of the tunnel and in temporary measurement trenches (Bergab, 2007b). The amount of inflow was measured every 14th day, or every 7th day in sensitive areas.

3.3.4 Grouting design

The Lerum utility tunnel was sealed with continuous pregrouting using cement, and where the inflow was not meeting the inflow requirements, postgrouting was used (Bergab, 2007a). Grouting was performed in order to limit the groundwater drawdown in soil and rock, and to ensure the functionality of the tunnel (Gryaab, 2007). Sealing requirements were given on rock prognosis drawings to ensure that the previously described design goals were met.

The sealing requirements for the Lerum tunnel were based on three grouting classes in order to get adequate sealing of the tunnel (Bergab, 2007a). The grouting design for the tunnel sections was updated as the tunneling proceeded and more detailed information was received of the rock quality and groundwater flow. For example, the borehole geometry, pattern, grout and length could be adapted according to the prevailing geologic conditions. The grouting design of the three grouting classes is illustrated in Figure 3.5, and the profile of the grouting design is illustrated in Figure A.3. The grouting in grouting class 1 and 2, and the first round in grouting class 3 was expected to be satisfactory when using cement grout (Gryaab, 2007). In grouting class 2 and 3, control holes were drilled to ensure that the sealing was sufficient, see Figure 3.5.

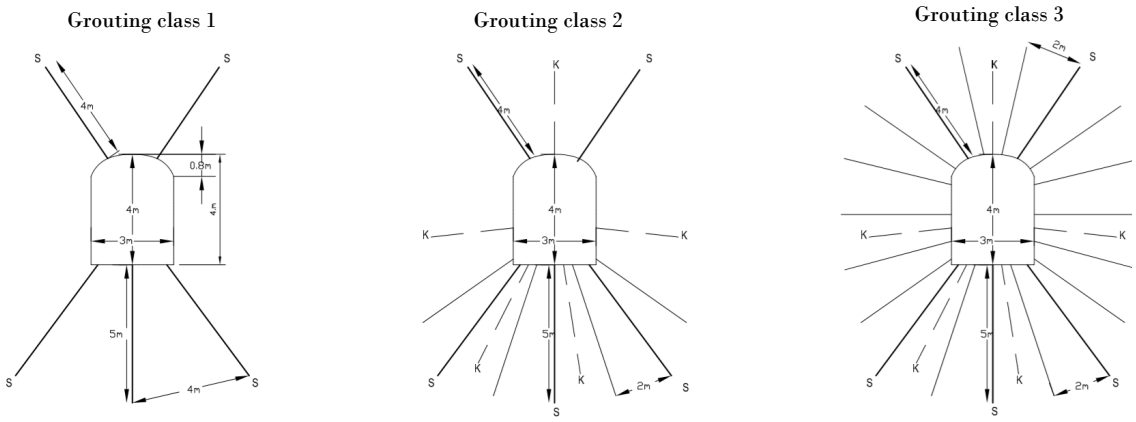

Figure 3.5: Design of grouting classes for the Lerum tunnel (Technical drawing 762G1410-1027).

The following is the description of the three grouting classes given in the document from the preliminary investigation regarding rock prognosis (Bergab, 2007a), and in the technical description used during the tunnel construction (Bergab, 2002). The grouting process for the three grouting classes can be seen in Table 3.5.

- **Grouting class 1:** were used when the rock quality was good and the groundwater flow small.

- **Grouting class 2:** were used in tectonic zones where there were increased fracturing and groundwater flow and in zones with good rock quality and moderate groundwater flow.
- **Grouting class 3:** were used in tectonic zones with large groundwater flow and in sections where the sealing received with grouting class 2 was not satisfactory and additional grouting was needed.

Table 3.5: Grouting process for the three grouting classes in the Lerum tunnel (Bergab, 2002, 2007a). Each grouting class is denoted IK. To clarify, IK3 is chosen when WLMs in probe holes are ≥0.1 Lu in zones with high fracture frequency. Two grouting rounds were always performed for IK3.

Work process IK1	**Work process IK2**	**Work process IK3**
Chosen when WLMs probe <0.1 Lu	*Chosen when WLMs probe ≥0.1 Lu, control <0.1 Lu*	*Chosen when WLMs control ≥0.1 Lu, probe ≥0.1 Lu (when high fracture frequency)*
Probe holes with WLMs	Probe holes with WLMs	Probe holes with WLMs
Grouting holes drilled	Grouting holes drilled	Grouting holes drilled
Grouting round 1	Grouting round 1	Grouting round 1
	Control holes with WLMs	Control holes with WLMs
	If >0.1 Lu, grouting round 2 using IK3. *If <0.1 Lu*, finished.	*If <0.1 Lu*, grouting round 2 using IK2. *If ≥0.1 Lu*, grouting round 2 with additional holes around control hole.

Five probe holes per grouting fan were used to evaluate the groundwater flow, and thus also grouting class, in the rock in the upcoming section of the tunnel (Gryaab, 2007). Normally, the probe holes were 20 meters long with a diameter of 54 mm (Internal document, Bergab, 2012-05-23), but the lengths were adapted with respect to locations of known water bearing zones. This to make sure that each grouting fan included, if possible, a uniform section from a sealing point of view. If the probe holes showed increased fracturing in the rock mass, the probe holes were complemented with grouting and control boreholes according to grouting class 2 and 3 (Internal document, Bergab, 2012-05-23), see Figure 3.5.

The grouting was performed until a stop pressure was reached (Gryaab, 2007). The stop pressure is adapted to, among other, the prevailing overburden and distance to existing infrastructure. However, the stop pressure was generally aimed to be 2.5 MPa above the groundwater pressure. The grouting was stopped when the stop pressure had been achieved and the flow of grout had been smaller than 2 l/min during 5 minutes. If these requirements were not reached during grouting, a maximum volume of grout was given where the grouting was stopped.

Water loss measurements were used to evaluate the groundwater flow in the probe and control holes along the whole tunnel stretch (Gryaab, 2007). The measurement was performed with an overpressure of 0.5 MPa above the groundwater pressure. A

packer was placed at least 1 meter into the borehole, and the pressure had to be held for 2 minutes to ensure that a steady state was achieved. The communication between the boreholes was tested for each borehole by temporarily opening the closed packers.

If inflow still existed after the pregrouting, postgrouting was used (Gryaab, 2007). As for the pregrouting, postgrouting was performed continuously with primarily cement based grouts, and the execution of the postgrouting was adapted for the site conditions.

3.4 Västlänken service tunnels

The West Link (*sv:Västlänken*) is an ongoing project, which consists of a 6 km long double tracked railway tunnel for commuter traffic that passes underneath the central parts of Gothenburg (Trafikverket, n.d.-b). New stations are being built at the central station, Korsvägen and Haga, see Figure 3.6. The project aims to decrease travel times, increase the frequency of the rail services and make it possible for travellers to reach more destinations in Gothenburg without having to change travel modes (Trafikverket, n.d.-b). The construction of three of the service tunnels was started in 2018 and 2019, and the project is planned to be finished in 2026.

In total, Västlänken consist of approximately 8 km of railway for commuter traffic (Trafikverket, n.d.-a), and approximately two thirds of Västlänken will be constructed in rock (Vänersborgs district court, case number M638-16, verdict 2018-01-31). In the east, Västlänken will connect to the Olskroken Project, which will convert the Olskroken railway junction into a grade separated junction (Trafikverket, n.d.-c). Olskroken is a railway node that connects Gothenburg to the western Sweden railway system.

The three service tunnels that are analysed in this thesis have the construction names ST206, ST207 and ST210 (Trafikverket, 2016b):

- Service tunnel 206 (ST206) is located at Korsvägen, and is blasted from Södra vägen towards Renströmsgatan, next to the Chalmers tunnel. The tunnel will be 506 meters long .
- Service tunnel 207 (ST207) is located at Korsvägen, and is blasted through Liseberget from Södra vägen. The tunnel will be 309 meters long.
- Service tunnel 210 (ST210) is located in Haga, and is blasted from Linnéplatsen towards Södra Viktoriagatan. The tunnel will be 910 meters long.

The cross-sectional area of each of the three service tunnels (ST206, ST207 and ST210) will be approximately 70 m^2 (Trafikverket, 2016b). Several existing rock facilities are located close to all three service tunnels (Trafikverket, 2016a), one of which is the Chalmers tunnel, that is located next to ST206.

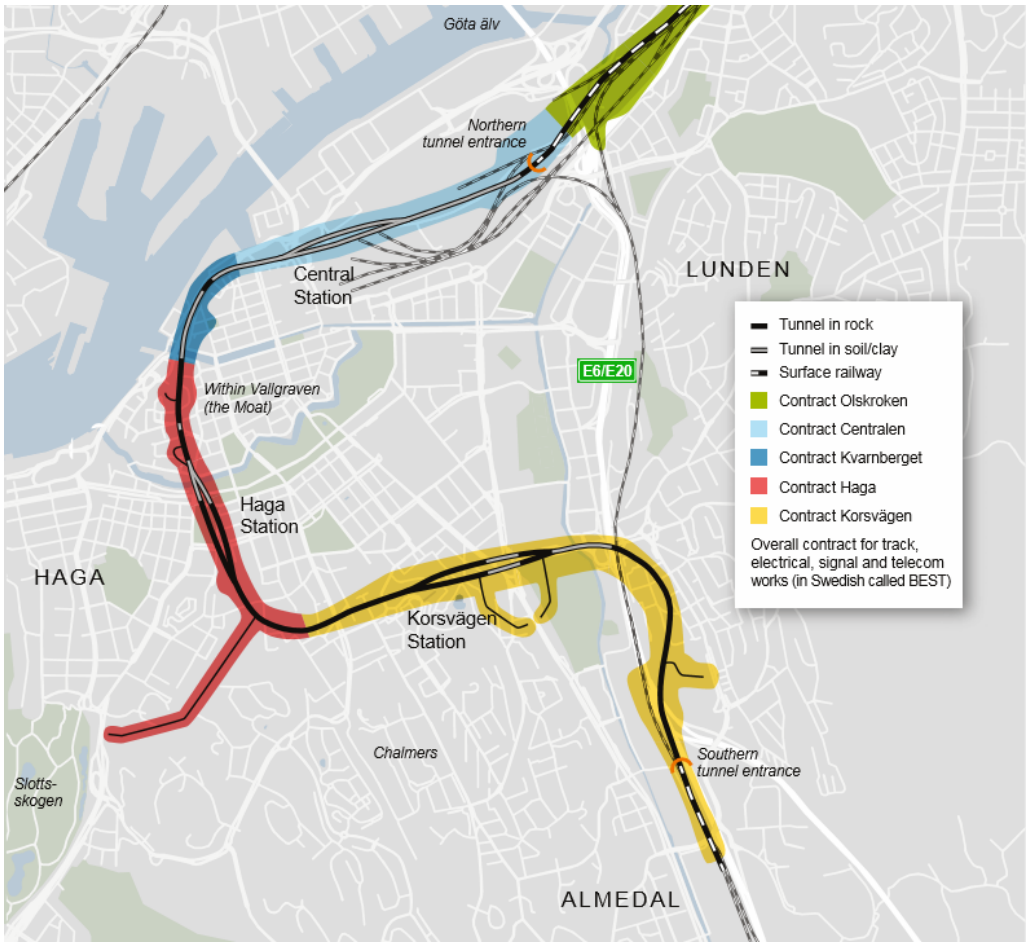

Figure 3.6: Location of the Västlänken railway tunnel and the service tunnels (Trafikverket, n.d.-c).

3.4.1 Geologic conditions

The bedrock mainly consist of a fine to medium grained gneiss, which is heavily foliated (Trafikverket, 2016c). Smaller elements of a less foliated, medium to coarse grained gneiss can be seen in the more heavily foliated gneiss. Dikes of pegmatite and a fine grained metabasite are also present in the rock mass. Further, in the area investigated for ST210, breccia and mylonite can be found.

The rock mass consist of three dominating fracture sets (Trafikverket, 2016c). The most dominating fracture set is located in the same direction as the foliation of the bedrock. Some of the common fracture fillings are quarts, chlorite and calcite. Swelling clays can be also found as fillings in fractures, which may cause additional stresses on the surrounding rock.

ST210 are located in a highland area with a lot of uncovered bedrock, and variations in ground levels between +20 and +76 (Trafikverket, 2016a). ST207 is going through Liseberget, on which the western parts of the amusement park Liseberg is located. ST206 is passing underneath Calanderska hospital and residential houses. Both ST206 and ST207 are located adjacent to Södra vägen, which is a soil covered

valley.

In a supporting document produced for the hydrogeological PM that was used in the permit application to the Land and Environmental Court (Trafikverket, 2016a), approximate locations of fracture zones were given:

- ST206 is expected to have a fracture zone almost parallel to the tunnel stretch.
- ST207 is not expected to cross any fracture zone. Two fracture zones are however expected on both sides of the tunnel.
- ST210 is expected to cross several smaller fracture zones, and a larger one just before the second turn of the tunnel, close to Konstepidemin.

3.4.2 Hydrogeologic conditions

The hydrogeologic conditions were characterised by core drilled and percussion boreholes, and hydrogeological tests and test pumpings performed in boreholes (Trafikverket, 2016a). 10 percussion boreholes and 6 core drilled boreholes were drilled to characterise the rock mass where the three service tunnels are located.

WLMs were performed in the core drilled boreholes in sections of three meters, the whole borehole length, and in half the borehole length (Trafikverket, 2016a). Three tests were performed for each section with the pressures 0.3 MPa, 0.5 MPa and 0.3 MPa above the groundwater pressure, and each test had the duration of 5 minutes. The evaluated core drilled boreholes for the three service tunnels considered can be seen in Table 3.6, where the boreholes denoted with *KK* are located over ST206 and ST207, and the boreholes denoted with *HK* are located over ST210. The measurement limit for these tests were set to be 1 liter per 5 minutes, which corresponds to an approximate hydraulic conductivity of $3{\cdot}10^{-8}$ m/s.

Table 3.6: Evaluated hydraulic transmissivity in core drilled boreholes through water loss measurements using one packer at 10 - 20 meter below rock surface (Trafikverket, 2016a).

Borehole	**Borehole length in rock [m]**	**Transmissivity [m^2/s]**	**Measured length [m]**
KK625KBH	100.8	$2.9{\cdot}10^{-6}$	90.8
KK626KBH	88.4	$9.3{\cdot}10^{-6}$	85.5
KK627KBH	76.8	$5.7{\cdot}10^{-5}$	76.7
HK628KBH	50.0	$4.9{\cdot}10^{-7}$	39.0
HK629KBH	73.0	$4.7{\cdot}10^{-5}$	70.3
HK630KBH	42.5	$1.3{\cdot}10^{-5}$	41.5

However, only approximately 37% of the tested sections in all the 28 boreholes evaluated were estimated to lie within the measurement limits of the equipment used (Trafikverket, 2016c). Because of this, complementary WLMs were performed with a measurement limit of 0.005 l/min to get a more accurate result of the sections with low permeability, see Table 3.7. The new WLMs were performed with one

pressure interval of 0.3 MPa over the groundwater pressure until stationary conditions prevailed and the variation in flow was below 5%, but at least during 10 minutes. Using the new equipment with higher measuring accuracy, approximately 77% of the tested sections in four boreholes gave results within the measurement limits. The calculated means of the hydraulic conductivity estimated using the four complementary WLMs can be seen in Table 3.8.

The groundwater levels are expected to mostly follow the topography (Trafikverket, 2016c). The distance between the ground level and groundwater level are however expected to increase as the ground level increases. The groundwater level can also be lower in areas where existing rock facilities are located.

Table 3.7: The complementary WLMs located near Korsvägen station and Haga station performed during 2015 (Internal working document). The hydraulic conductivity was calculated using Moye's formula.

Borehole	**Transmissivity [m^2/s]**	**Hydraulic conductivity [m/s]**	**Measured length [m]**
KK606KBH	$1.98{\cdot}10^{-6}$	$6.08{\cdot}10^{-8}$	32.5
HH636KBH	$6.63{\cdot}10^{-6}$	$9.60{\cdot}10^{-8}$	69.0

Table 3.8: The estimated means of the hydraulic conductivity [m/s] for the complementary WLMs located near Korsvägen and Haga station (Trafikverket, 2016c). The estimation is based on WLMs in three meter sections in core drilled boreholes.

Core drilled boreholes	$\mathbf{K}_a$	$\mathbf{K}_{median}$	$\mathbf{K}_{3D}$
HH636KBH	$9.6{\cdot}10^{-8}$	$3.5{\cdot}10^{-9}$	$1.6{\cdot}10^{-8}$
KK606KBH	$6.0{\cdot}10^{-8}$	$2.0{\cdot}10^{-9}$	$5.3{\cdot}10^{-9}$
All 4 boreholes	$2.3{\cdot}10^{-7}$	$1.0{\cdot}10^{-8}$	$3.3{\cdot}10^{-8}$

3.4.3 Inflow requirements

The following is a translation of the Environmental ruling from the Environmental Court for the Lerum utility tunnel (Vänersborgs district court, case number M638-16, verdict 2018-01-31), where the following is stated concerning the three service tunnels:

- *During construction, inflow of groundwater to the tunnel and rock facilities can not exceed the flows given in the table below, calculated as guideline values and monthly mean values. Inflow in open rock excavations are not included in the stated values.*
- *After construction, inflow of groundwater to the tunnel and rock facilities can not exceed the flows given in the table below. The values given are limiting values and annual mean values.*

Rock facilities in the following sections	***Inflow [l/min]***
Station Korsvägen West *460+660 - 461+000*	*50*
Station Korsvägen East and *concrete tunnel Mölndalsåns valley* *461+000 - 461+550*	*55*
Service tunnel Haga, 920 m	*40*

The inflow requirements for some of the different tunnel sections covers several rock facilities. For example, in Station Korsvägen West, service tunnel ST206 is included together with main tunnels and station areas, while in Station Korsvägen East and concrete tunnel Mölndalsåns valley, service tunnel ST207 is included together with main tunnels and station areas.

Detailed requirements are given to specified tunnel sections, where the inflow given in the environmental permit is distributed over the different tunnel sections and rock facilities located between measurement weirs. Based on the reports used to get the environmental permit, the inflow to the tunnel was estimated to be in the order of 2-8 l/min·100m (Trafikverket, 2016c). During construction, an inflow budget is produced in order to have continuous monitoring of the inflow to the different tunnel sections. The estimated inflow is compared to the actual inflow for shorter tunnel stretches, in order to ensure that the permitted inflow is not exceeded.

3.4.4 Grouting design

In this study, only the general grouting design will be used to evaluate the performance of the grouting in the service tunnels. Thus, the following section will only consider the general grouting design for Västlänken described in PM Typinjektering (*en: General grouting design*) (Trafikverket, 2016c). Adaptations in the grouting design are, among other, performed where the rock cover is less than 10 meters, in the tunnel openings, and for the first 20 meters from the tunnel opening.

The grouting will mainly be performed using cement based grouts, with silica sol and polyurethane based grouts as alternatives under certain conditions (Trafikverket, 2016c). Three grouting classes have been created, and the choice of grouting class is based on the inflow requirement and the hydraulic conductivity of the ungrouted rock mass (Trafikverket, 2016c). The choice between grouting class 1 and 2 are made through inflow from probe holes, more described below, and the groundwater head for the considered tunnel section. The value of the two parameters define which class to use, which is specified in PM Typinjektering (Trafikverket, 2016c).

The following is a description from PM Typinjektering, describing the three grouting classes that will be used during construction (Trafikverket, 2016c). The grouting process for each grouting class can be seen in Table 3.9.

- **Grouting class 1:** will be used in areas with moderately strict to less strict requirements on inflow and in areas with no large water-bearing zones. Grouting will be performed in one round using a cement based grout with complemen-

tary grouting when needed.

- **Grouting class 2:** will be used in areas with permeable rock mass and water-bearing zones with a risk of remaining large inflows. Grouting will be performed in two rounds using a cement based grout.
- **Grouting class 3:** will be used in areas with strict requirements on inflow, where a high final sealing is required. Generally, this means a high degree of sealing is required. To achieve this, the grouting will be performed in two rounds. In the second round, a non-cement based grout, silica sol, can be required.

Table 3.9: Grouting process for the three grouting classes in the general design for the Västlänken tunnels (Trafikverket, 2016c). Each grouting class is denoted IK. a is the vertical distance from the tip of the borehole to the theoretical tunnel contour, b is the horizontal distance between the tip of the boreholes, and c is the overlap of each fan. Complementary grouting is performed where the grouting did not reach the grouting overpressure of 10 minutes, or reached the maximum volume, or if the limit for WLM in control holes are exceeded.

Work process IK1	**Work process IK2**	**Work process IK3**
Grouting boreholes $\leq$*25m* b = *2.5m* $c \geq$ *6m*	*Grouting boreholes* $\leq$*25m* b = *2.5m* $c \geq$ *6m*	*Grouting boreholes* $\leq$*25m* b = *2.5m* $c \geq$ *6m*
Probe holes with WLMs	First round according to IK1 with no probe holes	First round according to IK1 with no probe holes
If $\geq$*2 probe holes exceed defined limits, IK2 used (2 rounds)*	Grouting holes drilled a = *4m*	Grouting holes drilled a = *4m*
Grouting holes drilled a = *6m*	Grouting round 2	Grouting round 2 (grout for fine apertures can be used)
Grouting round 1	Poss. additional grouting	Control holes with WLM Δp *1 MPa,* $\geq$*3 minutes*
Poss. additional grouting	Control holes can be used	Poss. additional grouting
Control holes can be used		

In tunnel ST207 and ST206, grouting class 3 is preliminary decided to be used along the tunnels (Internal documents, Trafikverket, 2016-09-14). The general grouting design for grouting class 3 in the service tunnels can be seen in Figure 3.7, and the profile of the general design in Figure A.4.

In order to achieve a continuously sealed rock mass, the penetration length of the grout has to at least has to be equal to the distance between the grouting holes (Trafikverket, 2016c). Further, the distance between the endpoint of the boreholes are set to be 2.5 meters in order to hit and grout the different fracture sets. Further, by setting the vertical distance from the tip of the borehole to the tunnel contour to be smaller in the second round, the probability of hitting different fracture orienta-

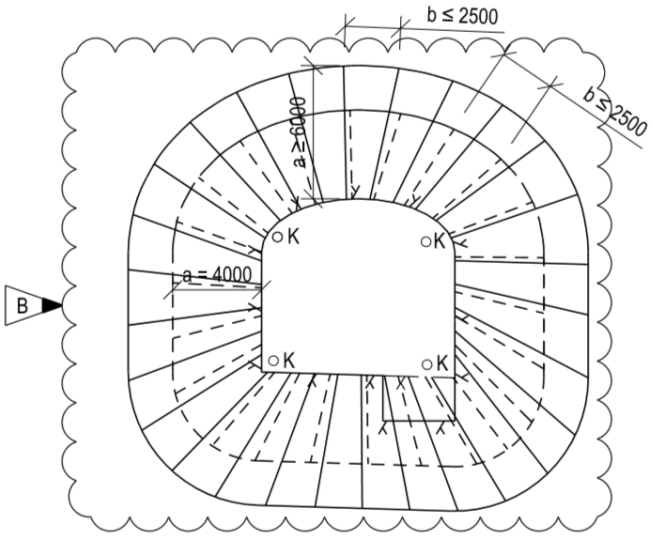

Figure 3.7: The grouting design of grouting class 3 for the service tunnels (Technical drawing E00-17-300-0000-013). The dotted lines are boreholes for the second round of grouting.

tions increase. The larger water-bearing zones can also be sealed in the first round when the larger vertical distance is used.

The stop criteria for the grouting is based on both a specified design time and a specified design pressure (Trafikverket, 2016c). The goal is to reach the grouting pressure as quickly as possible, and thereafter hold the pressure during the specified time. The following controls are performed in order to decide when to stop the grouting (translation from PM Typinjektering):

- Control of pressure and flow after 5 minutes
  - If the grouting overpressure is reached, the grouting will continue according to the stop criteria. For normal sealing, this means a grouting time of 15 minutes.
  - If the flow does not exceed 2 l/min during the 5 first minutes, the borehole can be denoted as a "zero-hole", and the grouting is discontinued.
  - If the grouting overpressure is not reached, a new control will be performed 10 minutes after the grouting began.
- Control of pressure after 10 minutes
  - If the grouting overpressure is reached, grouting will continue according to the stop criteria (15 minutes for normal sealing)
  - If the grouting overpressure has not been reached, this will be recorded and constitute a basis for decision of complementary grouting.
- Regardless the grouting time, the grouting will be stopped when a maximum volume of 400 liters have been injected into a single borehole. The boreholes in which the grouting has stopped because of the criteria on maximum volume

will be recorded and constitute a basis for the decision of complementary grouting in the same way as the boreholes that did not reach the grouting overpressure after 10 minutes.

An estimation of inflow for the general grouting design was performed for the different sealing categories and rock conditions evaluated with the complementary WLMs (Trafikverket, 2016c). In the evaluation, K_{3D} was used as a representative value for the hydraulic conductivity in the rock mass, the skin factor, ξ, was set to 3, the thickness of the grouted zone, t, was set to 6, and the hydraulic conductivity of the grouted rock mass, K_{gr}, was estimated for each sealing category. For the two boreholes located near the service tunnels considered in this study, the estimated K_{gr} ranged between approximately $1{\cdot}10^{-9}$ - $2{\cdot}10^{-8}$ dependent on the sealing category.

4

Methods

The following chapter describes how the data received from the tunnels was treated, and which methods were chosen to be used in the evaluation of the inflow to the tunnels considered in this thesis. Since the four tunneling projects uses different grouting designs, the method used in the evaluation of the hydraulic conductivities are slightly different depending on the design used. The tunnel stretches that are chosen to be evaluated in the analyses are sections with relatively "normally" fractured rock mass and for which inflow measurements has been performed.

Firstly, the method used to evaluate the hydraulic conductivity for the Chalmers and Lerum tunnel is described, which are followed by the methods used for the Göta tunnel and lastly the Västlänken service tunnels. Thereafter, the method used for calculating the inflow to the considered tunnel stretches is given, followed by a description of the sensitivity analyses performed.

4.1 Evaluation of hydraulic conductivity

In the evaluation of the hydraulic conductivity of the rock mass, the following general steps were used. However, the first and third step is slightly different for the four tunneling projects since different methods were used during grouting. A more detailed description of the methods used for the four tunneling projects are given in the following sections.

- The possible detection limit of the equipment used during the WLMs were found through the smallest reported flow in the data set, and all zero-reported measurements were replaced by the assumed measurement limit. Measurements performed in fracture zones were removed from the data set, as the hydraulic conductivity of the "normally" fractured bedrock was sought for. Further, the first ten meters of measurements in boreholes drilled from ground surface were removed as they were assumed to have a higher fracture frequency.
- The hydraulic conductivity was calculated using Equation 2.13, which is the modification of Moye's formula performed by A. Ylinen.
- The control holes that were assumed to represent the hydraulic conductivity of the grouted rock mass was chosen using the description of the grouting classes in the projects. Probe holes were assumed to represent the ungrouted rock mass.

- In order to see how well the data set fit a log-normal distribution, the empirical CDF was plotted against the log-normal CDF.
- The geometric mean and the 3D mean using Matheron's conjecture was calculated for the hydraulic conductivity in each fan and the whole considered tunnel stretch. These means were then plotted with the individual hydraulic conductivities in order to illustrate the scale dependence between the values.

4.1.1 Evaluation for the Chalmers and Lerum tunnel

To begin with, data exploration was conducted on the compiled water loss measurements in order to get an understanding of what possible detection limits there could have been on the equipment used in the tests. The water bearing capacity of the rock mass was reported to be zero for a quite large portion of the data, meaning that no water was able to enter as the test was performed. However, these measurements do not mean that all test sections where a zero value was measured had a hydraulic conductivity of zero, but that the equipment most probably did not detect the flows below a certain limit. Thus, the measurement accuracy had to be evaluated to see how detailed the flow meters used could have been. As no documentation was found on which equipment was used, a measurement limit was assumed for each tunnel based on the lowest measured flow in the tests. The smallest value measured for the Chalmers tunnel was found to be 1 l/min. Thus, the measurement limit was set to be 0.5 l/min in order to be slightly lower than the smallest measured value. This measurement limit approximately corresponds to $7.0 \cdot 10^{-9}$ m/s (depending on the test length of the evaluated borehole). Further, the smallest value measured for the Lerum tunnel was 0.1 l/min, and thus the measurement limit was set to be 0.05 l/min (which was also a requirement in the technical description (Bergab, 2002)).

If no measurement limit were to be assumed, the hydraulic conductivity of the rock mass could be underestimated as some of the measured zero-values might be higher than that. However, the assumed measurement limit might give a hydraulic conductivity of the rock mass that is higher than in reality, but the calculations will result in conservative values.

In older projects, there were generally no strict requirements on the detection limits of the equipment nor on the time the test had to be performed for to get accurate results (Personal communication, Thomas Wallroth, 2020-02-28). If the measurement is taken to early during a WLM, when stationary conditions has not yet occured, the measurement will most probably overestimate the transmissivity of the rock mass as the flow successively decrease during the test until it reaches stationary conditions (Internal document, Bergab, 2012-05-23). Today, the Swedish Standard SS-EN ISO 22282-3:2012 specifies the requirements of WLMs that is carried out as a part of a geotechnical investigation.

After the zero-values had been replaced by the assumed measurement limit, the hydraulic conductivity for each borehole was calculated using Equation 2.13, which is the modification of Moye's formula performed by A. Ylinen. Equation 2.13 is used because, as described in section 2.2, it gives more accurate results of the hydraulic conductivity when the test length is larger than 30 times the radius of the borehole.

When considering the boreholes used when performing the WLMs in the Chalmers tunnel, the test length ($\approx$ 19m) is 792 times larger than the radius of the borehole (0.024m). In the Lerum tunnel, the test length ($\approx$ 21m) is 703 times larger than the radius of the borehole (0.027m).

In the calculations, the probe holes were used to represent the hydraulic properties of the ungrouted rock mass, and the control holes were used to represent the grouted rock mass. However, the control holes that represent the final grouting result had to be identified. As have been described in Chapter 3, the Chalmers and Lerum tunnel used different grouting designs. For the Chalmers tunnel, control holes were only drilled in grouting class 3, in which split-spacing of the probe holes were performed. This means that probe holes were firstly drilled, followed by two grouting rounds with altering grouting boreholes, and lastly the drilling of control holes. Thus, the WLMs performed in probe holes before the first grouting round were used to evaluate the ungrouted rock mass, and the control holes performed after the last grouting round was used to evaluate the grouted rock mass.

For the Lerum tunnel, grouting class 2 consisted of either one or two grouting rounds, depending on if the WLMs were above or below 0.1 Lu. For grouting class 3, two grouting rounds were performed with WLMs in between. The WLMs performed when using grouting class 3 did therefore not show the final result of the hydraulic conductivity of the grouted rock mass, as an additional grouting round was performed after the measurements in control holes. Hence, the control holes used when performing grouting class 2 were only used in the evaluation of the hydraulic conductivity of the grouted rock mass. However, an additional grouting round could have been performed after the control holes were tested in grouting class 2 as well, as described in section 3.3.4. Therefore, two evaluations were performed: one using only the fans from IK2 having control holes with Lu<0.1 (as ideally an additional grouting round would have been performed if Lu>0.1), and one using all fans with control holes from IK2 (as some control holes most probably will have a higher water loss than 0.1 Lu). The upper and lower boundary are then achieved of the hydraulic conductivity of the grouted rock mass, with one case overestimating K_{gr}, and one case underestimating K_{gr}.

In order to see how well the measured data fits a log-normal distribution, the empirical cumulative distribution function (CDF) was plotted against the log-normal CDF constructed with the mean and standard deviation according to measured data. The empirical CDF is only dependent on the sampled values, while the log-normal CDF is defined according to its distribution. The empirical CDF is generated by cumulatively counting the fraction of sampled values. As an example: if the sampled values are 2, 6, 13, the cumulative function is: $\mathrm{ECDF}(\{2, 6, 13\}) = \{\frac{1}{3}, \frac{2}{3}, \frac{3}{3}\}$.

The geometric mean and the 3D mean using Matheron's conejcture was then calculated for each fan and for the chosen tunnel stretch using Equation 2.8 and Equation 2.9. Both the 3D and the geometric mean was calculated for the hydraulic conductivity as a grouting fan has boreholes with different directions, and it is hard to know in advance which mean will fit the data best. The calculated inflow achieved with the two different means was later compared with the actual inflow in order to see which fit the results best.

Figure 4.1 illustrates the three scales for which the two means were calculated for. The smallest scale represents the borehole through which the WLMs are performed, the mid-scale represents each grouting fan and the largest scale represents the evaluated tunnel stretch. The calculated geometrical mean and 3D mean for each fan and section was then plotted together with each individual hydraulic conductivity calculated from the tested boreholes to illustrate the scale dependence.

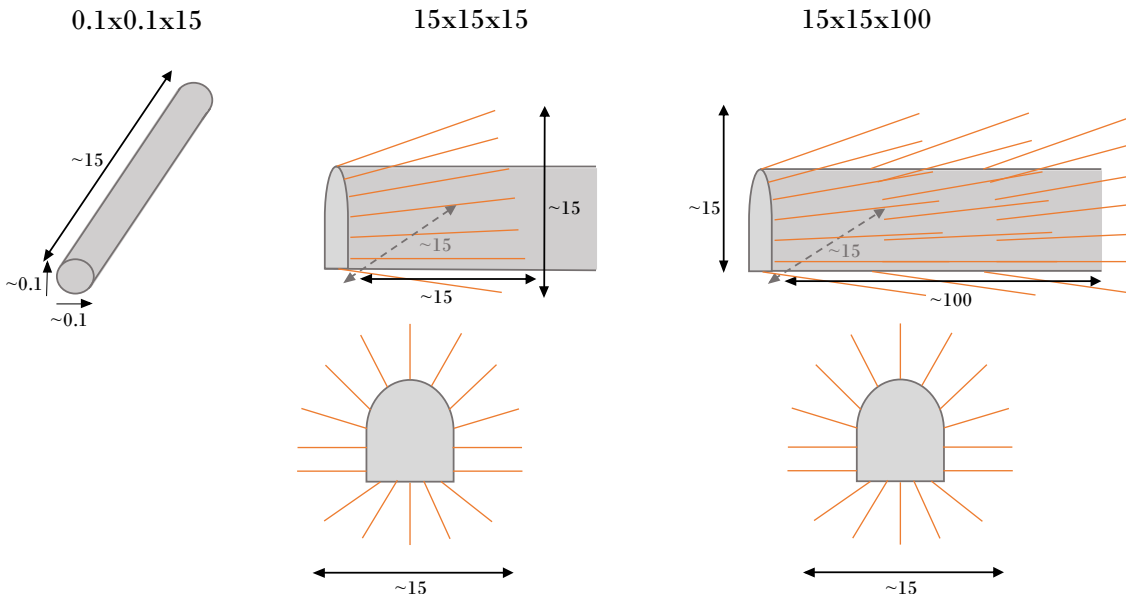

Figure 4.1: The different scales that the geometric mean and the mean using Matherons conjecture were calculated for, based on the length of the considered tunnel stretch in the Chalmers tunnel.

4.1.2 Evaluation for the Göta tunnel

In contrary to the Lerum and the Chalmers tunnel, the evaluation of the hydraulic conductivity of the rock mass for the Göta tunnel were based on WLMs performed in core drilled boreholes that were tested during the preliminary investigations. This is since the GIN method was used during the construction, which is based on an active stop criteria (that considers the grouting pressure and volume). Thus no continuous WLMs were performed. The estimated hydraulic conductivity will therefore not be as precise for the considered tunnel stretch as for the Chalmers and Lerum tunnel.

Firstly, the data from the WLMs performed in the core drilled boreholes located closest to the considered tunnel section were compiled, and the possible detection limit of the measurements were estimated to be 0.05 l/min. As two of the longer core drilled boreholes (180 and 292 meters long) had a large portion of measured zero-values, the detection limit was adjusted slightly from the lowest measured Lugeon value in order to get a median value that were closer to the one estimated in the preliminary investigations (see Table 3.2). Otherwise, the large portion of zero values in these two longer boreholes made the geometric mean of the hydraulic conductivity unreasonably low. The values measured in detected fracture zones

were then removed from the data set, as the hydraulic conductivity of the rock domain with "normally" fractured rock was sought for. Further, if the borehole was drilled from the land surface, the first ten drilled meters were removed from the data set as these were assumed to be more highly fractured and not representing the conditions at tunnel depth.

In the preliminary investigations, WLMs were performed using both 0.2 and 0.4 MPa overpressure. The measurements achieved when using 0.4 MPa were chosen to be used in the further calculations. This since the received flow during the test with the higher overpressure will be larger, and it is thus more likely to lie within the interval of the detection limit for the flow meter, resulting in more stable results.

The adjusted data set were then used to calculate the hydraulic conductivity of the rock mass using Equation 2.13. Using the same reasoning as in section 4.1.1, the ratio between the borehole radius (0.028m) and the test length ($\approx$ 3m) is 107, indicating that Ylinen's equation will produce more accurate results. The geometric mean and the 3D mean using Matheron's conjecture was thereafter calculated for the hydraulic conductivity. In order to see how well the measured data fit a log-normal distribution, the log-normal CDF was plotted together with the empirical CDF of the data set, as described in section 4.1.1.

Since the GIN-method was used during grouting of the Göta tunnel, no WLMs from control holes in the grouted rock mass were found when collecting the data needed for the evaluation of the rock mass. Thus, no information on the hydraulic conductivity of the grouted rock mass was given. The evaluation of the grouting design for the Göta tunnel was therefore based on finding an interval of K_{gr} using data on measured inflow.

4.1.3 Evaluation for the Västlänken service tunnels

Since Västlänken is an ongoing project, there is not much data that is published in reports available to the general public. The data sets used in the analyses in this thesis have thus not passed through a final review. However, the data sets have passed through internal controls, and can therefore be seen as trustworthy. Since the data is not available to the general public, the original data sets will not be referenced to in this thesis.

As for the Göta tunnel, core drilled boreholes performed during the preliminary investigations were used to estimate the hydraulic conductivity of the ungrouted rock mass. One of the complementary core drilled boreholes (KK606KBH) were drilled close to the two service tunnels located at Korsvägen (ST206 and ST207), see Table 3.7. Hence, this borehole was assumed to represent the hydrogeologic conditions of the ungrouted rock mass for ST207 and ST206. The WLMs were performed in 3-meter sections. The measurement accuracy of the new equipment used in the WLMs was given to be 0.005 l/min in the general grouting design (Trafikverket, 2016c), resulting in more accurate results of the less fractured rock mass. Thus, all measurements reported to be below 0.005 l/min was replaced by this measurement limit.

The complementary core drilled borehole performed to evaluate the hydrogeologic conditions in Haga was however not assumed to be representative for ST210, as the rock mass where ST210 is to be constructed is expected to have a higher fracture frequency. Thus, WLMs performed in two core drilled boreholes (HK629KBH and HK628KBH) drilled along the tunnel stretch of ST210 were used, see Table 3.6. These tests were not performed with the same measurement accuracy, and according to notes taken during the tests in one of the boreholes, some difficulties occured during the tests performed in 3-meter sections. Thus, only the WLMs performed in the entire borehole were used. These tests were seen as more representative as the test lengths were longer, and in combination with a higher overpressure pressure the flow have a larger probability of reaching the measurement limit and hence give more reliable results. It should however be noted that in the tests using the whole borehole length, it is the fracture zones discrete permeability that is measured and averaged along the borehole length. Hence, the resulting calculated mean will give an indication of the upper limit of the hydraulic conductivity in the "normally" fractured rock mass.

Out of the three measurements performed using the entire borehole length in HK629-KBH and HK628KBH, the first and second test (with 0.3 respective 0.5 MPa over-pressure) was chosen to be used in the evaluation, as it was assumed that some water might return to the borehole after the 0.5 MPa test, influencing the third and last test (with 0.3 MPa overpressure). Thus, four WLMs performed in the whole core drilled boreholes were used to evaluate the hydraulic conductivity of the un-grouted rock mass for ST210; two WLMs from HK628KBH and two WLMs from HK629KBH.

The hydraulic conductivity of the grouted rock mass was determined through data sets of WLMs from control holes performed in grouting class 3. The measurement accuracy for the control holes in ST206 and ST207 was given in internal documents, were a flow of 0.2 l/min was seen as reliable for the equipment used. Thus, all measurements from these two tunnels reported to be lower than 0.2 l/min were replaced by this value. The WLMs performed in the first sections close to the tunnel opening was removed from the data set as those have a small rock cover and could be affected by the tunnel opening. Measurements that had a comment of having surface leakages were also removed.

For the WLMs performed in control holes in ST210, no information was found on the possible detection limit of the equipment. And since no measurements were found to be reported as zero, no measurement limit was set. Thus, the resulting calculated mean of the hydraulic conductivity might be underestimating the hydraulic conductivity of the grouted rock mass, if some of the measurements are below the measurement limit corresponding to reliable measurements for the equipment used.

In the data set received with control holes from the three service tunnels, control holes were drilled both on the outside and the inside of the tunnel contour during a test period in order to evaluate the result of the two methods. The control holes drilled on the outside of the tunnel contour in the grouted rock mass was chosen to be used in this thesis, based on the conclusion of a report evaluating the result of the two methods (Internal document, Trafikverket, 2019-10-31).

As for the other tunnels, Equation 2.13 was used to calculate the hydraulic conductivity, from which the geometric mean and the 3D mean using Matheron's conjecture then was calculated for the above stated scales. Ylinen's equation is a good fit for these performed tests as well, since all tests have a test length that is larger than 30 times the radius of the borehole. For example, the shortest length of a control used in the data set is 11 meters, and have a radius of 0.032 meters. Thus, the test length is approximately 340 times longer than the radius of the borehole. Thereafter, the log-normal CDF of the measured data was plotted against the empirical CDF to see how well the data fit a log-normal distribution. However, as only four measurements were used in the evaluation of the ungrouted rock mass for ST210, no CDF:s were produced for these values.

4.2 Method used to evaluate the inflow

One of the main goals of the calculations performed in this thesis is to evaluate how well the inflow equation generally manages to estimate an inflow that coincides with the actual measured inflows in the tunnels. However, the execution of the grouting might not always be according to the design, since, among other, changes might have to be made when the conditions change.

After the representative hydraulic conductivity had been calculated for the respective tunnel, the inflow was estimated using Equation 2.22. The inflow was calculated with both the geometric and the 3D mean of the hydraulic conductivity to see which was the most representative value for the rock mass by comparing the calculated inflow to the actual measured inflow. In this calculation, the selected values of the parameters needed in the equation were chosen as follows:

- The groundwater pressure from the middle of the tunnel to the groundwater table, H, was estimated from technical drawings and recorded groundwater data. As the groundwater table often fluctuates, an approximate mean was chosen. When the chosen tunnel section was quite long, it was divided into smaller sections with several estimated values of H.
- The grouted thickness, t, was chosen to be the mean of the distance between the tunnel and the tip of the grouting boreholes in the tunnel roof and in the tunnel invert given in the grouting design.
- The skin factor, ξ was chosen according to the choice made in the estimations of the inflow from the technical documents. For example, a value of 5 corresponds to rock mass with very low fracture frequency, while a value of 3 corresponds to normally fractured rock.
- The radius of the tunnel, r_t, was calculated with Equation 2.20, using the tunnel area given in the technical documents. The tunnel radius will however vary slightly as the tunnel is blasted.

As can be seen in the grouting designs for all tunnels considered in this study, a larger thickness of the grouted rock mass was used in the bottom of the tunnel. When the tunnel is constructed, the rock is more heavily blasted in the bottom of

the tunnel, as described in section 2.3, which will create a larger damage zone in the tunnel invert. This, in combination with the larger depth below the groundwater table, will result in larger groundwater flow through the tunnel floor. Thus, a larger thickness of the grouted zone is needed in the tunnel invert to decrease the inflow.

Moreover, the thickness of the grouted zone is not constant as the penetration length of the grout is larger in the wider apertures than in the smaller ones. The thickness may also be smaller than the theoretical thickness if some fractures are not fully grouted. Fractures may not be fully grouted if the grouting boreholes do not cut the fractures along the fracture planes, meaning that there is no hydraulic contact. It can also be the result if fractures are partially filled with clay which will prohibit the penetration of grout (Petro Bloc AB, 1999). Further, the thickness will vary depending on the amount of boreholes that are used during grouting, see Figure 4.2. When using more boreholes, the grout will get more evenly distributed as each borehole will create smaller but closer "cylinders" of grouted rock mass, while less boreholes will lead to more defined "cylinders" of grouted rock mass that vary in penetration length.

In order to take into account the possible differences in all parameters needed in the evaluation of the inflow and their possible impact on the result, sensitivity analyses were performed. This was achieved by keeping all but one parameter constant, and changing the value to evaluate its influence on the inflow to the tunnel. A sealing factor was calculated for each tunnel by dividing the median hydraulic conductivity of the ungrouted rock mass with the median hydraulic conductivity of the grouted rock mass.

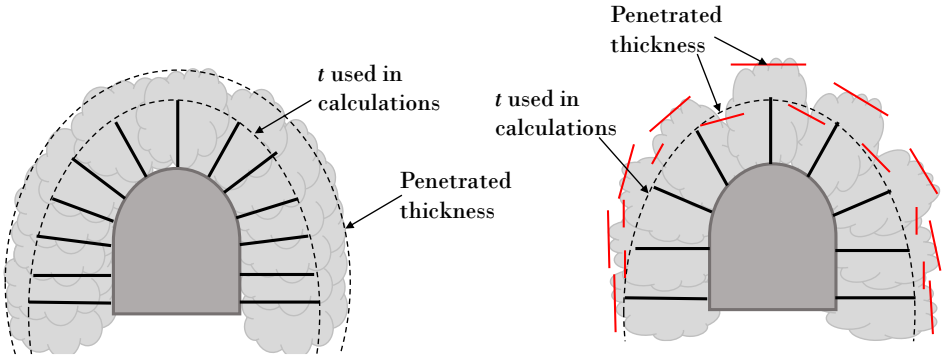

Figure 4.2: Illustration of how the penetration of grout and the thickness of the grouted zone can vary with number of grouting holes. The figure is adapted from grouting class 1 in the Chalmers tunnel.

4.2.1 Correction of inflow for two symmetrical tunnels

In two of the study objects, the Chalmers and Göta tunnel, two symmetrical tunnel tubes are located next to each other. The inflow equation used in the calculations assumes that groundwater can enter a tunnel from all sides. However, the rock mass located between the two tunnels will not be able to transport as much water as the

surrounding rock mass since water-bearing fractures most likely are disrupted by the tunnel tubes. As the two tunnels will use the same rock volume in the calculations, the inflowing water from the pillar between the tunnels will be counted twice. Thus, the calculated inflow may be overestimated.

The amount of flow that will move to each symmetrical tunnel tube will most likely depend on the amount of rock mass that is located between the tunnel tubes. A factor of 0.5 could then be applied on the estimated inflow if the tunnels are located next to each other with no wall in between, and 1.0 if the tunnels are independent of each other. Based on this, an approximate correction factor that will account for the symmetry of two tunnels was calculated through a geometric rough estimate. By using the geometry of the tunnels and the distance under the groundwater level, an area of the circular sector that might not contribute to the inflow was estimated. This was then divided by an area calculated through an approximated radius of influence ending to the groundwater table, resulting in a factor between 0.5 and 1.0. However, since the calculations are based on approximations, the correction factor can only be viewed as a qualified guess.

Thus, in order to take into account the effect of the symmetry of the tunnel tubes for the Chalmers tunnel, a factor of 0.65 could be applied on the inflow based on its geometry. Consequently, a factor of 1.30 could be applied to get the total inflow to both tunnel tubes, if the inflow to both tunnels are assumed to be the same. When performing the calculation using the geometry of the Göta tunnel, the estimated correction factor became 0.7.

An other way to try to take into account the effect of the symmetry of two tunnel tubes located close to each other is illustrated in Figure 4.3. Here, an approximate radius is calculated through Equation 4.1 taking into account the area of both tunnel tubes. The new radius is then used in the calculation of the inflow, resulting in the inflow that would occur to both tunnel tubes.

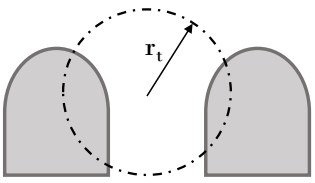

Figure 4.3: An approximate radius calculated through the area of both tunnel tubes.

$$r_t = \sqrt{\frac{A_t + A_t}{\pi}} \tag{4.1}$$

5

Results

In the following chapter, the results from the calculations performed on the studied tunnel stretches are presented. The results based on the three already constructed tunneling projects are presented first, followed by the three service tunnels in Västlänken.

As several of the parameters used in the evaluation are based on assumptions, two significant figures are given in the results. This to see the variation in the results.

5.1 Chalmers tunnel

The tunnel stretch considered for the Chalmers tunnel is located between section 7/285 and 7/372 in the southern tunnel tube, and between section 5/288 and 5/392 in the northern tunnel tube.

5.1.1 Evaluation of hydraulic conductivity

Figure 5.1 illustrates the empirical CDF and the log-normal CDF for the probe and control holes for the considered tunnel stretches in the Chalmers tunnel. From these graphs it can be seen that the hydraulic conductivities were reasonably log-normal distributed, as the empirical and log-normal CDF followed each other quite well. Since only 45 measurement values could be used in the evaluation of the control holes, the empirical CDF became quite edgy and not as smooth as the graph for the probe holes. The straight line that can be seen in the beginning of both graphs was a result of the defined measurement limit that is replacing all values that are reported as zero, as described in section 4.1.1. The straight line shifts slightly as a result of the difference in borehole lengths used in the calculations. If the zero values were removed from the data set, the empirical distribution get a better fit to the log-normal CDF, which can be seen in Figure 5.1. However, when the zero-values are removed from the data set, the distribution is not an as good representation of the hydraulic conditions of the rock mass.

The scale dependence between the means calculated for the two scales and the individual hydraulic conductivities calculated from each borehole can be seen in Figure 5.2. As the scale increases, the variation in hydraulic conductivity decreases. It can also be seen that there were a slight difference between the values calculated with the geometric mean and the 3D mean using Matheron's conjecture.

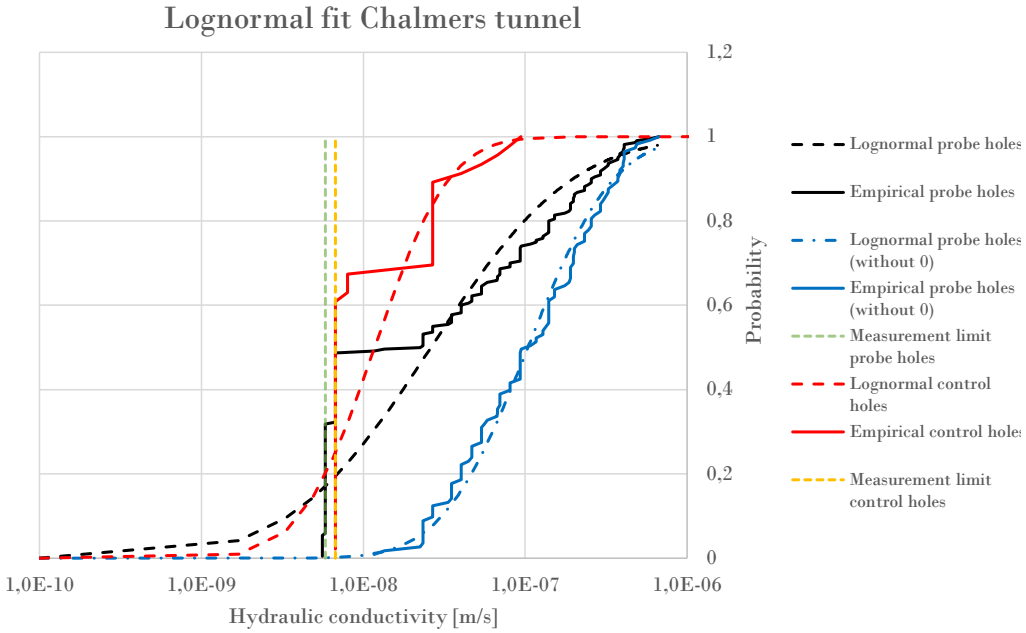

Figure 5.1: The log-normal and empirical CDF for the probe and control holes in the considered tunnel stretches in the Chalmers tunnel. 220 measured values were used in the evaluation of the probe holes, where 113 values were non-zero, and 46 measurement values were used in the evaluation of the control holes, where 14 values were non-zero.

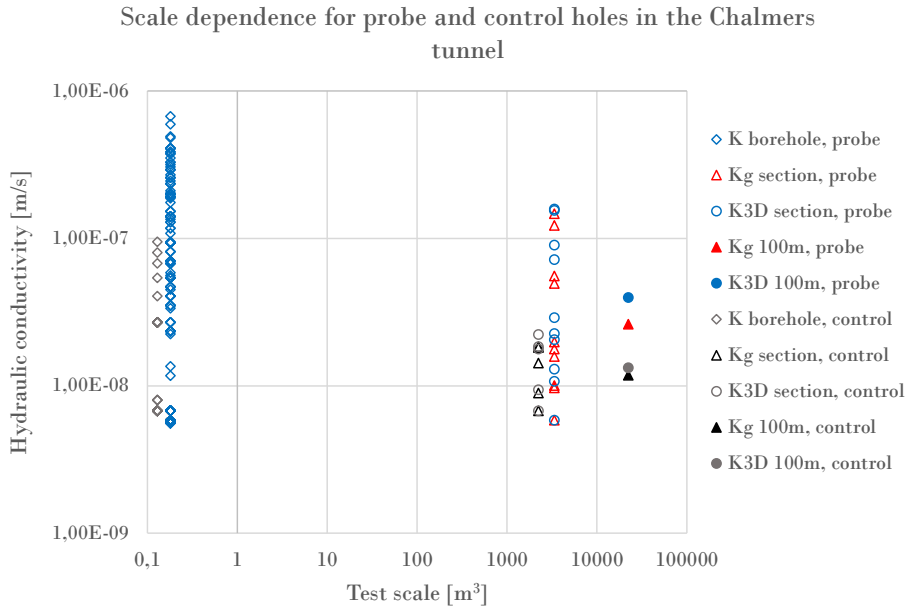

Figure 5.2: The scale dependence between the different means for the Chalmers tunnel. The data consists of 220 measured values in probe holes, 10 sections of grouting fans and the tunnel stretch of approximately 100 meters. The means calculated for the control holes per section is slightly shifted on the x-axis.

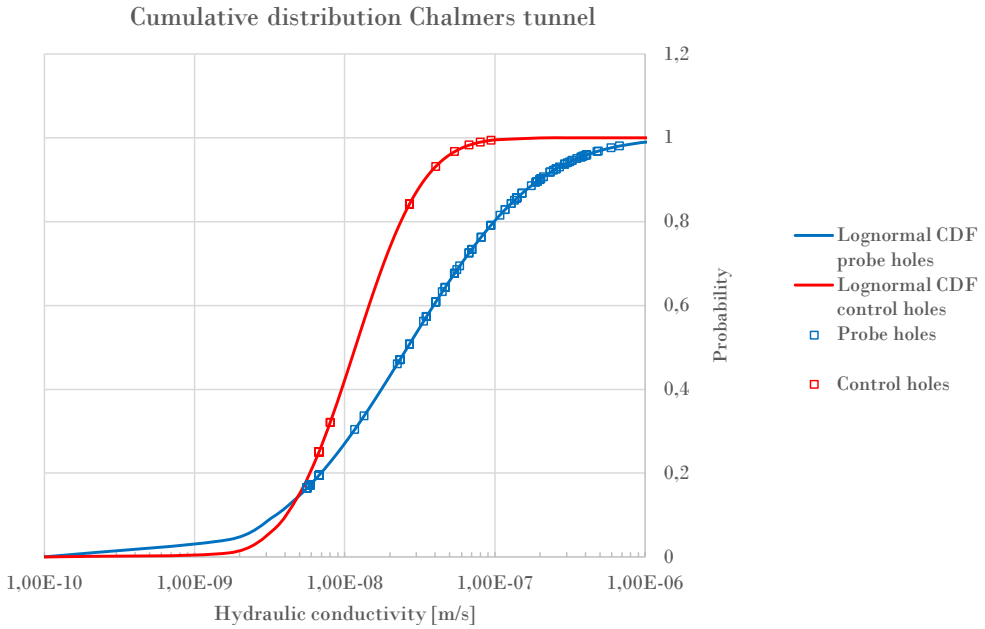

Figure 5.3: Cumulative distributions of the hydraulic conductivity for the two considered stretches in the Chalmers tunnel. The lines represent the calculated log-normal CDF, while the points are the calculated values of the hydraulic conductivity from water loss measurements. The probe holes have 220 measurement points, while the control holes have 46 measurement points.

The cumulative distribution illustrates the probability of a measured value to be equal to or lower than a certain value. It is constructed with a log-normal CDF with the mean and standard deviation according to the measured data. As can be seen in Figure 5.3, illustrating the calculated hydraulic conductivities for both tunnel stretches, the control holes had a hydraulic conductivity that was smaller than the hydraulic conductivity for the probe holes. Thus, the grouting caused a decrease in groundwater flow through the rock mass. The cumulative distribution illustrating the sealing effect for the southern and northern tunnel separately can be seen in Figure B.1. Here, it can be seen that the southern tunnel received a larger sealing effect than the northern tunnel.

The median hydraulic conductivity for the ungrouted rock mass was $2.3 \cdot 10^{-8}$ m/s, while the median for the grouted rock mass was $6.7 \cdot 10^{-9}$ m/s. In Figure 5.3, it can be seen that a large portion of the hydraulic conductivity of the ungrouted rock mass lie in the range of 10^{-8} to 10^{-7}. Further, a large portion of the hydraulic conductivity of the grouted rock mass were in the range of 10^{-9} to 10^{-8} m/s. When considering the hydraulic conductivities for both tunnel tubes, the sealing factor $\frac{K}{K_{gr}}$ based on median values was calculated to be 3.4. Hence, the water-bearing capacity of the rock mass decreased with approximately 3.4 times as a result of the grouting.

5.1.2 Evaluation of inflow to the considered tunnel sections

The estimated groundwater pressures for the tunnel stretches considered are given in Table B.1, which were ranging between 15 and 21 meters. A mean value is made for the considered tunnel stretch in each tunnel tube, which were then used in the calculations of the inflow (see Table 5.3).

The estimation of the inflow can be seen in Table 5.1. The inflow was calculated using the geometric mean and the 3D mean for the considered tunnel stretch in the southern respectively the northern tunnel tube, and the selected best fit values of the input parameters in Table 5.3. Table 5.2 consists of the measured inflows performed during and after the construction of the tunnel. Since it is not known where the tunnel front was located during the measurements performed in the construction phase, it is hard to know how representative the measurements are. Thus, more confidence is given to the measurements performed after the construction was finished. When comparing Table 5.1 and Table 5.2, it can be seen that the geometric mean gave calculated inflows that were closer to the actual inflow to the tunnel stretches in the Chalmers tunnel. Therefore, the geometric mean was used in the further evaluation.

Table 5.1: Calculated means for the tunnel stretch studied in the Chalmers tunnel, and the corresponding calculated inflow.

Chalmers tunnel	**K_g Probe**	**K_g Control**	**K_{3D} Probe**	**K_{3D} Control**
Southern	$5.3 \cdot 10^{-8}$	$9.6 \cdot 10^{-9}$	$1.4 \cdot 10^{-7}$	$1.0 \cdot 10^{-8}$
Inflow	*3.5 l/min·100m*		*4.4 l/min·100m*	
Northern	$1.8 \cdot 10^{-8}$	$1.7 \cdot 10^{-8}$	$3.6 \cdot 10^{-8}$	$1.9 \cdot 10^{-8}$
Inflow	*2.0 l/min·100m*		*2.7 l/min·100m*	

Table 5.2: Measured inflow (l/min·100m) to the considered tunnel stretch in the Chalmers tunnel after the construction of the tunnel (2007) and during construction (2001) (Internal documents). The measured inflows are then added to represent the inflow to both tunnel tubes.

Measured inflow	**Southern tube**	**Northern tube**	**Both tubes**
2007-07-30	2.4	1.4	3.8
2007-08-02	2.3	2.1	4.4
2001, week 12	1.5	1.5	2.9
2001, week 15	1.6	1.2	2.8
2001, week 20	1.4	0.9	2.3
2001, week 21	1.1	1.5	2.5
2001, week 22	1.6	1.6	3.2
2001, week 23	1.0	1.6	2.6

Table 5.3: The selected values for the input parameters used when estimating the inflow that are seen as the best fit for the prevailing conditions for the considered tunnel stretches in the Chalmers tunnel.

Parameter	Southern tunnel	Northern tunnel
K	$5.3 \cdot 10^{-8}$ m/s	$1.8 \cdot 10^{-8}$ m/s
K_{gr}	$9.6 \cdot 10^{-9}$ m/s	$1.7 \cdot 10^{-8}$ m/s
H	17 m	19 m
t	4.5 m	4.5 m
r_t	3.5 m	3.5 m
Skin factor	4.0	4.0

5.1.3 Sensitivity analysis on the estimated inflow

In order to take into account the effect of the symmetry of the two tunnel tubes, a correction factor of 0.65 was calculated according to the method described in section 4.2.1. The results from the sensitivity analysis performed on the correction factor, see Table 5.4, can be compared with the measured inflows in Table 5.2. Further, the radius of a circular tunnel that is equal to both tunnel areas was calculated, as illustrated in Figure 4.3, resulting in an approximate tunnel radius of 4.9 meters. By using the selected best fit values of the input parameters and changing the radius of the tunnel to 4.9 meters, a new inflow was calculated, which can be seen in the last two rows of Table 5.4.

Table 5.4: The corrected inflow (l/min·100m) to the considered tunnel stretches in the Chalmers tunnel taking into account the effect of the symmetry of the two tunnel tubes. The inflow written in italic corresponds to the calculated correction factor. The two last rows are the corrected inflow into one tunnel using an approximate radius of 4.9 calculated using both tunnel areas.

Inflow	Southern tunnel	Northern tunnel	Both tubes
Inflow K_g	3.5	2.0	5.4
Corrected inflow (0.5)	1.7	1.0	2.7
Corrected inflow (0.6)	2.1	1.2	3.2
Corrected inflow (0.65)	*2.2*	*1.3*	*3.5*
Corrected inflow (0.7)	2.4	1.4	3.8
Corrected inflow (0.8)	2.8	1.6	4.3
Corrected inflow using K_g and r_t=4.9 m	-	-	**2.6**
Corrected inflow using K_{3D} and r_t=4.9 m	-	-	**3.7**

The sensitivity analysis performed on the input parameters for the inflow equation can be seen in Figure 5.4, and in Appendix B, Figure B.2a to Figure B.2e. From these analyses, it can be seen that K_g had the highest influence on the calculated inflow, followed by K_{gr} and the groundwater head. Since the ratio between K_g and K_{gr} is 1.04 for the northern tunnel, the effect of the input parameters that are

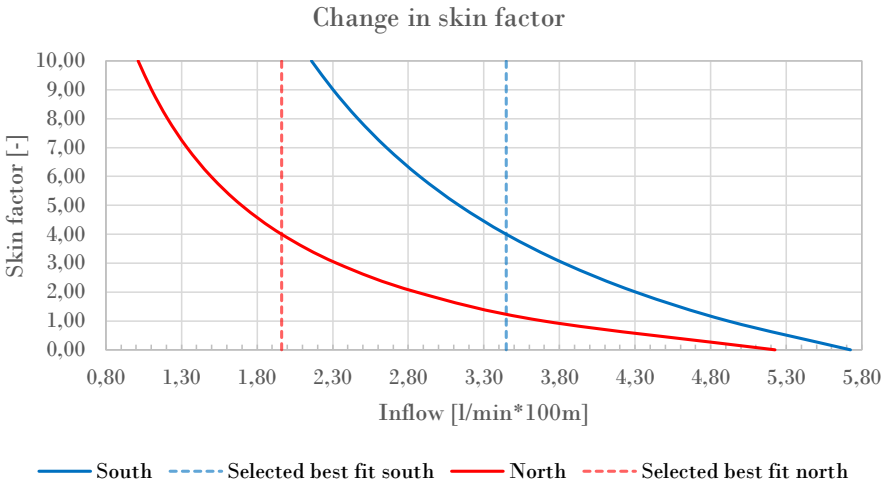

Figure 5.4: Sensitivity analysis of the skin factor for the Chalmers tunnel.

multiplied with this ratio in the denominator, t and r_t, will be very small, see Figure B.2d and Figure B.2e. For the southern tunnel, the ratio between K_g and K_{gr} is 5.5, and a larger variation in inflow can be seen. The choice of skin factor was also having a quite large effect on the calculated inflow, see Figure 5.4. When looking at the interval of 2-5 in skin factor, which is mostly used for the bedrock in Sweden, the change in inflow was approximately 1.2 l/min·100m.

5.2 Lerum tunnel

The tunnel stretch considered for the Lerum tunnel is located between section 3/543 and 5/290.

5.2.1 Evaluation of hydraulic conductivity

As was described in section 4.1.1, a division was made between the control holes used in the evaluation of the inflow. The upper boundary of the hydraulic conductivity of the grouted rock mass was represented by all control holes used in the sections where grouting class 2 (IK2) were used. Further, the lower boundary of the hydraulic conductivity of the grouted rock mass was represented by the control holes used in the sections where IK2 were used, and whose water-loss was less than 0.1 Lu in all control holes in each grouting fan. Thus, two cases are presented in the evaluation of the inflow; the actual conditions will lie somewhere in between these.

Figure 5.5 illustrates the empirical CDF and the log-normal CDF for the probe and control holes for the considered tunnel stretch in the Lerum tunnel. No clear straight line can be seen in the beginning of the graphs as a larger percentage of the values are non-zero than for the Chalmers tunnel. However, in the case where the control holes of Lu<0.1 were used, the low hydraulic conductivity creates a steep inclination of the graph. For this data set, IK2 Lu<0.1, the largest hydraulic conductivity was $1.7 \cdot 10^{-8}$ m/s.

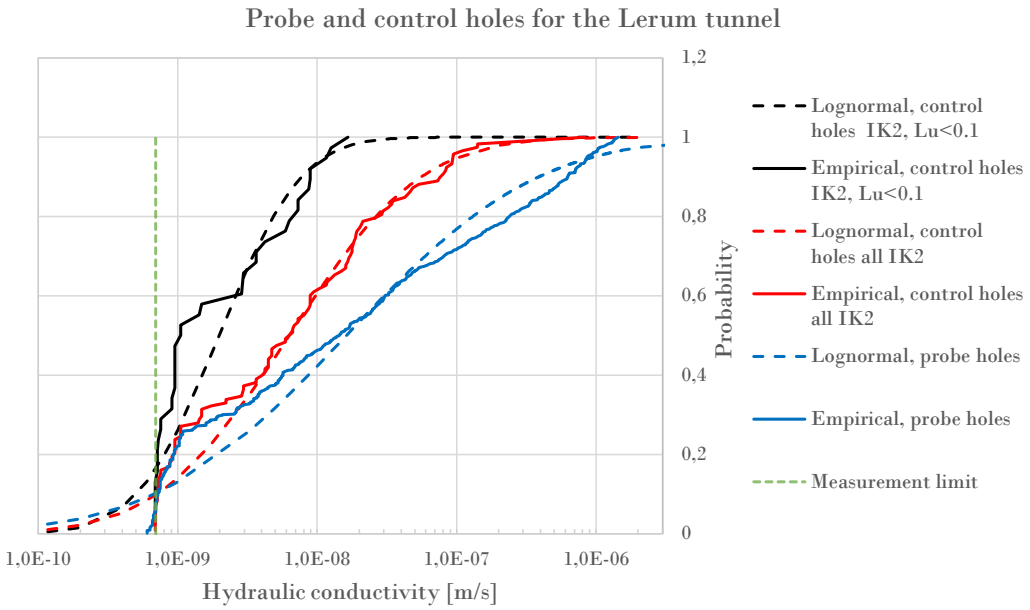

Figure 5.5: The log-normal and empirical CDF for the probe and control holes for the considered tunnel stretch in the Lerum tunnel. 639 measured values were used in the evaluation for the probe holes, where 473 values were non-zero. 38 measured values were used in the evaluation of the control holes of grouting class IK2 where Lu<0.1, where 19 values were non-zero. 118 measured values were used in the evaluation for all the control holes of grouting class IK2, where 84 values were non-zero.

The scale dependence between the individual hydraulic conductivities and the two different scales with mean values can be seen in Figure 5.6 and Figure 5.7. Since each fan had around seven boreholes, and 119 sections of fans with probe holes were used, the amount of mean values that represents the different sections were large and covers almost the same interval of hydraulic conductivities as the individual boreholes. Further, since the majority of the grouting fans consist of only 7 boreholes, a large spread is seen between the different means calculated for each grouting fan.

The cumulative distribution of the hydraulic conductivity can be seen in Figure 5.8. The lines represent the calculated log-normal CDF, while the points are the calculated values of the hydraulic conductivity from water loss measurements. In the graph, it can be seen that the log-normal CDF for the control holes where only the fans where Lu<0.1 were used had the lowest hydraulic conductivities, followed by the control holes where all fans of IK2 were used and lastly the probe holes. It can also be seen that the probe holes had a large variety in hydraulic conductivity, with measurements that cover the log-normal CDF almost evenly. It can also be seen that a large portion of the hydraulic conductivity for the ungrouted rock mass lie below $1.0 \cdot 10^{-7}$ m/s.

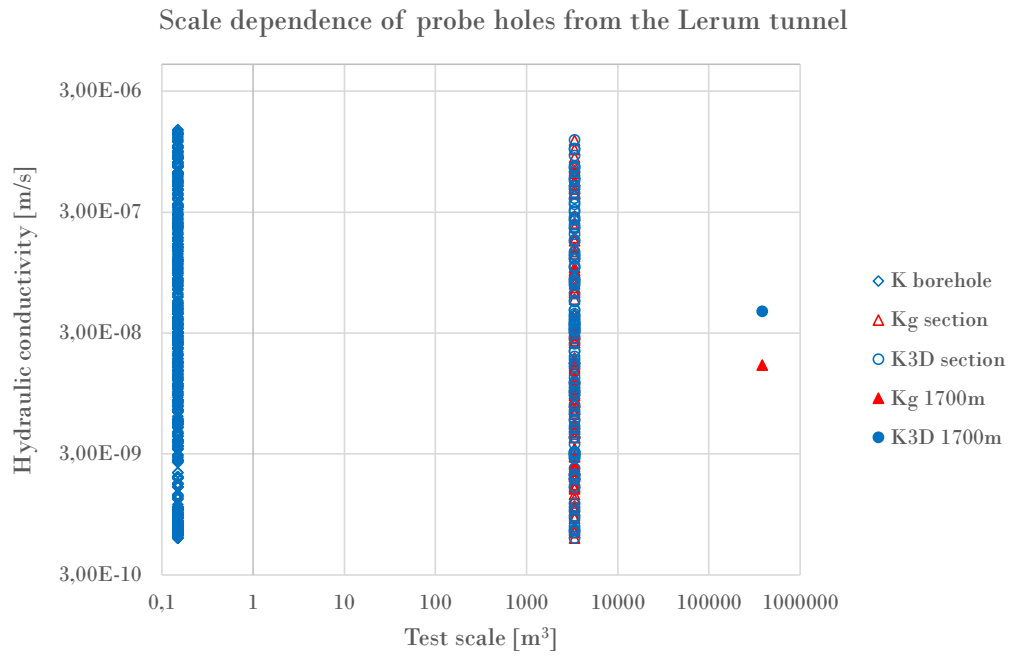

Figure 5.6: The scale dependence between the different means for the Lerum tunnel. The data consists of 639 measured values in probe holes, 119 sections of grouting fans and the tunnel stretch of approximately 1700 meters.

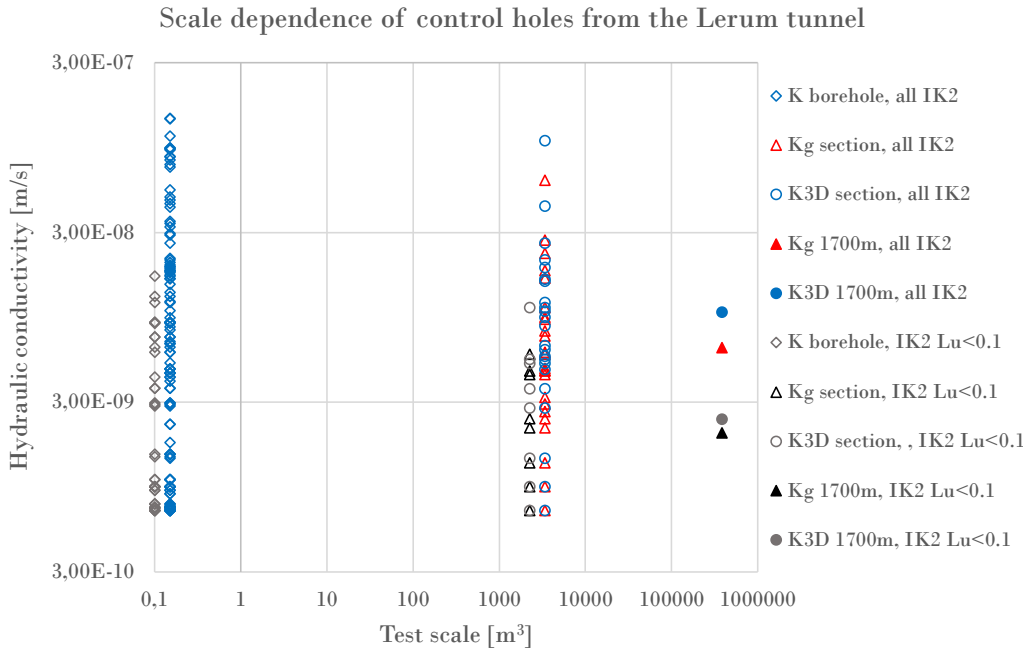

Figure 5.7: The scale dependence between the different means for the Lerum tunnel. The data for all IK2 consists of 118 measured values in probe holes, 24 sections of grouting fans, while IK2 with Lu<0.1 consists of 38 measured values in probe holes, 8 sections of grouting fans. The tunnel whole tunnel stretch is approximately 1700 meters. The values for IK2 Lu<0.1 are shifted slightly to the left on the x-axis.

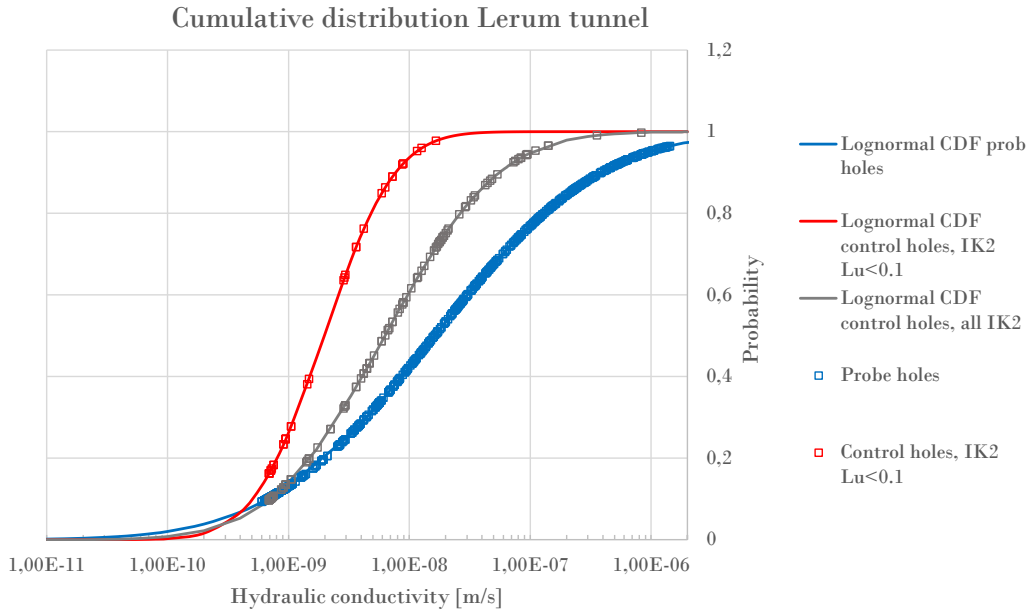

Figure 5.8: Cumulative distributions of the hydraulic conductivity for the considered tunnel stretch in the Lerum tunnel. The probe holes have 639 measurement points, the control holes with all fans from IK2 have 188 measurement points, and the control holes with all fans from IK2 with Lu<0.1 have 38 measurement points.

The median hydraulic conductivity for the grouted rock mass where Lu<0.1 was $1.0 \cdot 10^{-9}$ m/s, the median for the grouted rock mass using all control holes from IK2 was $6.5 \cdot 10^{-9}$ m/s, and the median for the ungrouted rock mass was $1.4 \cdot 10^{-8}$ m/s. The sealing factor $\frac{K}{K_{gr}}$ based on the median hydraulic conductivities became 2.2 for the upper boundary (all IK2), and 13.7 for the lower boundary (IK2 with Lu<0.1).

5.2.2 Evaluation of inflow to the considered tunnel section

The approximate groundwater pressures over the tunnel stretch considered can be seen in Table C.1. Since the studied tunnel stretch is 1700 meters long, the groundwater pressure was estimated in sections covering 100 meters each. The groundwater pressure ranged between 67 to 77 meters, with a mean of 72 meters.

The estimation of the inflow can be seen in Table 5.5. When comparing the predicted inflow in Table 5.5 with the measured inflows in Table 5.6, it can be seen that the inflow calculated with the geometric mean corresponded quite well with the measured inflow. Further, the calculated upper and lower boundary of the hydraulic conductivity for the grouted rock mass gave results that coincided well with the lowest and highest measured inflow during this given time period. Hence, the geometric mean was used in the further analyses.

The selected values for the input parameters that are seen as the best fit for the prevailing conditions for the Lerum tunnel are shown in Table 5.7.

Table 5.5: Calculated means for the tunnel stretch studied in the Lerum tunnel, and the corresponding calculated inflow.

Lerum tunnel	**K_g Probe**	**K_g Control**	**K_{3D} Probe**	**K_{3D} Control**
IK2 all	$1.6 \cdot 10^{-8}$	$6.3 \cdot 10^{-9}$	$4.5 \cdot 10^{-8}$	$1.0 \cdot 10^{-8}$
Inflow	*3.9 l/min·100m*		*9.0 l/min·100m*	
IK2, Lu<0.1	$1.6 \cdot 10^{-8}$	$2.0 \cdot 10^{-9}$	$4.5 \cdot 10^{-8}$	$2.4 \cdot 10^{-9}$
Inflow	*2.4 l/min·100m*		*3.9 l/min·100m*	

Table 5.6: Measured inflow between section 3/543-5/290 in the Lerum tunnel after the construction of the tunnel (Bergab, 2012).

Date	**Measured inflow [l/min·100m]**
2010-01-18	3.1
2010-01-28	2.1
2010-02-01	2.1
2010-02-15	3.0
2010-03-01	2.9
2010-03-29	3.7
2010-05-10	3.6
2010-05-24	3.2
2010-06-07	3.5
2010-06-21	4.0

Table 5.7: The selected values for the input parameters used when estimating the inflow that are seen as the best fit for the prevailing conditions for the considered tunnel stretch in the Lerum tunnel.

Parameter	**Using all IK2**	**Using the IK2 where Lu<0.1**
K	$1.6 \cdot 10^{-8}$ m/s	$1.6 \cdot 10^{-8}$ m/s
K_{gr}	$6.3 \cdot 10^{-9}$ m/s	$2.0 \cdot 10^{-9}$ m/s
H	72 m	72 m
t	4.5 m	4.5 m
r_t	1.8 m	1.8 m
Skin factor	5.0	5.0

Figure 5.9 illustrates how the inflow varies with the estimated range of the hydraulic head along the tunnel stretch. The estimated inflow varied with approximately 0.3 - 0.5 l/min·100m when the hydraulic head ranged between 67 to 77 meters.

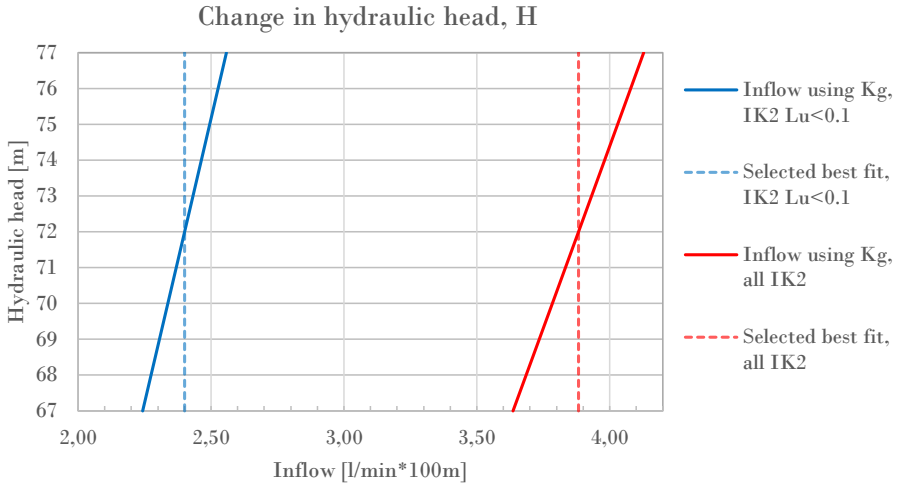

Figure 5.9: How the variation in H along the tunnel stretch affects the calculated inflow for the two cases of calculated K_{gr}.

5.2.3 Sensitivity analysis on the estimated inflow

The sensitivity analysis performed on the input parameters for the inflow equation can be seen in Figure 5.10a, Figure 5.10b and in Appendix C, Figure C.1b to Figure C.1e. In the figures, the parameters that are denoted 1 represent the case using the lower boundary of K_{gr}, while the parameters denoted 2 represent the case using the upper boundary of K_{gr}.

For the case of the upper boundary of K_{gr} (where all control holes from IK2 were used), the ratio of K_g and K_{gr} became 2.6, and for the case of the lower boundary of K_{gr} (where all control holes from IK2 where Lu<0.1 were used), the ratio became 8.2. Since this ratio is located in the denominator of the Equation 2.22, a smaller ratio of K_g and K_{gr} will result in a larger inflow. This can be seen in Figure 5.10a, where a change in hydraulic conductivity of the ungrouted rock mass results in a larger variation in inflow for the case using all control holes from IK2. Further, the influence of the input parameters that are included in the multiplication with the ratio of K_g and K_{gr}, t and r_t, are also affected by the size of the ratio. As the lower boundary have a larger ratio of K_g and K_{gr}, the effect of the change in t and r_t on the inflow becomes larger, see Figure C.1d and Figure C.1e. This effect can also be seen when the evaluating the impact of the skin factor; the upper boundary with a smaller ratio of K_g and K_{gr} had a larger variation in inflow with change in skin factor (see Figure 5.10b). When focusing on the interval of 2-5 in skin factor, the variation in inflow was approximately 1.4 l/min·100m for the upper boundary, while the lower boundary had a change in inflow of approximately 0.5 l/min·100m.

Lastly, the theoretical hydraulic conductivity back-calculated through the measured inflow can be seen in Figure 5.11. The illustrated interval corresponds quite well with the calculated upper and lower boundary of K_{gr} from water loss measurements.

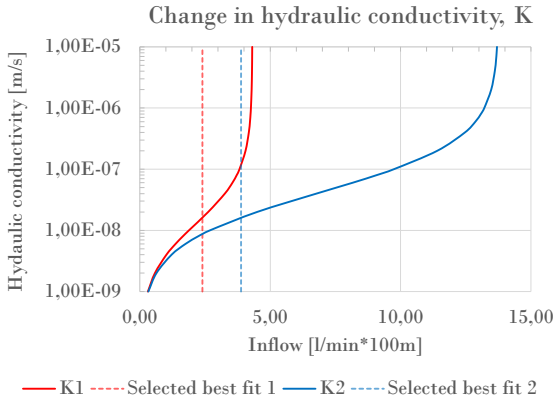

(a) Sensitivity analysis of the hydraulic conductivity.

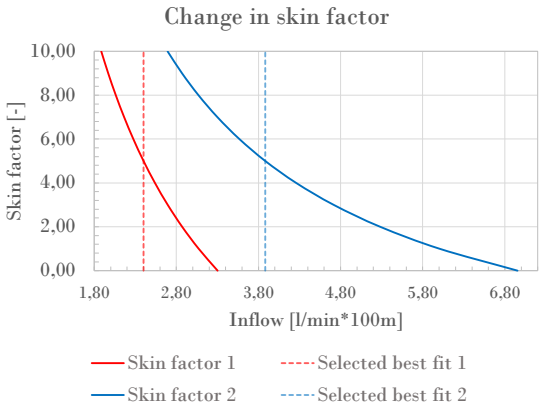

(b) Sensitivity analysis of the skin factor.

Figure 5.10: Sensitivity analyses performed for the considered tunnel stretch in the Lerum tunnel.

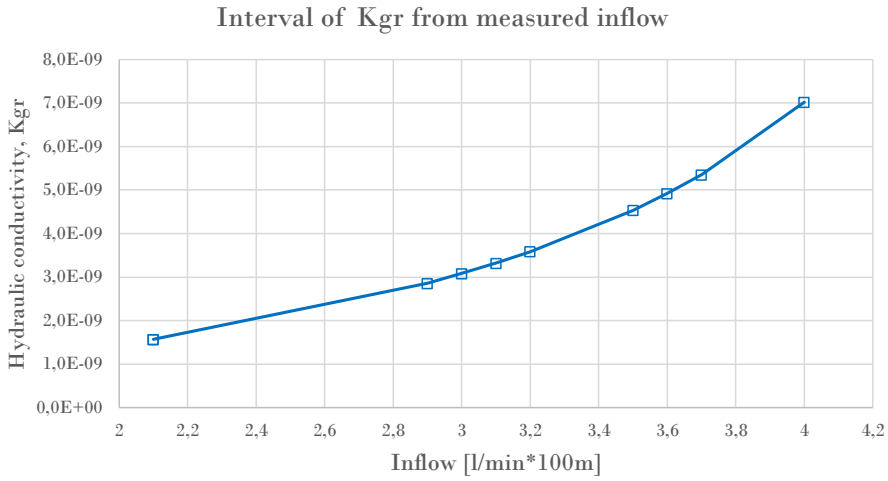

Figure 5.11: Calculated K_{gr} from the measured inflow and the selected best fit values of the input parameters.

5.3 Göta tunnel

The tunnel stretch considered for the Göta tunnel is located between section 2/285 and 2/460 in the southern tunnel tube, and between section 21/275 and 21/430 in the northern tunnel tube.

5.3.1 Evaluation of hydraulic conductivity

Figure 5.12 illustrates the empirical CDF and the log-normal CDF for the hydraulic conductivity calculated through the core drilled boreholes from the preliminary investigations. As a large portion of the values were measured as zero, a straight line forms in the beginning of the empirical graph. These zero values were, as described in section 4.1.2, replaced with the chosen value of the measurement limit. Hence, the

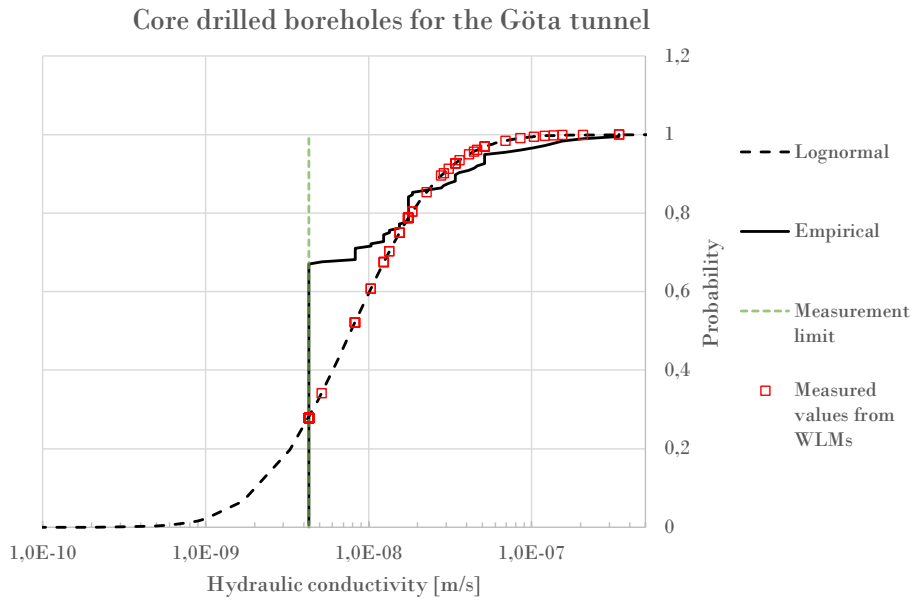

Figure 5.12: The log-normal and empirical CDF for the calculated hydraulic conductivity from core drilled boreholes considered for the Göta tunnel. 176 measured values are used in the evaluation, where 59 values are non-zero. The points represent the calculated values of the hydraulic conductivity from water loss measurements.

straight line of the empirical CDF followed the value of the corresponding hydraulic conductivity of the measurement limit. Approximately at the probability 0.7, the measured non-zero values began, and the graph started to follow the log-normal distribution. The estimated median of the hydraulic conductivity of the ungrouted rock mass was $4.3 \cdot 10^{-9}$ m/s. Further, 125 out of 176 values were below $1.0 \cdot 10^{-8}$ m/s, indicating that the hydraulic conductivity of the rock mass was low.

5.3.2 Evaluation of inflow to the considered tunnel sections

The approximate groundwater pressures over the tunnel stretches considered can be seen in Table D.1. The estimated groundwater pressure ranged between 22 and 25 meters for the southern tunnel tube, and between 18 to 24 meters for the northern tunnel tube. As the majority of the considered tunnel stretch had a groundwater pressure of 22 respectively 19 meters, these values were considered to be the selected best fit for the further calculations.

The hydraulic conductivities used in the estimation of the inflow can be seen in Table 5.8. As the calculated inflow where geometric mean was used corresponds well to the measured inflow for the Lerum and Chalmers tunnel, the geometric mean was chosen to be used in the further calculations for the Göta tunnel as well. The inflows measured after the tunnel was finished were thereafter used to estimate the approximate hydraulic conductivity of the grouted rock mass, see Table 5.9. For tunnel stretch 2/285 - 2/460, the arithmetic mean of the calculated K_{gr} became $1.0 \cdot 10^{-10}$ m/s, and for 21/275 - 21/430, the arithmetic mean became $1.9 \cdot 10^{-10}$ m/s.

The selected values that are seen as the best fit for the input parameters and the

Table 5.8: Calculated inflow using the geometric mean of the hydraulic conductivity of the ungrouted rock mass for the considered tunnel stretches in the Göta tunnel.

Göta tunnel	$\mathbf{K}_g$	$\mathbf{K}_{gr}$	**Inflow**
Southern tube	$7.8 \cdot 10^{-9}$	$1.0 \cdot 10^{-10}$	0.11 l/min·100m
Southern tube	$7.8 \cdot 10^{-9}$	$1.9 \cdot 10^{-10}$	0.16 l/min·100m

Table 5.9: Calculated K_{gr} from the inflow measured after the tunnel was constructed between section 2/285-2/460 and 21/275-21/430 in the Göta tunnel. The measured inflows were collected from the data base TMO, 2020-04-07. All inflows are given in the unit l/min·100m.

	Section 2/285 - 2/460		*Section 21/275 - 21/430*	
Date	**Measured inflow**	**Calculated $\mathbf{K}_{gr}$ [m/s]**	**Measured inflow**	**Calculated $\mathbf{K}_{gr}$ [m/s]**
2008-06-09	0.11	$1.1 \cdot 10^{-10}$	0.19	$2.3 \cdot 10^{-10}$
2007-11-21	0.09	$7.7 \cdot 10^{-11}$	0.13	$1.4 \cdot 10^{-10}$
2007-05-21	0.10	$8.8 \cdot 10^{-11}$	0.16	$1.9 \cdot 10^{-10}$
2007-04-17	0.13	$1.2 \cdot 10^{-10}$	0.19	$2.3 \cdot 10^{-10}$
2006-12-06	0.14	$1.4 \cdot 10^{-10}$	0.19	$2.3 \cdot 10^{-10}$
2006-10-16	0.11	$1.1 \cdot 10^{-10}$	0.13	$1.4 \cdot 10^{-10}$
2006-06-08	0.11	$1.1 \cdot 10^{-10}$	0.13	$1.4 \cdot 10^{-10}$
2006-05-08	0.11	$1.1 \cdot 10^{-10}$	0.19	$2.3 \cdot 10^{-10}$

prevailing conditions for the Göta tunnel are shown in Table 5.10.

Table 5.10: The selected values for the input parameters used when estimating the inflow that are seen as the best fit for the prevailing conditions for the considered tunnel stretches in the Göta tunnel.

Parameter	**21/275-21/430**	**2/285-2/460**
K	$7.8 \cdot 10^{-9}$ m/s	$7.8 \cdot 10^{-9}$ m/s
K_{gr}	$1.9 \cdot 10^{-10}$ m/s	$1.0 \cdot 10^{-10}$ m/s
H	19 m	22 m
t	6.0 m	6.0 m
r_t	6.2 m	6.2 m
Skin factor	5.0	5.0

5.3.3 Sensitivity analysis on the estimated inflow

The sensitivity analysis performed for the considered tunnel stretches in the Göta tunnel can be seen in Figure 5.13 and in Appendix D, Figure D.1b to Figure D.1f. In Figure 5.13, a larger variation can be seen in the inflow for section 21/275 - 21/430 when the hydraulic conductivity is changed than for section 2/285 - 2/460. This is since the ratio between K_g and K_{gr} for tunnel section 2/285 - 2/460 was 78, while the ratio for tunnel section 21/275 - 21/430 was 41. A larger variation can also be seen in the inflow when the grouted thickness and tunnel radius were changed, see Figure D.1d and Figure D.1e. Generally, as the hydraulic conductivity for the considered sections in the Göta tunnel were smaller than for the tunnel stretches evaluated in the Lerum and Chalmers tunnel, the change in input parameters caused a smaller change in predicted inflow.

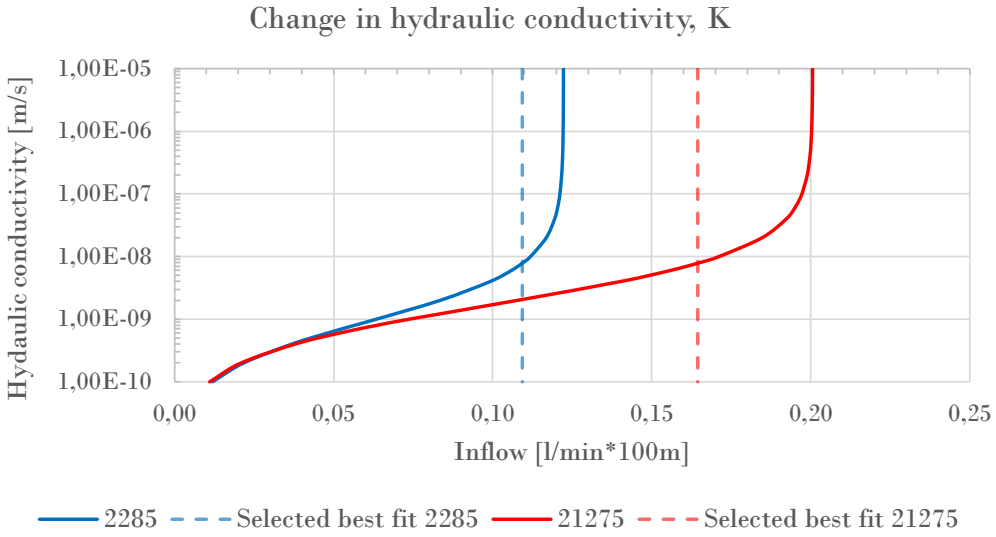

Figure 5.13: Sensitivity analysis of the hydraulic conductivity for the Göta tunnel.

Table D.2 shows the corrected inflow when taking into the effect of the symmetry of the two tunnel tubes, and the corresponding new hydraulic conductivity of the grouted rock mass. The estimated factor calculated from the approximate circle sector that will contribute to the inflow for one tunnel tube was 0.7. From the corrected inflow, the arithmetic mean of the calculated hydraulic conductivity of the grouted rock mass became $1.0 \cdot 10^{-10}$ m/s for tunnel stretch between 2/285 - 2/460, and $6.9 \cdot 10^{-11}$ m/s for tunnel stretch between sections 21/275 - 21/430.

The inflow calculated with the selected best fit values of the input parameters was then corrected using the radius corresponding to both tunnel areas according to Figure 4.3. The new radius became 8.7 meters. When using the new radius with the input values for section 2/285 - 2/460, the corrected inflow became 0.14 l/min·100m, and when using it for section 21/275 - 21/430, the corrected inflow became 0.2 l/min·100m. These values are supposed to correspond to an inflow to both tunnel tubes. However, when adding the measured inflows from both tunnel tubes in Table 5.9 together, the calculated corrected inflows using this method are too small.

5.4 Västlänken

The tunnel stretches considered in the Västlänken service tunnels are the following:

- **ST206**: one tunnel stretch (ST206-02) that is 42 meters.
- **ST207**: one tunnel stretch that is 43 meters (ST207-01), and one that is 90 meters (ST207-03).
- **ST210**: one tunnel stretch that is 42 meters (ST210-02), one that is 67 meters (ST210-03), one that is 102 meters (ST210-04), and one that is 97 meters (ST210-05).

5.4.1 Evaluation of hydraulic conductivity

Figure 5.14 illustrates the empirical CDF and the log-normal CDF for the core drilled borehole KK606KBH and the control holes for the considered service tunnels. From these graphs, it can be seen that the data is reasonably log-normally distributed. It can also be seen that the core drilled borehole KK606KBH and the control holes for ST207 have the lowest distribution of the hydraulic conductivity, and that ST210 have the highest. Further, the straight lines in the beginning in the graphs show that a quite large portion of the measured values for ST207 and ST206 were replaced with the measurement limit. The calculated hydraulic conductivity corresponding to the measurement limit shift slightly for the reported zero-measurements, as the length of the control holes differ. Since only 11 measurements were made in KK606KBH, the empirical CDF becomes quite rough.

The scale dependence between the means calculated for the two scales and the individual hydraulic conductivities calculated from each borehole can be seen in Figure 5.15 and Figure 5.16. In both graphs, it can be seen that as the scale increases, the variation in the calculated hydraulic conductivity decreases. Further, the difference between the geometric mean and the 3D mean using Matheron's conjecture for the whole considered tunnel stretch is quite small for ST206 and ST207, and slightly larger for ST210.

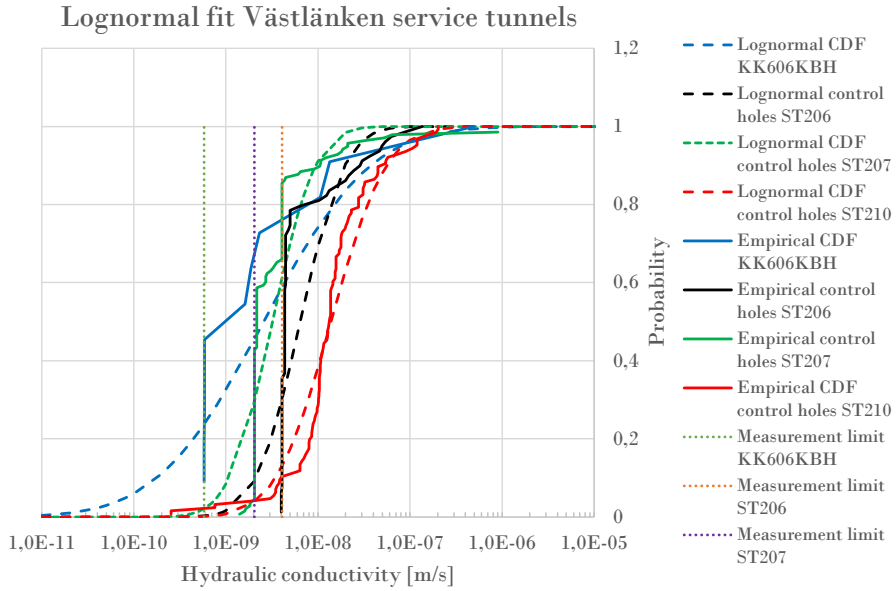

Figure 5.14: The log-normal and empirical CDF for the calculated hydraulic conductivities. 11 measured values are used for KK606KBH where 9 values are non-zero, 81 measured values are used for ST206 where 28 values are non-zero, 148 measured values are used for ST207 where 52 values are non-zero, 126 measured values are used for ST210 where all values are non-zero.

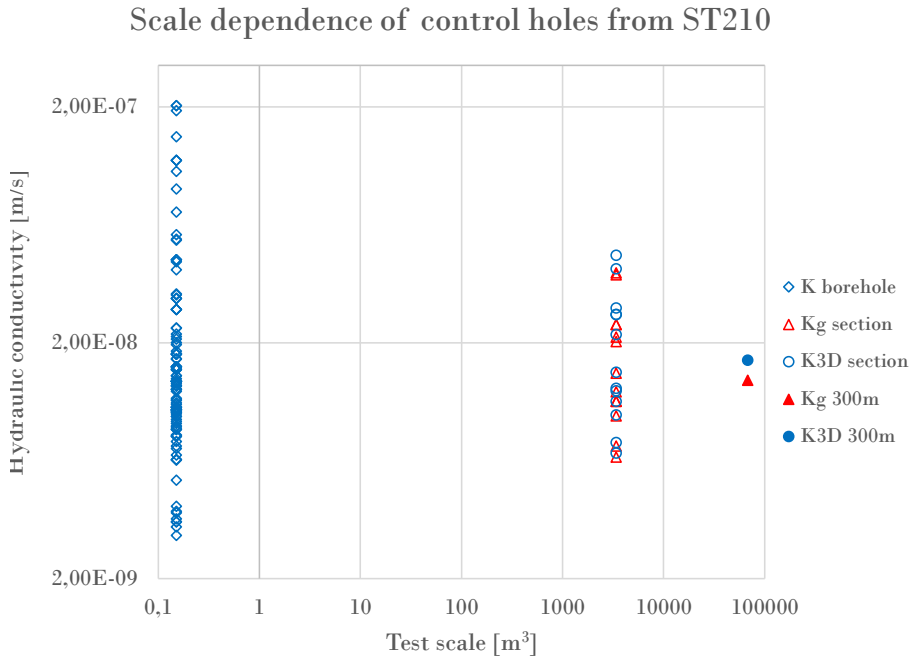

Figure 5.16: The scale dependence between the different means for ST210. The data consists of 126 measured values in control holes, 14 sections of grouting fans and the tunnel stretch of approximately 300 meters.

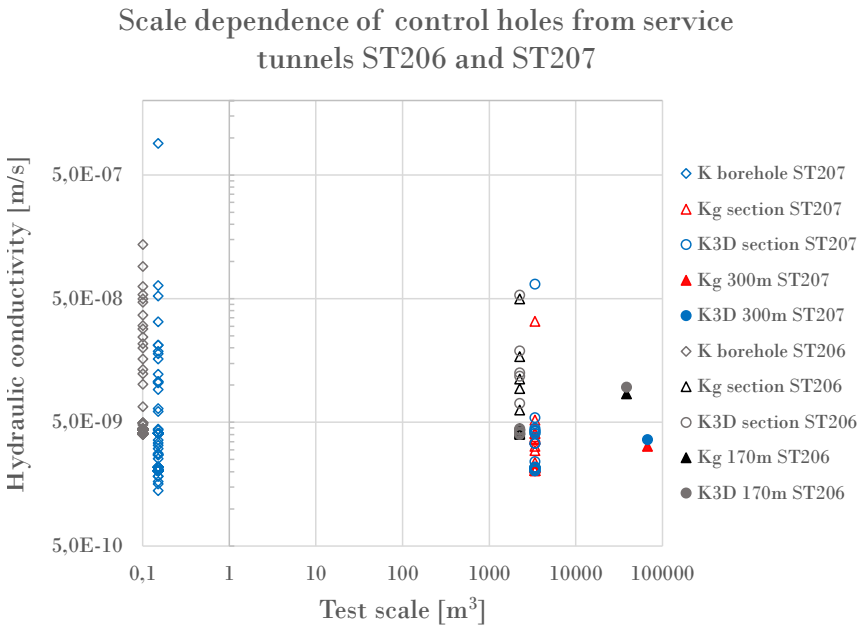

Figure 5.15: The scale dependence between the different means for ST206 and ST207. The data of ST206 consists of 81 measured values in control holes, 13 sections of grouting fans and the tunnel stretch of approximately 170 meters, while the data of ST207 consists of 148 measured values in control holes, 22 sections of grouting fans and the tunnel stretch of approximately 300 meters. The individual values of K and the mean values for each grouting fan in ST206 is slightly shifted to the left.

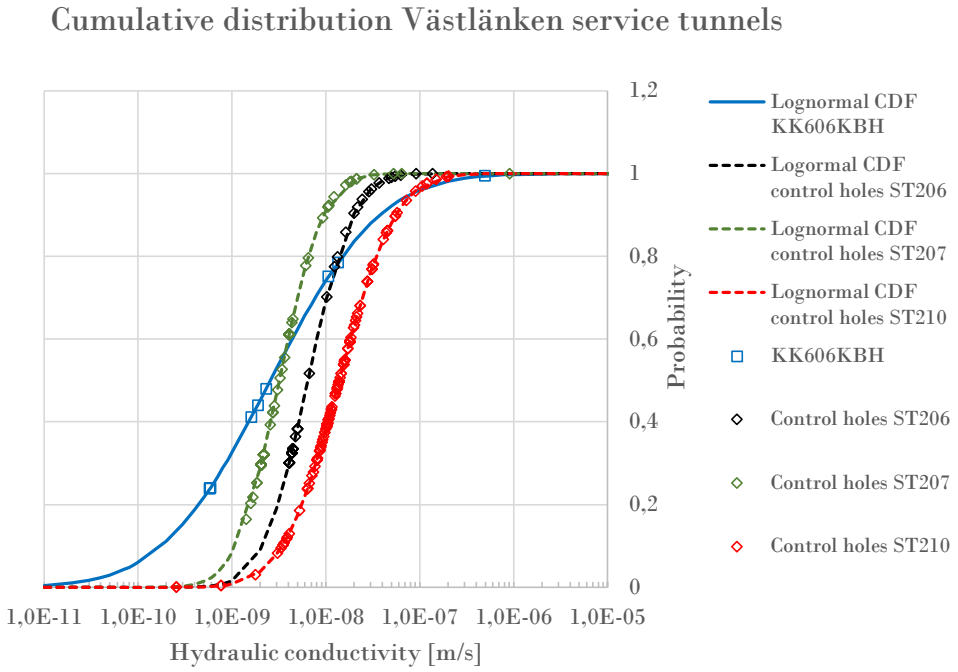

Figure 5.17: Cumulative distributions of the hydraulic conductivity for the Västlänken service tunnels. The lines represent the calculated log-normal CDF, while the points are the calculated values of the hydraulic conductivity from water loss measurements in core drilled boreholes and control holes.

The cumulative distribution for the considered tunnel stretches in the service tunnels can be seen in Figure 5.17. Since the core drilled borehole KK606KBH is used to estimate the hydraulic conductivity of the ungrouted rock mass for ST207 and ST206, it should have a CDF that have a higher hydraulic conductivity than the CDf for the control holes. However, as can be seen in Figure 5.17, there is an approximately 60% probability that the hydraulic conductivity of the ungrouted rock mass is lower than that of the control holes in ST207, and a corresponding probability of 80% for ST206. Thus, KK606KBH might not give a completely representative estimate of the ungrouted rock mass. That is however reasonable, as the hydraulic conductivity of the ungrouted rock mass is characterised through only one core drilled borehole. The control holes are oriented in different directions, while the core drilled borehole is only located in one direction. Therefore, the control holes have a larger probability hitting fractures of different orientations, thus characterising the rock mass better. Since the rock mass can have quite large local variations in hydraulic conductivity, more tests would be needed of the ungrouted rock mass along the considered tunnel stretches to receive a better fit of the distributions. The lack of data for estimating the hydraulic conductivity of the ungrouted rock mass will be further reflected in the estimation of the inflow.

5.4.2 Evaluation of inflow to the considered tunnel sections

The approximate groundwater head for the tunnel stretches considered in the Västlänken service tunnels can be seen in Table E.1. The groundwater head ranged between approximately 5 to 35 meters. Estimated mean values for the considered tunnel stretches can be seen in Table E.1, and in the summary in Table 5.14 and Table 5.15.

The estimation of the inflow can be seen in Table 5.11, whose values can be compared with the measured inflow to the considered tunnel stretches in Table 5.12 and Table 5.13. The measured inflow to the considered tunnel stretches are measurements performed after 2020-01-01 up until today (May 2020). In Table 5.11, the estimation of the inflow using the geometric mean for ST206-02 and ST207-01 is not included. This is since the geometric means for these two tunnel stretches were calculated to be higher than the estimated geometric mean for the ungrouted rock mass from the core drilled borehole KK606KBH, which is unreasonable. Thus, it was decided to only use K_{3D} when estimating the inflow to tunnels ST206 and ST207. However, for tunnel ST210, the inflow calculated with the geometric mean corresponded better to the actual measured inflow to the four considered tunnel stretches. Thus, the geometric mean was seen as the best fit for the estimation of inflow to ST210.

As can be seen in the tables, the measured inflow to ST207-01 is quite much larger than the estimated inflow. This could be caused by individual discrete fractures that has not been completely sealed. Further, this was the first section constructed in the start of the project, during which the experience of the construction design was probably not yet high.

Table 5.11: Calculated means for the tunnel stretch studied in the Västlänken service tunnels, and the corresponding calculated inflow.

Lerum tunnel	**K_g KBH**	**K_g Control**	**K_{3D} KBH**	**K_{3D} Control**
ST206-02	$2.6 \cdot 10^{-9}$	$4.3 \cdot 10^{-9}$	$5.3 \cdot 10^{-9}$	$4.3 \cdot 10^{-9}$
Inflow	-		*0.55 l/min·100m*	
ST207-01	$2.6 \cdot 10^{-9}$	$2.9 \cdot 10^{-9}$	$5.3 \cdot 10^{-9}$	$3.2 \cdot 10^{-9}$
Inflow	-		*0.3 l/min·100m*	
ST207-03	$2.6 \cdot 10^{-9}$	$2.2 \cdot 10^{-9}$	$5.3 \cdot 10^{-9}$	$2.3 \cdot 10^{-9}$
Inflow	*0.5 l/min·100m*		*0.9 l/min·100m*	
ST210-02	$6.0 \cdot 10^{-8}$	$8.6 \cdot 10^{-9}$	$1.8 \cdot 10^{-7}$	$9.3 \cdot 10^{-9}$
Inflow	*5.3 l/min·100m*		*8.9 l/min·100m*	
ST210-03	$6.0 \cdot 10^{-8}$	$1.4 \cdot 10^{-8}$	$1.8 \cdot 10^{-7}$	$1.5 \cdot 10^{-8}$
Inflow	*8.3 l/min·100m*		*15.5 l/min·100m*	
ST210-04	$6.0 \cdot 10^{-8}$	$1.9 \cdot 10^{-8}$	$1.8 \cdot 10^{-7}$	$2.1 \cdot 10^{-8}$
Inflow	*9.5 l/min·100m*		*19 l/min·100m*	
ST210-05	$6.0 \cdot 10^{-8}$	$1.2 \cdot 10^{-8}$	$1.8 \cdot 10^{-7}$	$1.9 \cdot 10^{-8}$
Inflow	*8.3 l/min·100m*		*18 l/min·100m*	

Estimations of the hydraulic conductivities and the inflow were also performed for the tunnel section located in between ST207-01 and ST207-03. For this section (ST207-02), the estimated hydraulic conductivity for the grouted rock mass was higher than the hydraulic conductivity for the ungrouted rock mass for both K_g and K_{gr}, which is unreasonable. During visits in tunnel ST207, systematic leakages had been observed along the tunnel wall for some sections (Personal communication, Johan Thörn, 2020-05-04). Thus, the homogeneous assumption of the grouted thickness in the inflow equation might not work that well during these conditions. Backward calculations could be performed through the measured inflow, but since the measured inflow to this section did not seem to represent the actual inflow, this is not performed.

The selected values for the input parameters that are seen as the best fit for the prevailing conditions for the Västlänken service tunnels are shown in Table 5.14 and Table 5.15.

Table 5.12: Measured inflow [l/min·100m] between measurement wiers located in the Västlänken service tunnels ST206 and ST207. The measurements from 2020-03-28 to 2020-05-02 are an average value of 24 hours of measurements made from Saturday 00:00 to Sunday 00:00.

Date	ST206-02	ST207-01	ST207-03
2020-01-07	0.4	-	-
2020-02-22	0.1	-	-
2020-03-15	0.1	-	-
2020-03-28	-	0.7	0.6
2020-04-04	-	0.6	0.7
2020-04-11	-	1.1	0.9
2020-04-18	-	0.8	0.8
2020-04-25	-	0.8	0.8
2020-05-02	-	0.9	1.1

Table 5.13: Measured inflow [l/min·100m] between measurement wiers located in the Västlänken service tunnel ST210.

Date	ST210-02	ST210-03	ST210-04	ST210-05
2020-01-13	0.4	0.7	0.5	-
2020-01-27	2.4	1.3	10	6.8
2020-02-09	3.9	1.2	4.2	14
2020-02-29	3.1	0.3	4.5	23
2020-03-09	-	2.1	3.4	8.5
2020-03-23	1.4	2.2	5.9	12
2020-04-06	3.2	2.6	-	17
2020-04-20	7.0	2.6	11	15
2020-04-22	4.5	5.0	10	16

Table 5.14: The selected values for the input parameters used when estimating the inflow that are seen as the best fit for the prevailing conditions for the considered tunnel stretches in the Västlänken service tunnels ST206 and ST207.

Parameter	ST206-02	ST207-01	ST207-02
K	$5.3 \cdot 10^{-9}$ m/s	$5.3 \cdot 10^{-9}$ m/s	$5.3 \cdot 10^{-9}$ m/s
K_{gr}	$4.3 \cdot 10^{-9}$ m/s	$3.2 \cdot 10^{-9}$ m/s	$2.3 \cdot 10^{-9}$ m/s
H	17 m	9 m	35 m
t	5 m	5 m	5 m
r_t	4.7 m	4.7 m	4.7 m
Skin factor	4.0	4.0	4.0

Table 5.15: The selected values for the input parameters used when estimating the inflow that are seen as the best fit for the prevailing conditions for the considered tunnel stretches in the Västlänken service tunnel ST210.

Parameter	**ST210-02**	**ST210-03**	**ST210-04**	**ST210-05**
K	$6.0 \cdot 10^{-8}$ m/s	$6.0 \cdot 10^{-8}$ m/s	$6.0 \cdot 10^{-8}$ m/s	$6.0 \cdot 10^{-8}$ m/s
K_{gr}	$8.6 \cdot 10^{-9}$ m/s	$1.4 \cdot 10^{-8}$ m/s	$1.9 \cdot 10^{-8}$ m/s	$1.2 \cdot 10^{-8}$ m/s
H	25 m	33.5 m	35 m	35 m
t	5 m	5 m	5 m	5 m
r_t	4.7 m	4.7 m	4.7 m	4.7 m
Skin factor	4.0	4.0	4.0	4.0

5.4.3 Sensitivity analysis on the estimated inflow

The sensetivity analysis performed for the Västlänken service tunnels can be seen in Figure 5.18 and Figure 5.19, and in Appendix E, Figure E.2 to Figure E.5.

In the general grouting design described in PM Typinjektering (Trafikverket, 2016c), it was given that the minimum penetration length of the grout had to be equal to the length between the boreholes (2.5 meters). Through geometry, see Figure E.1, the upper limit of the grouted thickness according to the design could then be calculated to be 8.2 meters. However, as has been discussed earlier, the penetration length of the grout can vary, and a locally greater (and lesser) thickness can occur. Thus, in Figure 5.18, the upper limit of the grouted thickness according to the geometry of the design should be 8 meters.

In Figure 5.18, it can also be seen that the considered tunnel stretches in tunnel ST210 have a larger range of estimated inflows when the length of the grouted thickness is changed. This can be seen in all the sensitivity analyses performed; a change in input parameter causes a larger change in the estimated inflow. This is most probably the result of ST210's larger hydraulic conductivities, and larger ratios of K and K_{gr}. This can also be seen in Figure 5.19, where the estimated inflow with change in hydraulic conductivity of the ungrouted rock mass causes the inflow to increase significantly. At the hydraulic conductivity of $1 \cdot 10^{-5}$, ST210-03 reaches 24 l/min·100m, ST210-04 reaches 33 l/min·100m, and ST210-05 reaches 22 l/min·100m.

Further, it can be seen that a change in skin factor causes a larger change in estimated inflow for the considered tunnel stretches in ST210 compared to ST206 and ST207. A change in skin factor between 2-5 causes a change in inflow of approximately 0.4 l/min·100m for ST206, between 0.2-0.4 l/min·100m for the considered stretches in ST207, and between 2-4 l/min·100m for the considered stretches in ST210. Thus, a change in skin factor causes a change in inflow in ST210 that is approximately 10 times larger than the change in ST206 and ST207 when it is varied between 2 and 5.

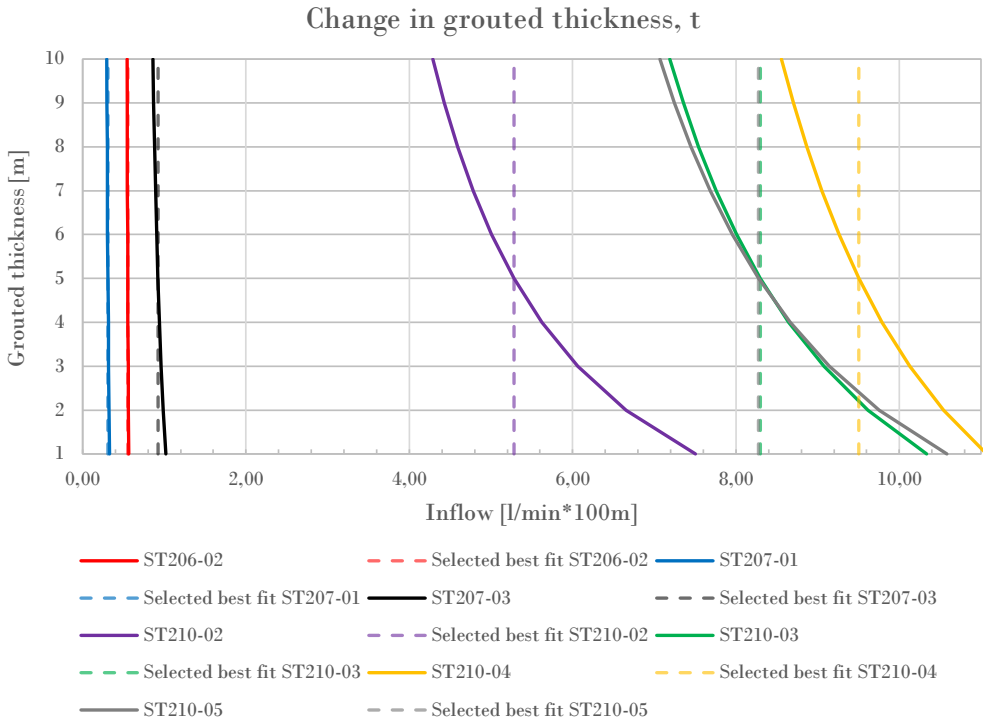

Figure 5.18: Sensitivity analysis of the thickness of the grouted rock mass for the Västlänken service tunnels.

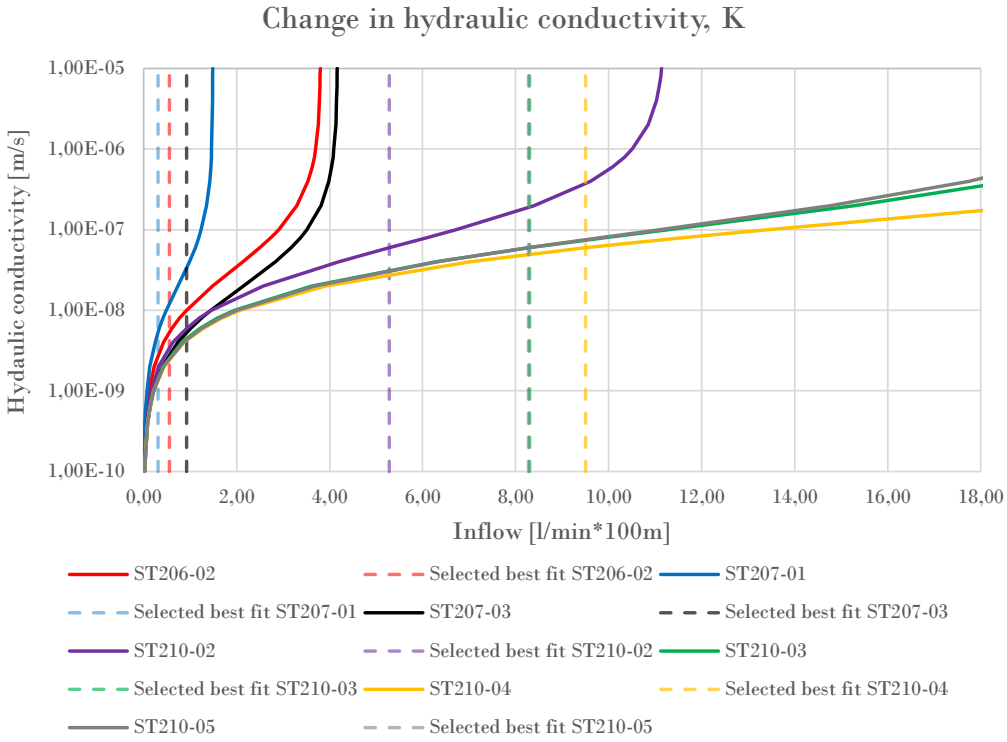

Figure 5.19: Sensitivity analysis of the hydraulic conductivity for the Västlänken service tunnels.

6

Discussion

The following chapter will discuss the results and uncertainties for the four tunneling projects. Firstly, the uncertainties related to the data from WLMs used in the evaluation of the hydraulic conductivity is discussed, followed by a discussion of the impact of the input parameters on the calculated inflow and their uncertainties. Thereafter, comparisons between the results from the four tunneling projects are made. Lastly, the applicability of the inflow equation for different rock domains is discussed, and the correspondence of the calculated inflow to the measured inflow for the tunneling projects is evaluated.

6.1 Uncertainties in collected data of hydraulic conductivity

When data from older projects are collected, it is hard to know how representative the data is of the hydrogeologic conditions that prevailed, and of what quality it is. Since it was not known what equipment that was used during the WLMs of the three older tunneling projects, the detection limit of the equipment had to be assumed. The resulting calculated hydraulic conductivities of the measurements reported as zero might therefore be either higher or lower than what the actual conditions were. Additionally, no detection limit could be found from the WLMs in the control holes in the Västlänken service tunnel ST210.

As described in section 4.1.1, the execution of the test will also affect the outcome of the results. If the tests were not performed at stationary conditions, the measurement would most probably overestimate the transmissivity of the rock mass. Consequently, for the two tunneling projects where probe holes were drilled continuously (the Lerum and Chalmers tunnel), a too strict grouting class would have been chosen based on the results of those WLMs. Accurate results of the hydraulic tests do therefore require competent workers that perform the tests according to the given requirements.

Further, it is difficult to assess data when not being a part in the projects considered and knowing the conditions of the tests. For example, challenging conditions might have made certain sections of WLMs harder to perform and might therefore not get as representative measurements. However, as these were not known, all data that has been found were used in the evaluations, except for the selections made mentioned in section 4.1 (such as removing the first fans with small rock cover from

the data set).

Moreover, for all considered tunnels in this thesis, the WLMs performed in the control holes might not give results of the final sealing of the rock mass, as additional grouting could have been performed if some of the WLMs in the control holes indicated a need. Some of the evaluated hydraulic conductivities of the grouted rock mass might therefore be higher than what the actual conditions show.

In the two following subsections, the uncertainties related to the estimation of the hydraulic conductivity are divided into two parts: one for the older already constructed tunneling projects, and one for the ongoing Västlänken project.

6.1.1 The Lerum, Chalmers and Göta tunnel

During the data collection, it was hard to find data from the construction of the Chalmers and Göta tunnel. The tunnel sections considered for the Chalmers tunnel is located in a valley, and it was found in internal documents that these tunnel stretches were a bit problematic during construction and required post grouting. This is most likely why these WLMs were kept in the archive, as some further investigations were performed on the groundwater levels and the flow of groundwater. The tunnel stretch considered for the Chalmers tunnel is therefore probably not representative for a "normally" fractured rock mass, but a section with a somewhat higher fracture frequency.

As described earlier, no detailed information regarding the hydraulic properties of the rock mass for the Göta tunnel was found. Thus, five core drilled boreholes tested during the preliminary investigations were chosen, as those were located close to the tunnel stretch of the Göta tunnel with the least amount of fracture zones. The resulting hydraulic conductivity for the considered tunnel stretch is hence a rough estimate of the prevailing conditions, resulting in an imprecise result. And as described in section 4.1.2, some of the core drilled boreholes were long with a large amount of zero-reported measurements, making the choice of measurement limit cause a quite large impact on the resulting mean of the hydraulic conductivity. The measurement limit for the Göta tunnel was therefore hard to estimate as the resulting mean of the hydraulic conductivity when using the lowest measured flow in the core drilled boreholes became unreasonably low. Thus, the measurement limit for the Göta tunnel was chosen so that the calculated hydraulic conductivity for the value of the measurement limit was in the same order as for the Chalmers tunnel, and so that the resulting mean of the hydraulic conductivity was close to the one calculated in the preliminary investigations. However, as the chosen measurement limit for the Chalmers tunnel is the largest of the four tunneling projects, the hydraulic conductivity calculated for the more intact rock mass in the Chalmers tunnel might be overestimated.

As the grouting design for the Göta tunnel did not include as detailed controls of the grouted rock mass, no results from continuous control holes were found for the Göta tunnel. Consequently, no data of the hydraulic conductivity of the grouted rock mass could be used in the analyses, resulting in even more imprecise results. Since the hydraulic conductivities are the parameters influencing the results of the

inflow equation the most, as will be discussed in section 6.2, large uncertainties were linked to the results of the Göta tunnel. The results achieved in this thesis for the considered tunnel stretch in the Göta tunnel is thus only a rough approximation of the actual conditions and can not be seen as a detailed analyses.

Since the choice of tunnel stretches in the old tunneling projects were based on the information that could be found, the tunnel stretches consisted of several different geologic domains. Consequently, several of the different specified grouting classes were used along these tunnel stretches. In the collected data, the gathered information was not seen as being enough to make possible subdivisions. In addition, only a small number of grouting fans were collected for the Chalmers tunnel, which would result in a very small data sets if subdivisions were considered possible. The comparison of the results of the four tunneling projects would have been better if tunnel stretches where only one grouting class were used and where inflow measurements were performed had been found. This since the values of the calculated hydraulic conductivities were averaged, and when several geologic domains are included in the tunnel stretch, the resulting mean value might not be completely representative of the prevailing conditions.

The data sets used from the Lerum utility tunnel were the largest of the old tunneling projects, with a large number of fans of both probe and control holes measured along the tunnel stretch. As only the fans where grouting class 2 had been used were chosen, as described in section 4.1.1, a large number of fans were disregarded from the data set. Thus, the evaluated hydraulic conductivities does not cover the entire considered tunnel stretch of 1700 meters. However, because of the large number of fans of both control and probe holes still used (approximately 120 of each) which are spread over the tunnel stretch, this evaluation most probably gave the most reliable results of all considered tunnels in this thesis.

For the Chalmers and Lerum tunnel, where continuous WLMs were performed in probe holes during the construction, an additional uncertainty might be related to these WLMs, since those were partly conducted in already grouted rock mass. The grouting fans were designed to create an overlap in order to ensure adequate sealing between the fans. An example of this can be seen in for example Figure A.3, where the overlap between the grouting fans in the Lerum tunnel are five meters. Hence, the calculated hydraulic conductivity for the ungrouted rock mass based on these tests might be slightly smaller than what it actually is. However, as the zero-reported measurements were replaced by a measurement limit, it might to some extent compensate for these possible lower measured flows.

6.1.2 Västlänken service tunnels

Only three core drilled boreholes were used to characterise the ungrouted rock mass for the three different Västlänken service tunnels; one for ST207 and ST206, and two for ST210. As a consequence of this, the resulting mean of the hydraulic conductivity was not based on data from WLMs performed at several locations. Hence, the results most probably only gave an indication of which order of magnitude the hydraulic conductivity of the ungrouted rock mass had. This can also be reflected in the

results, as the geometric mean for the grouted rock mass of ST206 and ST207 were higher than the hydraulic conductivity of the ungrouted rock mass, which is unreasonable. The geometric mean had been smaller than the 3D mean based on Matheron's conjecture for all studied tunnels, and resulted in evaluated inflows that corresponded better to the measured inflow for all of the older tunneling projects. However, in order to be able to perform the calculation for ST206 and ST207, K_{3D} had to be used. This uncertainty should be taken into consideration when viewing the results; since only a few core drilled boreholes were used to evaluate the hydraulic conductivity, the results only give an indication of in which order of magnitude the inflow is.

No measurement limit were used on the data from the control holes in ST210, as no could be found. Thus, the hydraulic conductivity of the grouted rock mass could be higher since there is probability that some measurements lie below the measurement limit of the equipment from which accurate results could be obtained. In order to achieve analyses with better results, more information regarding the measurement limit of the equipment used are needed, as well as more detailed data on the hydraulic conductivity of the ungrouted rock mass. As will be discussed below, the hydraulic conductivities K and K_{gr} are the two parameters that influence the results the most. Thus, those are of large importance to get right, if a detailed reliable result is wanted.

6.2 Impact of parameters on calculated inflow

Through the sensitivity analyses performed on the hydraulic conductivity of both the grouted and ungrouted rock mass (K and K_{gr}), it could be seen that these two parameters had the largest influence on the estimated inflow. These two parameters also have large variations in reality, as the flow through the fractures is largely dependent on the fracture apertures and the hydraulic connection of the fractures. Thus, the hydraulic conductivity have local variations which will influence the volume of inflow to the tunnel. The flow through the grouted rock mass can also vary, as there might be individual fractures that are not sufficiently grouted and cause discrete inflows to the tunnel. Thus, it is difficult to properly characterise the hydraulic conductivity through a mean value in the inflow equation since variations always occur.

It could also be seen in the sensitivity analyses that a change in hydraulic head results in a quite large change in estimated inflow. Further, it could also be seen that the increase was almost linear for all evaluated tunnels, which was expected and can be seen in the formulation of the equation. In the calculations, the mean hydraulic head was estimated from measured groundwater levels and through technical drawings of the vertical distance to the middle of the tunnel. Hence, the estimation of the inflow were based on an unaffected groundwater table where no groundwater had yet entered the tunnel. During the construction of a tunnel, the groundwater table fluctuate more or less along the tunnel stretch; both as a result of seasonal variations but also because of the tunnel driving. The calculated inflow will thus most probably be overestimated when the unaffected groundwater table were used to estimate the hydraulic head, as some drawdown is inevitable. And because the hydraulic head

had a quite large impact on the result, these variations should be taken into account in order to get an estimated inflow that corresponds well to the actual conditions.

The radius of the tunnel, r_t, is the parameter affecting the inflow least when it was changed. In the equation, r_t grow logarithmically, resulting in the inflow being less sensitive to small changes in the parameter value. This is reasonable since the radius of the tunnel will not have that large variations as it is a set parameter in the tunnel design, and do therefore not have a large interval of values it should range between. The variation in tunnel radius can be the result of blocks removed during scaling, blocks that will fall during blasting of the tunnel contour, or as a result of the inclination of the boreholes used during blasting. Further, if a larger tunnel area were to be blasted, it will result in higher costs for the contractors because of the larger rock volumes that has to be handled. The variation in tunnel area will therefore probably be kept as small as possible.

As was described in section 4.2, it is quite hard to estimate the mean thickness of the grouted zone, as fractures of different apertures will have different penetration lengths. In the grouting design, a larger thickness was also used in the floor of the tunnel than in the tunnel roof in order to, among other, account for the larger hydraulic head. Even though the value of t grows logarithmically in the inflow equation, the chosen mean thickness of the grouted zone can have a moderate effect on the estimated inflow if the difference between K and K_{gr} was larger. This can be seen clearly in the sensitivity analysis of t for the Lerum tunnel (see Figure C.1d), where the only difference between the two cases were the ratio of K and K_{gr}. Here, the case using the lower boundary of K_{gr} results in a larger change in inflow with change in t, as the ratio of K and K_{gr} is larger.

The change in skin factor is also affected by the size of the ratio of K and K_{gr}. When the ratio was smaller, the choice of skin factor causes a larger change in the estimated inflow than when the ratio was larger. Thus, it could be seen that the choice of skin factor affect the results differently depending on the geologic settings and the sealing effect of the grouting. Since the skin factor is chosen qualitatively, more care should be taken in the choice of the factor when a small sealing effect of the grouting can be expected, and when the surrounding conditions are similar.

From this, it can be said that the estimation of the hydraulic conductivity of both the grouted and ungrouted rock mass and the hydraulic head are the most important parameters to characterise in detail in order to get an estimation of the inflow that is closest to the actual inflow. Further, it is seen that the choice of skin factor will cause a larger influence on the results if the difference between the hydraulic conductivity of the grouted rock mass and ungrouted rock mass is relatively small.

However, it should also be noted that the size of the inflow to the tunnels is dependent on the groundwater supply. If the supply is small or drained, the inflow will decrease compared to when the aquifers are full with a resulting large hydraulic head. Thus, inflow to tunnels will be more constant in zones with large groundwater supplies, compared to in areas where the groundwater is not able to accumulate.

6.3 Comparison of results from the four tunneling projects

To summarize the results, the approximate sealing factor for each considered tunnel stretch is given in Table 6.1.

Table 6.1: The calculated sealing factor for the evaluated tunnel stretches in this thesis. The sealing factor for the Chalmers tunnel is calculated from the data of the two tunnel tubes combined. For ST207 and ST206, K_{3D} had to be used, as the median hydraulic conductivity of K became smaller than K_{gr}. The hydraulic conductivities marked with italic were characterised through core drilled boreholes or based on small data sets. The resulting sealing factor for these are therefore only an approximation.

Tunnel	**Tunnel section**	**Section length [m]**	**Median K [m/s]**	**Median K_{gr} [m/s]**	**Sealing factor [-]**
Chalmers tunnel	5/288-5/392 7/269-7/372	104	$2.3 \cdot 10^{-8}$	$6.7 \cdot 10^{-9}$	3.4
Lerum tunnel	3/543-5/290	1747	$1.4 \cdot 10^{-8}$	1.0 - 6.5 $\cdot 10^{-9}$	2.2 -14
Göta tunnel	2/285-2/460 21/275-21/430	175	$\mathit{4.3 \cdot 10^{-9}}$	$\mathit{1.0 - 1.7 \cdot 10^{-10}}$	25 - 43
ST210	ST210-02 - ST210-05	Between 42 - 108	$\mathit{2.5 \cdot 10^{-7}}$	$8.6 \cdot 10^{-9}$ - $1.6 \cdot 10^{-8}$	16 - 29
			K_{3D} [m/s]	**$K_{3D,gr}$ [m/s]**	
ST206	ST206-02	42	$\mathit{5.3 \cdot 10^{-9}}$	$4.3 \cdot 10^{-9}$	1.2
ST207	ST207-01 & ST207-03	43 & 90	$\mathit{5.3 \cdot 10^{-9}}$	2.3 - 3.2 $\cdot 10^{-9}$	1.7 - 2.4

The results achieved for the Göta tunnel are not completely comparable to the results achieved for the three other tunneling projects. This is since the evaluation of the hydraulic conductivity for the Göta tunnel was only based on five core drilled boreholes and with no WLMs from control holes. Thus, a backwards calculation was made from the measured inflow in order to estimate a possible range of the hydraulic conductivity of the grouted rock mass, as this was the unknown parameter. Further, two tunnel stretches with unusually low permeability had to be chosen in the Göta tunnel in order to be able to perform the evaluation of the hydraulic conductivity of the grouted rock mass.

During the evaluation of the tunnel stretches for the Göta tunnel presented in section 5.3, calculations were also performed on the adjacent tunnel sections 2/460 - 2/615 and 21/430 - 21/610. The measured inflow to these sections are approximately ten times higher than the inflow measured to the tunnel sections 2/285 - 2/460 and 21/275 - 21/430 considered in the results. As no detailed data of the different sections were used when characterising the rock mass, the hydraulic conductivity of the ungrouted rock mass given in Table 5.8 was used in these calculations as well. The calculated K_g is quite low, indicating that the rock domain considered

in the calculations have a low hydraulic conductivity. However, when using K_g in the calculations of K_{gr} for the sections with higher measured inflow, K_{gr} becomes negative. This is since the K_{gr} corresponding to the higher measured inflow has to be larger than K_g given in Table 5.8, which is unreasonable. In the technical drawings illustrating the rock prognosis along the tunnel stretch, a fracture zone was expected along sections 2/460 - 2/615 and 21/430 - 21/610. Hence, the higher inflow could be caused by individual discrete leakages through fractures that may not have been sealed as effectively as in the rock mass with lower fracture frequency. To be able to account for the higher fracture frequency in the calculations of sections with higher inflow, an additional rock domain would be necessary. As this is not within the scope of this thesis, this was not performed.

Since the evaluation performed of K for the Västlänken service tunnels were also based on core drilled boreholes, the results for these tunnel sections are thus not completely comparable with the results of the Lerum and Chalmers tunnel either. As mentioned above, the results for the Västlänken service tunnels only indicate the order of magnitude of the inflow and the possible impact of changes in input parameters, and was thus not an detailed analysis. It should also be noted that the larger inflows in ST210 is being subject to post grouting as this thesis is concluded.

For several of the considered tunnel stretches, sections of very small or no sealing effect could be seen when performing the evaluations. This is most probably due to the fact that the estimated means of hydraulic conductivity of the ungrouted rock mass for some of the tunnel stretches were based on less detailed investigations. Additionally, when information regarding fracture zones were noted on the measurements, the data sets were modified to represent the more "normally" fractured rock mass. Since the monitoring during construction were more detailed than these preliminary investigations, fracture zones might be included in those results, making the hydraulic conductivity of the grouted rock mass being close or higher than the hydraulic conductivity of the ungrouted rock mass. The results might therefore during certain conditions misrepresent the sealing effect of the grouting, making the sealing of the rock mass seem small when it in reality was larger. This might also be the case for some of the sections in the tunnel stretches where the ungrouted rock mass was characterised through probe holes. Since the control holes have a slightly different orientation than the probe holes, there is a possibility that the control holes might hit a more water-bearing fracture than the probe holes initially indicated.

6.3.1 Comparison of the influence in input parameters

For all considered tunnel stretches in this thesis, it could be seen that as the scale considered when estimating the mean of the hydraulic conductivity increases, the variance decreases. When looking at the means calculated for the entire tunnel stretches, the difference between the two means was quite small. It could also be seen that the geometric mean calculated for the whole considered tunnel stretch was smaller than the 3D mean calculated with Matheron's conjecture for all considered tunnel stretches. Further, it was found that the variance of the geometric mean calculated for each grouting fan were smaller than that of the 3D mean using Matheron's conjecture.

When estimating the inflow, the geometric mean gave results that were closer to the actual measured inflow for all considered tunnel stretches, except for the three Västlänken service tunnel sections where K_{3D} had to be used. The geometric mean might be a better fit for the calculations made since the groundwater head most likely was overestimated when it was assumed to be unaffected by drawdown. A smaller hydraulic conductivity could therefore result in estimations that were closer to the measured inflows. However, as the groundwater head most likely was overestimated, a drawdown could have been assumed in the calculations, which might result in K_{3D} being a better fit.

In the sensitivity analyses, it could be seen that the Chalmers and Lerum tunnel have larger variations in inflow with change in K and K_{gr} (see Figure 6.1 and 6.2) than the Göta tunnel. This is probably due to the fact that both the Chalmers and Lerum tunnel have hydraulic conductivities corresponding to more "normally" fractured rock mass, while the hydraulic conductivity for the evaluated sections in the Göta tunnel were very low. The estimated mean hydraulic conductivity of the grouted rock mass for the considered tunnel stretches Göta tunnel became between 1-2·10^{-10} m/s, whilst it became between 2-6·10^{-9} m/s for the considered stretch in the Lerum tunnel and between 1-2·10^{-8} m/s for the stretches in the Chalmers tunnel.

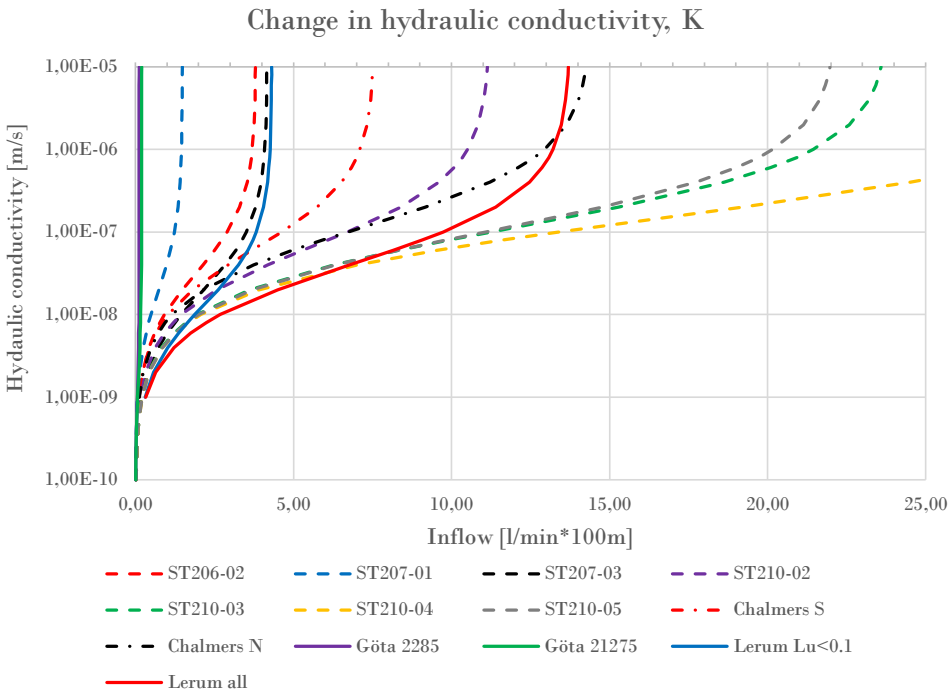

Figure 6.1: Sensitivity analyses of K performed for all considered tunnel stretches in this thesis.

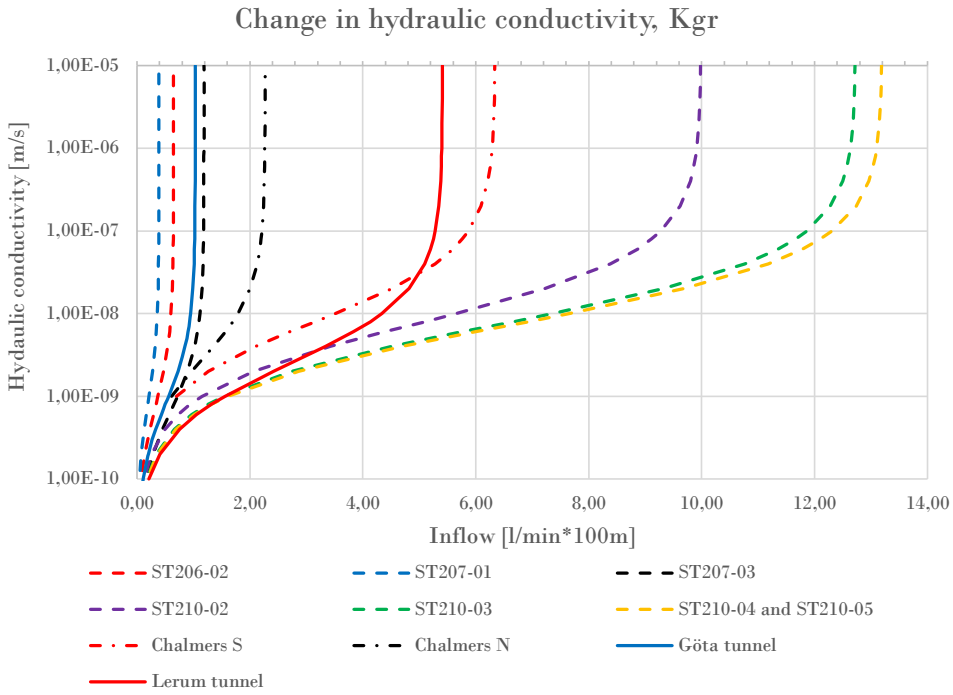

Figure 6.2: Sensitivity analyses of K_{gr} performed for all considered tunnel stretches in this thesis.

It is most probably not possible to achieve such low hydraulic conductivities as 1-2·10^{-10} m/s by using only cement-based grout. However, it was not found if any chemical grouting had been performed along the tunnel stretches considered in the Göta tunnel. If the grouting along this stretch were only performed using cement based grouts, the grouting of the larger apertures may have prevented the flow from the smaller fractures that had not been sealed, prohibiting the flow from these anyways.

In Figure 6.1, it could also be seen that the three considered tunnel stretches in ST206 and ST207 lie in the same order, or below, the range of estimated inflow for the considered stretch in the Lerum tunnel using only IK2<0.1 Lu and the southern Chalmers tunnel. The two later tunnel stretches were the ones with the lowest hydraulic conductivity analysed for the respective tunnel. Further, the sensitivity analyses made for K and K_{gr} in the four considered tunnel stretches in ST210 all lie far above the estimations performed for the other tunnels. ST210-04 stand out from these four, as it had the largest estimated inflows for all analyses performed. This is since it is the tunnel stretch with the largest evaluated K_{gr} of all considered tunnel stretches, and a large estimated hydraulic head; two of the parameters influencing the result the most.

The order of magnitude of the hydraulic conductivity also affects the results for the parameters multiplied with the ratio of K and K_{gr} in the denominator of the inflow equation (t and r_t), see factor (1) and (2) in Equation 6.1. The variation in input parameters in factor (2) cause very small changes in the estimated inflow to the Göta tunnel compared to the Chalmers and Lerum tunnel. This is also seen

for the Västlänken service tunnels; the four tunnel stretches considered in ST210 have almost 10 times larger variation in inflow when changing t and r_t than those considered in ST206 and ST207.

$$q = \frac{2\pi \overline{K} H}{ln(2H/r_t) + \underbrace{(\overline{K}/\overline{K}_{gr} - 1)}_{(1)} \cdot \underbrace{ln(1 + t/r_t)}_{(2)} + \underbrace{\xi}_{(3)}} \tag{6.1}$$

Further, as mentioned in section 6.2, the choice of skin factor is influencing the estimated inflow differently depending on the geologic setting and the performance of the grouting. As can be seen in Figure 6.3, the deviation of the estimated inflow when the skin factor was changed between 1-10 is larger when the ratio of K and K_{gr} is smaller, and grows smaller as the ratio of K and K_{gr} increases. Thus, when a large sealing effect is expected, the choice of skin factor will most probably not influence the result that much. Whereas in situations where a small sealing effect is expected (for example, when the ungrouted rock mass already has a low hydraulic conductivity), the skin factor might influence the estimated inflow more.

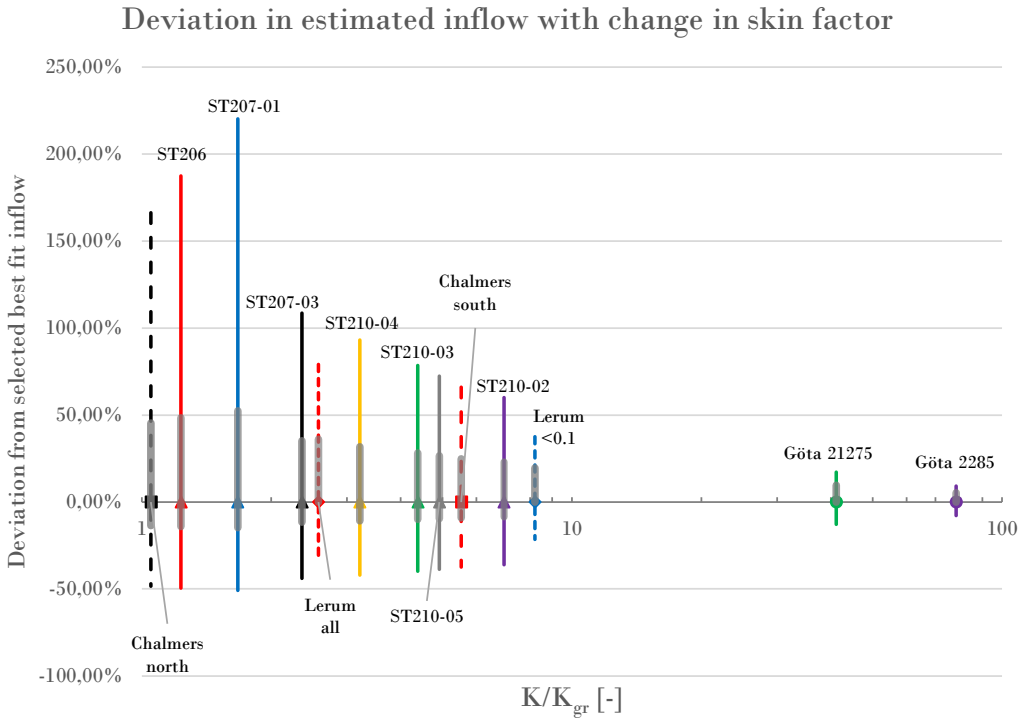

Figure 6.3: Deviation from the estimated inflow calculated with the selected best fit values of the input parameters when the skin factor is changed between 0-10, and the corresponding ratio of K and K_{gr} for the considered tunnel stretches. The grey highlighted thicker lines correspond to a change in skin factor between 2-5.

This effect can be seen in the formulation of the inflow equation, see Equation 6.1. When factor (1) is dominating factor (3), the effect of a change in factor (3) on the estimated inflow will not be very large. Further, when factor (3) is dominating factor (1) (when the sealing effect of the grouting is small), a change in factor (3)

will result in a larger variation in the estimated inflow. However, this requires that factor (2) is close to 1. For the considered tunnels in this thesis, factor (2) ranges between approximately 0.7-1.3 when using the selected best fit values of t and r_t. Thus, as factor (1) grows, it will most probably start to dominate factor (3). Figure F.1 illustrates the deviation of the estimated inflow with change in skin factor with the calculated value of the multiplication of factor (1) and (2). In this figure, it could be seen that some of the tunnels shifted slightly on the x-axis, but that the general distribution is similar. Hence, factor (2) does not influence the distribution significantly.

6.3.2 Comparison of corrected inflow

Since both the Chalmers and Göta tunnel are consisting of two tunnel tubes, the estimated inflow for the considered stretches was corrected according to the two methods described in section 4.2. The first method was based on calculating a factor between 0.5-1 based on the geometry of the tunnel, whilst the second method was using the radius of a circular tunnel corresponding to the area of both tunnel tubes.

The results for the Chalmers tunnel is summarized in Table 6.2, and it could be seen that the estimated inflows using the selected best fit values were larger than both considered median values for the measured inflow for all three tunnel stretches. The median measured inflow given in the second column in Table 6.2 is based on six measurements performed during the construction, and two after the construction was finished (given in Table 5.2). Further, the median of the measured inflow after construction in the third column is only based on the two measurements performed after construction. However, as described in the results, more confidence is given to the measurements performed after the construction was finished.

Table 6.2: The corrected inflow using the two methods, estimated inflow using the selected best fit parameters, and the median measured inflow for the Chalmers tunnel. The measured inflow to both tunnel tubes are the added individually measured inflow to the two tunnel tubes on the same date. All inflow are given in the unit l/min·100m.

Inflow	**Southern tube**	**Northern tube**	**Both tubes**
Median measured inflow all	1.5	1.5	2.9
Median measured inflow after constr.	2.3	1.8	4.1
Estimated inflow	3.5	2.0	5.4
Corrected inflow 0.65	2.2	1.3	3.5
Corrected inflow 0.7	2.4	1.4	3.8
Corrected inflow 0.8	2.8	1.6	4.3
Corrected inflow 2A	-	-	2.6

In Table 6.2 it could be seen that the corrected inflow using the radius corresponding to both tunnel areas was quite low when comparing it to measurements performed after construction, whereas it was relatively close to the median of all measured inflows. The corrected inflow using the factor of 0.65 was relatively close to the measurements made after construction for all three considered tunnel cases. Further, when varying the factor, it was seen that a factor of 0.7 was slightly closer to the median of the measured inflows after construction.

As only a few measurements of the inflow were found for the considered tunnel stretches, and since it was hard to evaluate the quality of the values, it was hard to prove either of the methods being better than the other. However, the corrected inflow using an estimated correction factor between 0.5-1 seem to give estimations that were closer to the actual measured values performed after construction for the Chalmers tunnel.

Since the calculations for the Göta tunnel were not based on estimations of the inflow, the two methods of correcting the inflow were used to estimate a new interval of hydraulic conductivities of the grouted rock mass, see Table 6.3. As can be seen, the corrected inflow made the hydraulic conductivity of the grouted rock mass decrease even more. However, since there were no measurements found of WLMs in the grouted rock mass for the Göta tunnel, it was difficult to evaluate the outcome. It could also be seen that the method using the radius of a circular tunnel corresponding to the two tunnel areas was giving way too small inflows. This is probably due to the very small hydraulic conductivity of the grouted rock mass.

Table 6.3: The corrected inflow using the two methods, estimated inflow using the selected best fit parameters, and the median measured inflow for the Göta tunnel. The values for the corrected inflow using the radius corresponding to two tunnel areas are representing the possible inflow to both tunnel tubes. All inflow are given in the unit l/min·100m.

Tunnel stretch	**Median measured inflow**	**Estimated K_{gr} [m/s]**	**Median corrected inflow 0.7**	**Median K_{gr} [m/s]**	**Corrected inflow 2A (both tubes)**
2/285	0.11	$1.0{\cdot}10^{-10}$	0.08	$1.0{\cdot}10^{-10}$	0.14
21/275	0.18	$1.9{\cdot}10^{-10}$	0.12	$6.9{\cdot}10^{-11}$	0.20

6.4 Applicability of the inflow equation and the correspondence with measured inflow

When performing the calculations for the four different tunneling projects, it was found that the inflow equation seemed to work better in geologic domains of "normally" fractured rock. For the considered sections where the hydraulic conductivities were very low, for example in the considered tunnel stretches in the Göta tunnel, ST206 and ST207, the equation did not perform as good. The reasons why the equation did not perform as expected in these conditions are outside the scope of this thesis. However, it could be due to the fact that in the domains of rock mass with low hydraulic conductivity, only a small increase caused by a fracture with higher water-bearing capacity could make the estimated mean of K_{gr} become larger than the estimated mean of K. An example of this was seen in the calculations performed for the adjacent tunnel stretches in the Göta tunnel described in the beginning section 6.3, which had an measured inflow that were ten times larger than the measured inflow to the stretches considered in the results. Because of that, the calculations were not possible as K_{gr} had to be larger than the estimated K for that section, which is unreasonable. Another reason might be related to the connectivity of the fracture systems, where the isotropic conditions reflected by the equation might suit better with a well-connected fracture system than a poorly connected system. In the poorly connected fracture system, few of the larger fractures might during grouting cancel out the flow in many otherwise ungroutable fractures.

When searching through literature, a dimensionality analysis of a tunnel section at the Äspö Hard Rock Laboratory performed by Hernqvist et al. (2012) was found. When performing an inflow prediction, a very small inflow was received, and they questioned if the inflow equation is suitable when 1D flow occur since the equation is based on radial flow. As described in section 2.1.2, the flow is 1D and channeled in fractures with large contact areas, 2D and radial in larger individual fractures, and 3D in connected fracture systems. Thus, this can be a further explanation of the difficulties performing predictions in rock mass of low hydraulic conductivity with a possible poorly connected fracture network.

Further, the calculated means of hydraulic conductivity that represented the considered tunnel stretch that was located between two measurement weirs worked well when evaluating and comparing inflow requirements. This might be since as the scale increases, the rock mass can be seen as more homogeneous. However, when evaluating individual boreholes, the probability of hitting water-bearing fractures are more random, and the evaluated rock mass becomes more heterogeneous. Thus, a larger scale of the evaluated mean of hydraulic conductivity might work better when using the inflow equation, or more defined smaller subsections with more similar and homogeneous rock mass.

One of the main objectives of this thesis was to evaluate how well the estimated inflow corresponds to the actual measured inflow for the considered tunnel stretches. This is illustrated and summarized in Figure 6.4, where the dotted black line have an inclination of 1:1. If the estimated inflow corresponds to the measured inflow,

the point for that tunnel stretch will lie on the black line. The points have the coordinates of the estimated inflow using the selected best fit parameters and the median measured inflow. The surrounding squares represent a sensitivity analysis in which the estimated inflow and measured inflow might fall within. On the x-axis, the value of the input parameters are changed with 20% that would cause a lower respectively higher estimated inflow, whereas the y-axis have a change of one standard deviation from the median measured inflow. A change in parameter value of 20% might be larger (e.g. for the tunnel radius) or smaller (e.g. for the hydraulic conductivity) than what the change in reality might fall within. However, the value of 20% was chosen to be consistent.

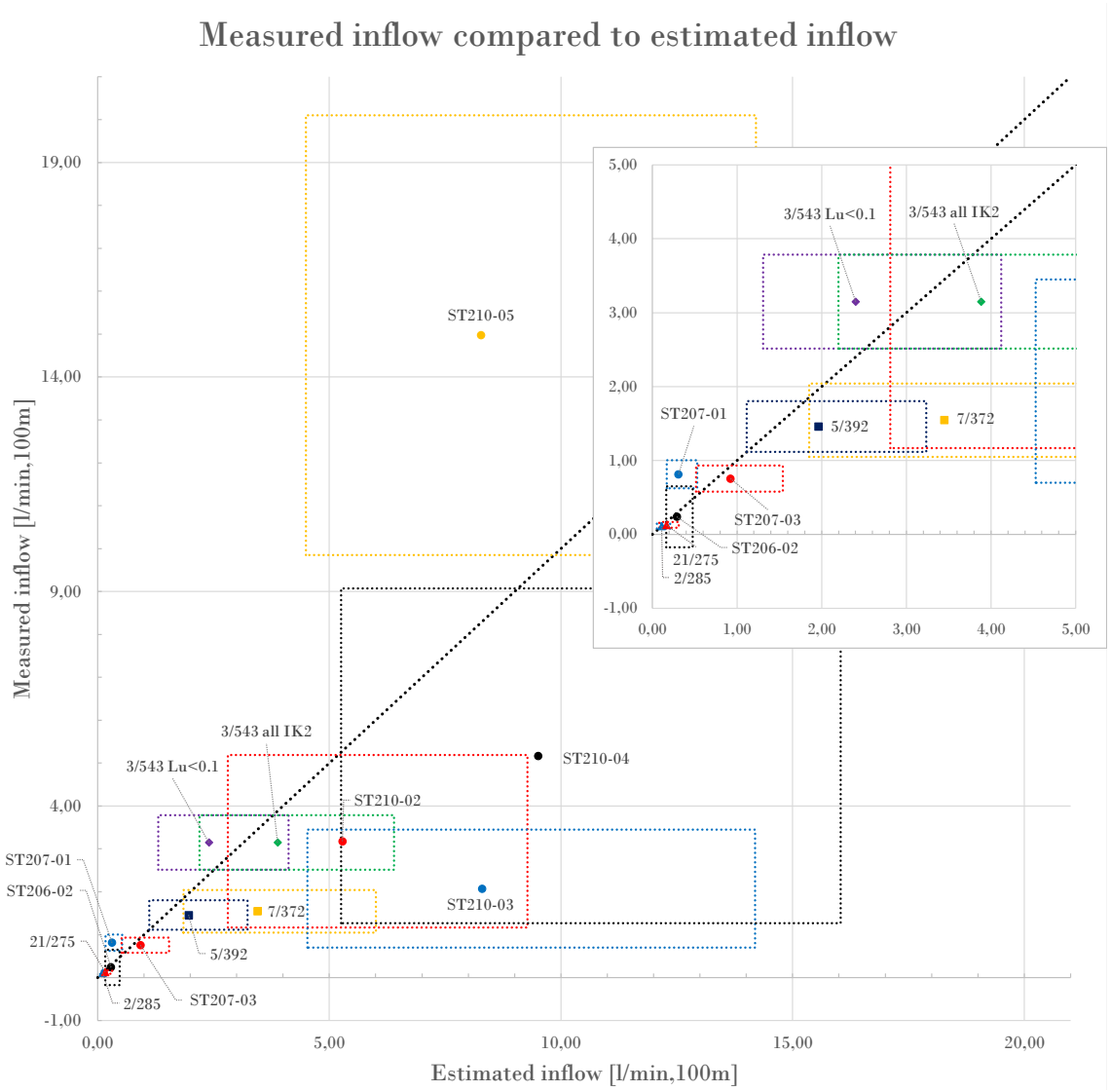

Figure 6.4: Comparison of the estimated inflow to the measured inflow for the considered tunnel stretches in this thesis. The boxes represent a change in input parameters of 20% that would result in a lower respectively higher inflow, and a standard deviation from the median of the actual measured inflows. The small box in the upper right corner is a zoomed graph of the lower left corner in the large graph.

The variation in the measured inflow was included in the graph as the inflow measurements performed have uncertainties that could affect the measured values. That could be problems related to the equipment used or if problems occured during the measurement. There will also be changes in inflow as a result of the availability in water supplies. Thus, the box represents values of measured inflows that have a relatively large probability to occur.

In Figure 6.4, it could be seen that none of the evaluated tunnel stretches have an estimated inflow that corresponds to the median measured inflow. However, through the sensitivity analyses, all tunnel stretches except ST210-03 and ST207-01 (and almost 7/372) have a possibility of having the estimated inflow to be equal to the measured inflow, with the change in values described above. It could also be seen that as the order of magnitude of the inflow increases, the size of the sensitivity-squares also increases, implying that a change in input parameter cause a larger change in estimated inflow. This is most probably the effect of the larger hydraulic conductivity that has to prevail in order to get these high inflows. When K was larger, a change in any of the other input parameter will result in a larger change in inflow compared to when K was smaller.

To summarize the results of Figure 6.4, no perfectly predicted inflow was achieved on either of the tunnel stretches considered. The sensitivity analyses do however indicate that most of the tunnel stretches have a relatively high probability of giving results close to the measured inflows. Further, the prediction generally overestimated the inflow for the considered tunnel stretches (approximately with 30%).

6.5 Work in a wider context

As described in the introduction, grouting is performed in order to avoid groundwater lowering that could cause harm on both the surrounding environment and humans. In order to keep the climate footprint as small as possible, active material choices has to be made. Further, as the tunnels considered in this thesis were funded by the state or municipalities, the money has to be well spent in order to avoid unnecessary costs.

The global construction sector accounted for 5.7 billion tons of total CO_2 in 2009, which are 23% of the total CO_2 emissions produced by the global economics activities (Huang, Krigsvoll, Johansen, Liu, & Zhang, 2018). Out of the 5.7 billion tons of total CO_2 emitted, 94% are coming from indirect sources of emissions, and the remaining 6% stem from direct emissions, which are dominated by fossil fuels. 15% of the indirect emissions are coming from non-energy use, which mainly are the result of production of cement. The cement production is a very carbon-intensive process, because of the calcination of limestone and combustion of fuels. When producing 1 ton of cement, 900 kg CO_2 are emitted to the atmosphere (Benhelal, Zahedi, Shamsaei, & Bahadori, 2013). Further, the production of cement is rising rapidly, with an increase of 54% between the year 2000 and 2006. One way of reducing the CO_2 emissions related to cement is by utilizing alternative materials. This can be performed using industrial by-products such as fly ash or blast furnace

slag. However, as the cement used during grouting is dependent of the grain size distribution, the diameters of the alternative materials particles has to be considered.

The choice of stop criterion of the maximum volume of grout that can be injected into a grouting borehole is thus important in order to decrease the use of cement. Further, by starting the grouting with a coarser first grouting round, followed by a finer grouting in the second round (as in grouting class 2 in the general grouting design in Västlänken), the volumes can be further reduced. If a finer grout would have been used also in the first grouting round, the criteria of maximum volume with no counterpressure would most probably be reached in a majority of the boreholes. Thus, the coarser grout will be able to seal the larger fractures in the first round, and the finer grout will seal the finer fractures in the second round, with less boreholes reaching the maximum volume of grout.

Polyurethane is a chemical grouting material that can be used when fine fractures has to be sealed (Vägverket, 2000). However, working environment and health-related risks are linked to this material, because of the risk being exposed to isocyanates (a reactive substance that are poisonous and sometimes mutagenic (Nationalencyklopedin, n.d.-b)). Further, the grouting material Rhoca Gil consists of, among other, acrylamide, which is seen as a possible carcinogenic substance (Nationalencyklopedin, n.d.-a). During the construction of the railway tunnel Hallandsåstunneln in 1997 Rhoca Gil was used, which poisoned construction workers, and through nearby streams also cattle. Therefore, health and ecological risks of grouting materials has to be carefully evaluated to ensure that no harm will be done.

If grouting were not to be performed, groundwater lowering with following subsidence will occur. Houses might then be damaged, which will either need economic compensation or a larger foundation (of most probably concrete). Additionally, an alternative of grouting tunnels is to use concrete lining. However, the prefabricated concrete shells consists of large amounts of material, which will most probably exceed the amount of cement used during grouting.

Thus, in order to decrease the impact of grouting, the emissions from equipment and machines as well as from the grouting material has to be reduced. If alternative climate friendly methods or materials exist, they should be used since the climate footprint from the construction sector has to be decreased substantially. Further, as the tunneling projects often are funded by the state or municipalities, an additional responsibility of protecting the environment is included as the projects are linked to the population. Grouting materials also has to be carefully evaluated to ensure that no harmful substances can be released to the environment. And by setting appropriate requirements of the grouting, such as stop criteria of volume of grout, the use of grouting material can be limited.

7

Conclusion

Grouting design has been shifted from being based on a rather empirical basis, to having more focus on calculations of fracture apertures and having the design being carried out in accordance with the observational method. In literature, limited data is available regarding follow-up on prognoses of grouting and inflow from projects based on both grouting design methods. This thesis therefore tried to illuminate how the theoretical method used to estimate inflow coincides with the measured inflow from four tunneling projects in the Gothenburg region.

The purpose of this thesis was to construct a method for follow-up on inflow through analyses on existing data from previous tunneling projects in the Gothenburg region, which would then be applied on the Västlänken service tunnels. The method were based on characterising the hydraulic conductivity of the rock mass from results of hydraulic tests in boreholes. The mean grouted thickness was thereafter selected based on the grouting design, and the tunnel radius was calculated from the area of the tunnel cross-sections. Furthermore, the hydraulic head was estimated from measured groundwater levels and technical drawings of the location of the tunnel, and the value of the skin factor was chosen according to the given values in the preliminary investigations. These six parameters were then used to make predictions of the inflow.

However, as different grouting designs were used in the four projects, the method used to evaluate the hydraulic conductivity had to be adapted according to the available data. Since probe and control holes were included in the grouting design for the Chalmers and Lerum tunnel, the rock mass was characterised in several different directions, giving the most reliable results of the hydraulic conductivity. For the Göta tunnel and the Västlänken service tunnels, the hydraulic conductivity of the ungrouted rock mass had to be evaluated using only a few core drilled boreholes. Additionally, as the GIN method used in the Göta tunnel did not include as detailed controls of the grouting, no control holes could be used in the evaluation. The results for the Göta tunnel and Västlänken service tunnels were therefore only seen as an approximation of the actual conditions.

The three grouting concepts represented in this thesis (stop pressure in the Chalmers and Lerum tunnel, active stop criterion in the Göta tunnel, and design pressure and design time for the Västlänken service tunnels) all seem to have the prerequisites to seal the rock mass. However, the follow-up of the inflow was hard to perform, since a lot of uncertainties were related to the estimation of the hydraulic conductivity of

both the grouted and ungrouted rock mass.

Additional uncertainties were linked to how well the grouting was performed in compliance with the design, and in which sections adaptations had been made. Such studies were impossible in the finished projects, and beyond the scope of the thesis for the ongoing project. Difficulties were also seen in assessing data quality of particularly the finished tunnels, as well as measurement limits for hydraulic tests. Moreover, the information gathered from the projects did not seem to be enough for making subdivisions of the rock mass. The resulting mean of the hydraulic conductivity used in the calculation of inflow might therefore not be completely representative of the prevailing conditions. The evaluated tunnel stretches considered consisted of several different rock domains (and hence also several of the different grouting classes), which became merged together when the mean values were calculated. A more detailed result could thus be achieved if geologic sections with more homogeneous characteristics were used, that would account for the local variations in hydraulic conductivity of the the rock mass.

Through the sensitivity analyses performed on the input parameters in the inflow equation, it was found that the hydraulic conductivity of both the grouted and ungrouted rock mass and the hydraulic head influenced the estimated inflow the most. It was also found that when the hydraulic conductivities were larger, the impact of the other input parameters generally also became larger. However, the largest uncertainties when estimating the parameter values were related to these three input parameters; K, K_{gr}, and H. It is therefore of large importance to characterise these three parameters in detail in order to get representative predicted inflows. Since the hydraulic head fluctuates as a result of the seasonal changes and the tunnel construction, a lower and upper boundary of the hydraulic head could be used to account for these variations. An upper and lower boundary of the hydraulic conductivity could also be used in order to account for the local variations in water-bearing capacity of the fractures in rock mass.

The tunnel radius had the smallest impact on the predicted inflow, followed by the thickness of the grouted zone. However, it was found that the ratio of K and K_{gr} influenced the results to a quite large extent. When the ratio of K and K_{gr} was larger, the impact of a change in grouted thickness became larger. Further, it was also seen that a larger ratio of K and K_{gr} resulted in a smaller impact of the skin factor. Since the skin factor is chosen qualitatively, one objective of this thesis was to particularly evaluate its influence on the predicted inflow. Through these analyses, it was therefore concluded that the skin factor have a larger influence when the sealing effect is lower, and a smaller influence when the sealing effect is larger. Thus, when a small sealing effect is expected (for example when the rock mass already have a low hydraulic conductivity), more care should be taken when choosing the skin factor.

The predicted inflow to the majority of the evaluated tunnel stretches were overestimated (approximately with 30%) when comparing it to the median measured inflow. Through sensitivity analyses on the evaluated input parameters and the median measured inflow, it was however found that a majority of the tunnel stretches considered do have a relatively high probability of predicting inflows that are close to

measured inflows. It can therefore be concluded that the inflow equation generally perform predictions that are larger than the actual inflows. This is most probably due to the fact that constant values were used for input parameters that in reality have large variations.

It can also be concluded that when predicting the inflow to two symmetrical tunnels, some kind of correction factor is needed. Otherwise, the predicted inflow to each individual tunnel tube will most probably be too large. Based on the small data set of measured inflows to the considered tunnel stretch in the Chalmers tunnel, the method used when estimating a correction factor between 0.5-1 based on geometry seemed to give the best predictions. However, it is difficult to say if this method consistently outperforms the other approach adding two tunnel areas to get a larger resulting tunnel radius.

Through the analyses of the four different tunneling projects, it was concluded that the inflow equation worked well in conditions of "normally" fractured rock mass. When the hydraulic conductivity of the rock mass was very low, the equation did not perform as well. The reasons why the equation might not perform as expected in these rock domains are not within the scope of the thesis. However, it could be the result of a small increase in the water-bearing capacity of a fracture in the low permeable rock mass, making the estimated mean of K_{gr} becoming larger than the estimated mean of K. Furthermore, it might be related to the connectivity of the fracture systems. The isotropic conditions reflected in the inflow equation might not work that well for a poorly connected system, where grouting of a few larger fractures might cancel out the flow in otherwise ungroutable fractures. It was also found that a larger scale of the evaluated means of hydraulic conductivity might work better when using the inflow equation, as the rock mass is then treated as more homogeneous. Although, in order to make more detailed evaluations, smaller subsections with more similar and homogeneous rock mass should be used. It should also be noted that the inflow equation does not take into account, for example, how well the layout of the fans are adapted to the water-bearing fracture orientations. Thus, the different predictions might not be completely comparable to each other as different conditions for evaluating the hydraulic conductivity prevailed.

7.1 Recommended future work

It is suggested that in order to get more detailed results, analyses should be performed using distributions on parameter values and not only constant values in the inflow equation, for example through Monte Carlo-simulations. In reality, several of the input parameters have variations that is not accounted for to the full extent in this thesis.

Since Västlänken is an ongoing project, follow-up on the inflow will be more easily performed as there is a possibility to ask questions to the project organisation, and since the data is kept digitally, making it more accessible. Moreover, since Västlänken is a large project, data from a very large number of measurement weirs and grouting fans can be used in the evaluations. Thus, statistics from the large

number of data sets can be used to form subsections based on different rock domains. Further, information regarding the equipment used during the WLMs is available, making it possible to properly evaluate the hydraulic conductivity from the water loss measurements.

References

Banks, D., & Robins, N. (2002). *An introduction to Groundwater in Crystalline Bedrock*. Geological Survey of Norway.

Benhelal, E., Zahedi, G., Shamsaei, E., & Bahadori, A. (2013). Global strategies and potentials to curb CO2 emissions in cement industry. *Journal of Cleaner Production*, *51*, 142–161. doi: https://doi.org/10.1016/j.jclepro.2012.10.049.

Bergab. (1999a). *Kringen, Tunnel Södra vägen-Chalmers: Förfrågningsunderlag Handling 11.4 Teknisk beskrivning - Bergarbeten.* Gothenburg.

Bergab. (1999b). *Kringen, tunnel Södra vägen-Chalmers: Förfrågningsunderlag Handling 13.2 - Rapport över geohydrologiska undersökningar (R hydro).* Gothenburg.

Bergab. (1999c). *Kringen, Tunnel Södra vägen-Chalmers: Tekniskt PM, Geohydrologi.* Gothenburg.

Bergab. (2002). *Spillvattentunnel Lerum-Partille: Teknisk beskrivning ingående i ansökan om tillstånd enligt 11 kap miljöbalken.* Gothenburg.

Bergab. (2007a). *Spillvattentunnel Lerum-Partille: Bygghandling 13.1 PM Bergteknik med bergprognos.* Gothenburg.

Bergab. (2007b). *Spillvattentunnel lerum-Partille: Bygghandling 13.5 PM Geohydrologi.* Gothenburg.

Bergab. (2012). *Spillvattentunnel Lerum-Partille: Resultat från utfört kontrollprogram för vattenverksamhet under byggskedet - Slutrapport byggskede.* Gothenburg.

Butron, C., Gustafson, G., & Funehag, J. (2008). *Grouting in the Nygård Tunnel: Pre-Grouting Design for Drip Sealing and Evaluation* (Tech. Rep. No. 2008:2). Gothenburg: Chalmers University of Technology.

Caine, J. S., Evans, J. P., & Forster, C. B. (1996). Fault zone architecture and permeability structure. *Geology*, *24*(11), 1025–1028. doi: DOI:10.1130/0091-7613(1996)024<1025:FZAAPS>2.3.CO;2

Chiocchini, U., & Castaldi, F. (2011). The impact of groundwater on the excavation of tunnels in two different hydrogeological settings in central Italy. *Hydrogeology Journal*, *19*(3), 651–669. doi: 10.1007/s10040-010-0702-1

Encyclopedia Britannica. (n.d.). *Sedimentary rock.* Retrieved from `https://www.britannica.com/science/sedimentary-rock` (2020-05-03)

Eriksson, M., & Stille, H. (2005). *Cementinjektering i hårt berg.* Stockholm: Swedish Rock Engineering Research (SveBeFo).

Fetter, C. W. (2014). *Applied Hydrogeology* (4th ed.). Pearson Education.

Fransson, Å. (2001). Characterisation of fracture geometry using specific capacities:

numerical and experimental study of a fracture replica. *Bulletin of Engineering Geology and the Environment*, *60*, 139–144. doi: https://doi.org/10.1007/s100640100100

Fransson, Å. (2008). *Grouting design based on characterization of the fractured rock: Presentation and demonstration of a methodology* (Tech. Rep. No. R-08-127). Stockholm: Swedish Nuclear Fuel and Waste Management Co.

Fransson, Å., & Hernqvist, L. (2010). Geology, Water Inflow Prognosis and Grout Selection for Tunnel Sealing: Case Studies from Two Tunnels in Hard Rock, Sweden. Vancouver: ITA-AITES World Tunnel Congress.

Funehag, J. (2007). *Grouting of Fractured Rock with Silica Sol: Grouting design based on penetration length* (PhD thesis). Chalmers University of Technology.

Funehag, J. (2011). *Hanledning för injektering med silica sol - för tätning i hårt berg* (Tech. Rep. No. BeFo 106). Stockholm: Rock Engineering Research Foundation (BeFo).

Gryaab. (2007). *Spillvattentunnel Lerum-Partille: Bygghandling 11.1 Teknisk beskrivning - bygg och anläggning, konventionell drivning.*

Gudmundsson, A. (2011). *Rock Fractures in Geological Processes*. Cambridge: Cambridge University Press. doi: 10.1017/CBO9780511975684

Gustafson, G. (1986). *Geohydrologiska förundersökningar i berg: Bakgrund-metodik-användning* (Tech. Rep. No. BeFo 84:1/86). Stockholm: Swedish Rock Engineering Research Foundation (BeFo).

Gustafson, G. (2012). *Hydrogeology for rock engineers*. Stockholm: Rock Engineering Research Foundation (BeFo).

Gustafson, G., Claesson, J., & Fransson, Å. (2013). Steering Parameters for Rock Grouting. *Journal of Applied Mathematics*, *2013*. doi: http://dx.doi.org/10.1155/2013/269594

Gustafson, G., & Fransson, Å. (2006). The use of the Pareto distribution for fracture transmissivity assessment. *Hydrogeology Journal*, *14*(1-2), 15–20. doi: 10.1007/s10040-005-0440-y

Gustafson, G., Fransson, Å., Funehag, J., & Axelsson, M. (2004). Ett nytt angreppssätt för bergbeskrivning och analysprocess för injektering. *Väg- och vattenbyggare*, *4*.

Hämäläinen, H., & Hurmerinta, E. (2013). *Monitoring Hydraulic Conductivity with HTU at Eurajoki, Olkiluoto, Drillholes OL-KR31 and OL-KR32, in 2012* (Tech. Rep. No. 2013-08).

Hawkins, M. (1956). A Note on the Skin Effect. *Journal of Petroleum Technology*, *8*(12), 65–66. doi: https://doi.org/10.2118/732-G

Heiniö, M. (1999). *Rock excavation handbook*. Sandvik Tamrock Corp.

Hernqvist, L. (2009). *Characterization of the Fracture System in Hard Rock for Tunnel Grouting* (PhD thesis). Chalmers University of Technology.

Hernqvist, L., Butrón, C., Fransson, Å., Gustafson, G., & Funehag, J. (2012). A hard rock tunnel case study: Characterization of the water-bearing fracture system for tunnel grouting. *Tunnelling and Underground Space Technology*, *30*, 132–144. doi: 10.1016/j.tust.2012.02.014

Hernqvist, L., Gustafson, G., Fransson, Å., & Norberg, T. (2013). A statistical grouting decision method based on water pressure tests for the tunnel con-

struction stage - A case study. *Tunnelling and Underground Space Technology*, *33*, 54–62. doi: 10.1016/j.tust.2012.08.004

Holmberg, M., & Stille, H. (2007). *Observationsmetodens grunder och dess tillämpning på design av konstruktioner i berg* (Tech. Rep. No. 80). Swedish Rock Engineering Research (SveBeFo).

Huang, L., Krigsvoll, G., Johansen, F., Liu, Y., & Zhang, X. (2018). Carbon emission of global construction sector. *Renewable and Sustainable Energy Reviews*, *81*(2), 1906–1916. doi: https://doi.org/10.1016/j.rser.2017.06.001

Kvartsberg, S. (2013). *On the Use of Engineering Geological Information in Rock Grouting Deisgn* (PhD thesis). Chalmers University of Technology.

Larsson, S. Å., & Tullborg, E.-L. (1993). *Tectonic regimes in the Baltic Shield during the last 1200 Ma - A review* (Tech. Rep. No. SKB 94-05). Stockholm: Swedish Nuclear Fuel and Waste Management CO.

Lindblom, U. (2010). *Bergbyggnad* (1st ed.). Stockholm: Liber AB.

Lindblom, U., Ludvig, B., & Axelsson, H. (2005). The Göta Tunnel - an impervious rock structure in a sensitive geotechnical environment. In *Bergmekanikdag 2005.* Swedish Rock Engineering Research (SveBeFo).

Lombardi, G., & Deere, D. (1993). Grouting design and control using the GIN principle. *Water Power and Dam Construction*, 15–22.

Merisalu, J., & Rosén, L. (2020). *Villkorsutformning för grundvattenbortledning vid undermarksbyggande* (Tech. Rep. No. ACE 2020:11). Gothenburg: Chalmers University of Technology.

Nationalencyklopedin. (n.d.-a). *Akrylamid.* Retrieved from `https://www-ne-se.proxy.lib.chalmers.se/uppslagsverk/encyklopedi/l%C3%A5ng/akrylamid` (2020-05-25)

Nationalencyklopedin. (n.d.-b). *Isocyanater.* Retrieved from `https://www-ne-se.proxy.lib.chalmers.se/uppslagsverk/encyklopedi/l%C3%A5ng/isocyanater` (2020-05-25)

Olofsson, B., Jacks, G., Knutsson, G., & Thunvik, R. (2001). Grundvatten i hårt berg – en analys av kunskapsläget. In *Kunskapsläget på kärnavfallsområdet 2001* (p. 113-189). Stockholm: Fritzes.

Patel, A. (2019). *Geotechnical Investigations and Improvement of Ground Conditions.* Elsevier.

Peck, R. (1969). Advantages and limitations of the observational method in applied soil mechanics. *Geotechnique 19*, *No.2*, 171-187.

Petro Bloc AB. (1991). *Götatunneln: Ingenjörsgeologisk undersökning Delrapport 3 - Beskrivning av bergmassan, bergklassificering och uppskattning av kostnader.* Gothenburg.

Petro Bloc AB. (1995). *Götatunneln: Kärnborrning Etapp 2.* Gothenburg.

Petro Bloc AB. (1999). *Väg 45, Götatunneln: Koncept - Tätning av tunneln med cementinjektering och vattentät inklädnad.*

Rodhe, A., & Bockgård, N. (2006). Groundwater recharge in a hard rock aquifer: A conceptual model including surface-loading effects. *Journal of Hydrology*, *330*(3-4), 389–401. doi: 10.1016/j.jhydrol.2006.03.032

Ryd, E. (2017). *Samband mellan kapacitet vid borrning och transmissivitet i kristallint och sedimentärt berg* (Master's thesis). Uppsala University.

SGU. (n.d.-a). *The bedrock of Sweden.* Retrieved from https://www.sgu.se/en/geology-of-sweden/the-bedrock-of-sweden/ (2020-03-10)

SGU. (n.d.-b). *Brunnsarkivet.* Retrieved from https://www.sgu.se/grundvatten/brunnar-och-dricksvatten/brunnsarkivet/ (2020-03-20)

SGU. (n.d.-c). *Morän - spår av inlandsisen.* Retrieved from https://www.sgu.se/om-geologi/jord/fran-istid-till-nutid/inlandsisen/moran-spar-av-inlandsisen/ (2020-02-22)

SGU. (2017). *Sveriges berggrund: hur, var och när.* Retrieved from http://resource.sgu.se/produkter/broschyrer/sveriges-berggrund-broschyr-nov2017-webb.pdf

SLU. (n.d.). *Liten geologisk encyklopedi.* Retrieved from http://www.geonord.org/ugs/LitenGeologiskEncyklopedFeb2015.pdf

Stille, B. (2016). *Grouting Theory and Grouting Practice: Distribution of hydraulic properties and rock mass response with regards to grouting aspects and seepage into tunnels* (PhD thesis). Chalmers University of Technology.

Stille, H. (2015). *Rock grouting: theories and applications.* Stockholm: Rock Engineering Research Foundation (BeFo).

Sundell, J. (2018). *Risk Estimation of Groundwater Drawdown in Subsidence Sensitive Areas* (PhD thesis). Chalmers University of Technology.

Thörn, J. (2015). *The Impact of Fracture Geometry on the Hydromechanical Behaviour of Crystalline Rock* (PhD thesis). Chalmers University of Technology.

Thörn, J., Kvartsberg, S., Runslätt, E., Almfeldt, S., & Fransson, Å. (2015). *Beräkningsverktyg för bergkaraktärisering vid injekteringsdesign - Teori och användarhandledning* (Tech. Rep. No. 143). Stockholm: Rock Engineering Research Foundation (BeFo).

Trafikverket. (n.d.-a). *Västlänken - lite kort om stora fördelar.* Retrieved from https://trafikverket.ineko.se/Files/sv-SE/10327/RelatedFiles/100687_vastlanken_lite_kort_om_stora_fordelar_utg2_201406.pdf (2020-04-25)

Trafikverket. (n.d.-b). *The West Link.* Retrieved from https://trafikverket.ineko.se/Files/sv-SE/11894/RelatedFiles/100576_the_west_link_utg3_201502.pdf (2020-04-25)

Trafikverket. (n.d.-c). *The West Link Project and the Olskroken Project.* Retrieved from https://www.trafikverket.se/contentassets/46d201b089d842efb233daeb43eb2aba/infofolder-eng-vastlanken-och-olskroken.pdf (2020-04-25)

Trafikverket. (2016a). *PM Hydrogeologi berg: Underlagsdokument till PM Hydrogeologi, ansökan om tillstånd till vattenverksamhet.*

Trafikverket. (2016b). *PM Hydrogeologiska beräkningar: Underlagsdokument till PM Hydrogeologi, ansökan om tillstånd enligt miljöbalken för anläggandet av Västlänken och Olskroken planskildhet.*

Trafikverket. (2016c). *Västlänken: Typinjektering.*

Vägverket. (2000). *Tätning av bergtunnlar – förutsättningar, bedömningsgrunder och strategi vid planering och utformning av tätningsinsatser.*

VBB Viak AB. (1997). *Väg 45, Göta tunneln: Ett projekt i Göteborgsöverkommelsen - Teknisk beskrivning till vattendomsansökan: hydrogeologiska förhållanden.*

Ylinen, A. (1994). *N-Dimensional Flow Behaviour in the Single Borehole Pumping Test.* Helsinki: Teollisuuden Voima Oy.

A

Appendix

Technical drawings of the profile of the grouting design for the tunnels considered.

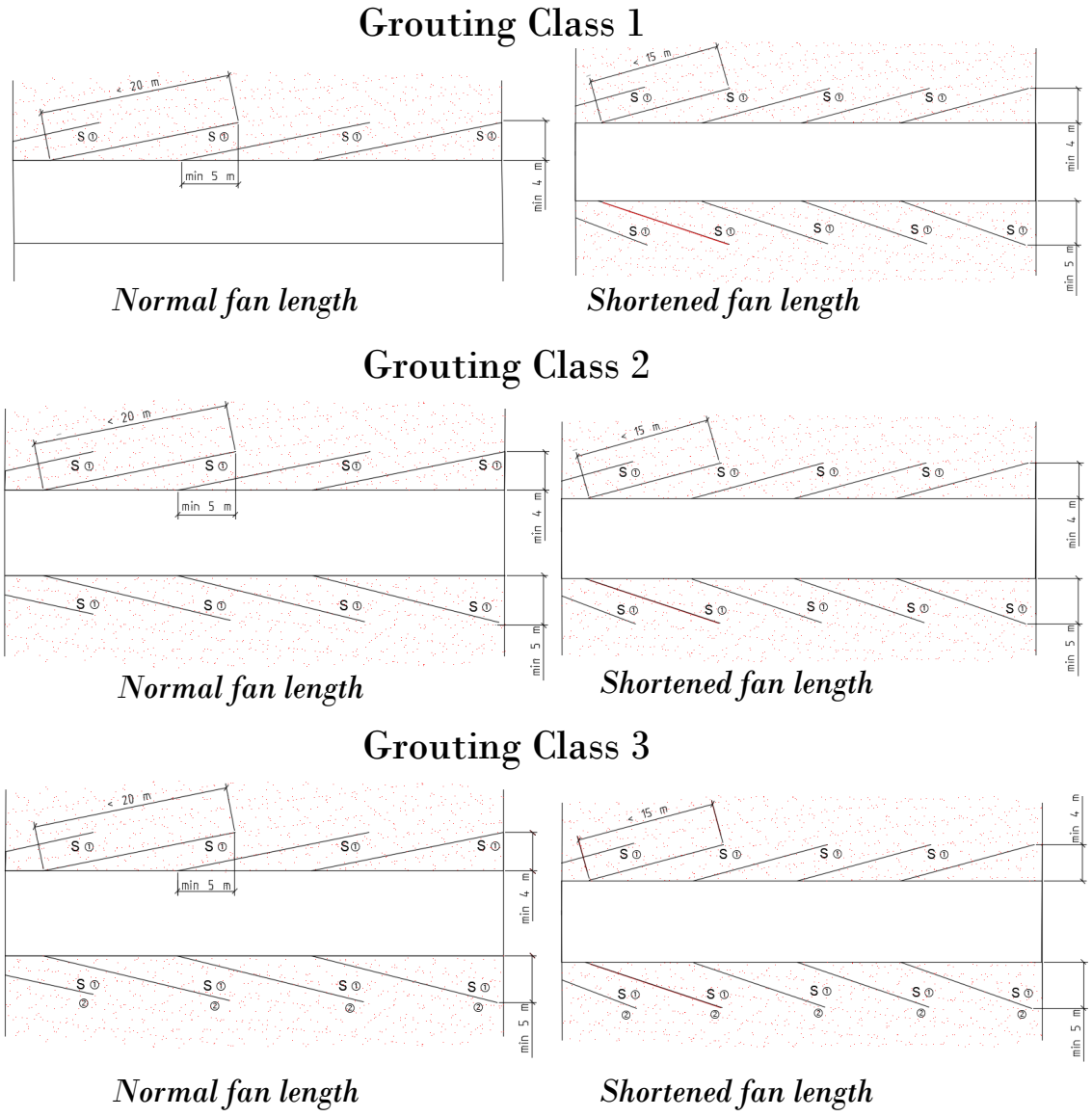

Figure A.1: The profile of the grouting design for grouting class 1,2 and 3 for the Chalmers tunnel (Technical drawing 620/98-9950).

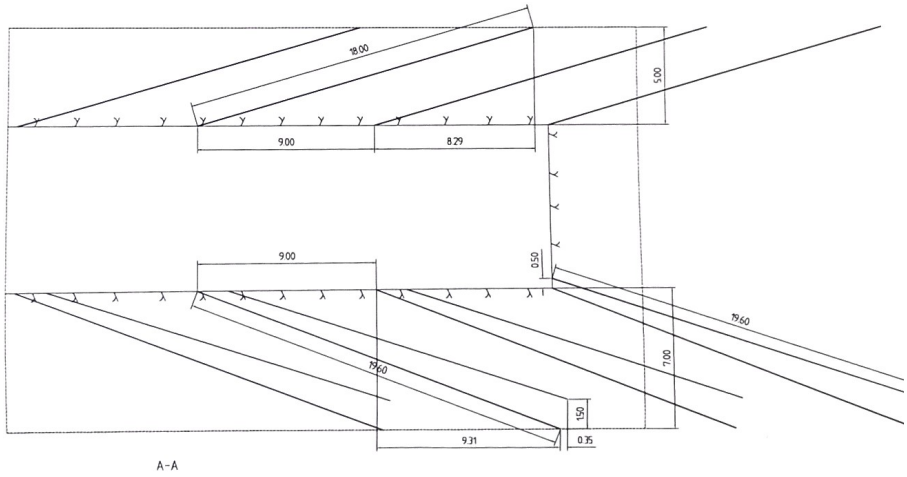

Figure A.2: A profile of the grouting design used for the main tunnel tubes for the Göta tunnel (Technical drawing 200B2442).

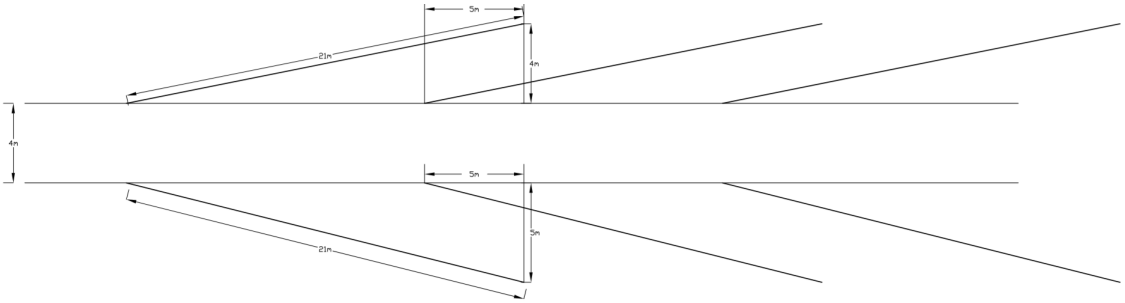

Figure A.3: Profile for the grouting design (Technical drawing 762G1410-1027).

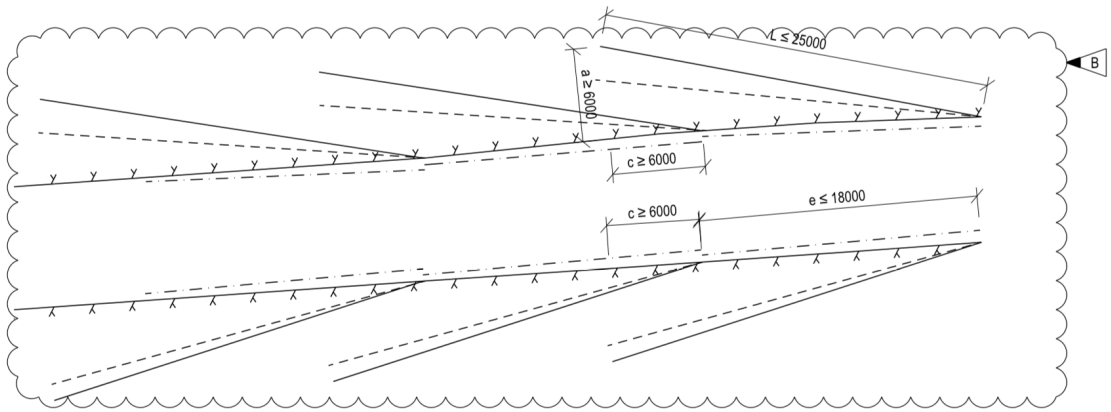

Figure A.4: Profile of the grouting design of grouting class 3 for the service tunnels (Technical drawing E00-17-300-0000-013). The dotted lines are boreholes for the second round of grouting.

B

Appendix

The following figures and tables show the results received for the Chalmers tunnel.

Table B.1: The groundwater pressure used in the calculation of inflow for the Chalmers tunnel. All levels are given in the unit meters.

Section	Level middle of tunnel	Level groundwater	Groundwater pressure	Mean value
7269	45	≈ 60	15	17.33
7300	43	≈ 60	17	
7372	40	≈ 60	20	
5288	44	≈ 60	16	18
5340	41.5	≈ 60	18.5	
5392	39	≈ 60	21	

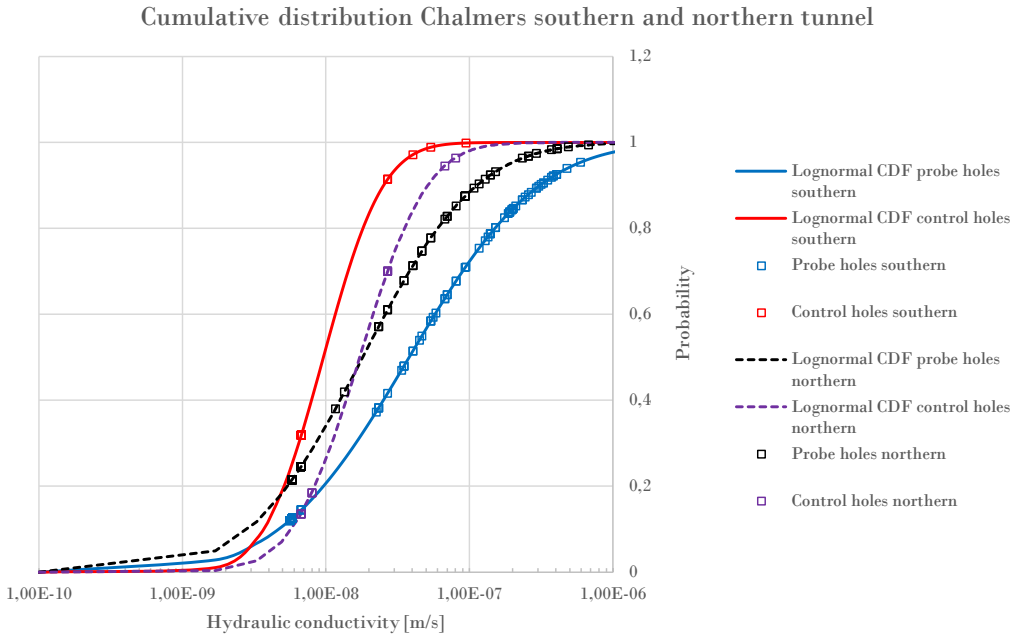

Figure B.1: A cumulative distribution for the northern and southern Chalmers tunnel. The lines represent the calculated log-normal CDF, while the points are the calculated values of the hydraulic conductivity from water loss measurements.

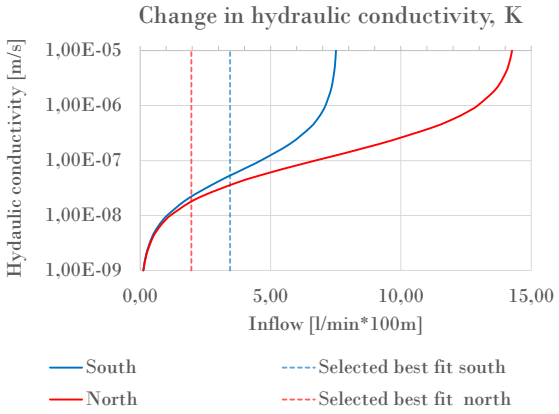

(a) Sensitivity analysis of the hydraulic conductivity.

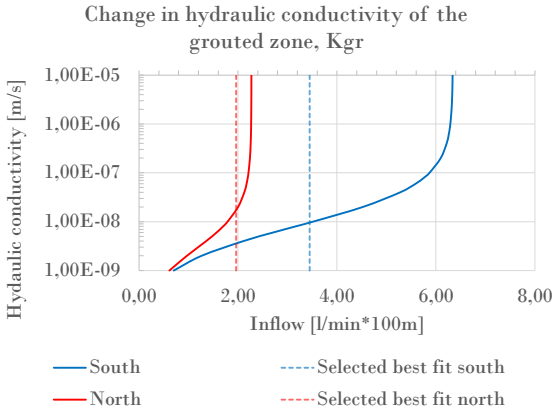

(b) Sensitivity analysis of the hydraulic conductivity of the grouted rock mass.

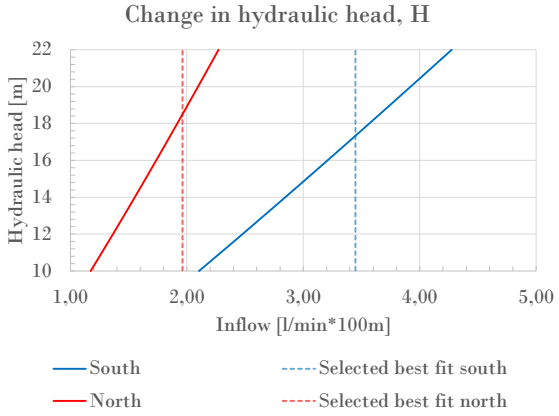

(c) Sensitivity analysis of the hydraulic head.

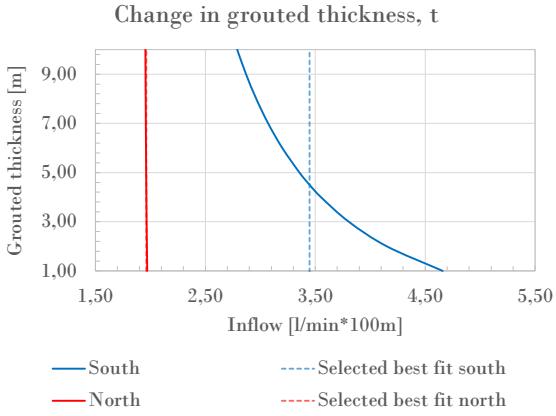

(d) Sensitivity analysis of the thickness of the grouted rock mass.

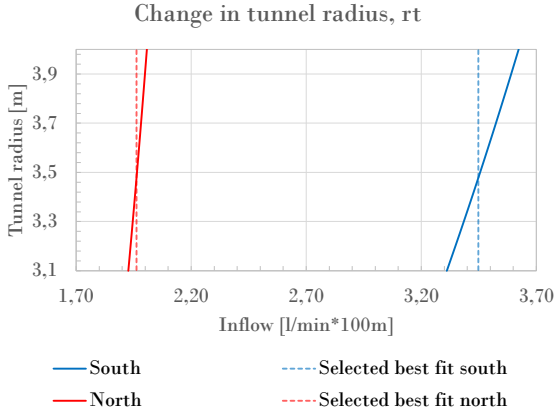

(e) Sensitivity analysis of the tunnel radius.

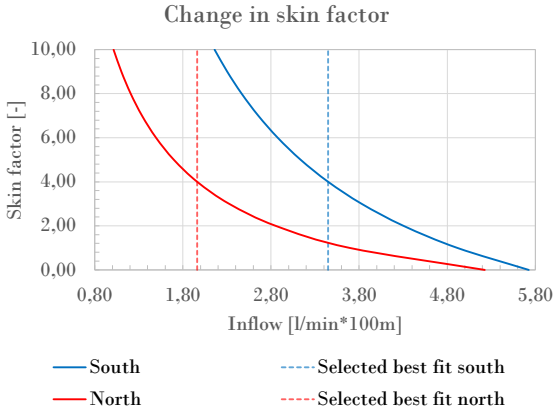

(f) Sensitivity analysis of the skin factor.

Figure B.2: Sensitivity analyses performed for the considered tunnel stretches in the Chalmers tunnel.

C

Appendix

The following figures and tables show the results calculated for the Lerum tunnel. For the sensitivity analyses, the parameters denoted with 1 is the case when all control holes from IK2, where Lu<0.1, are used, and the parameters denoted with 2 is the case when all control holes from IK2 are used.

Since all parameters except the hydraulic conductivity of the grouted rock mass was the same for the two cases, Figure C.1b will only have one graph when K_{gr} was changed.

Table C.1: The groundwater pressure used in the calculation of inflow for the Lerum tunnel. All levels are given in the unit meters.

Section	**Groundwater pressure [m]**
3600	≈ 67
3700	≈ 70
3800	≈ 75
3900	≈ 72
3900	≈ 73
4000	≈ 77
4100	≈ 73
4200	≈ 73
4300	≈ 73
4400	≈ 73
4500	≈ 73
4600	≈ 70
4700	≈ 67
4800	≈ 67
4900	≈ 74
5000	≈ 76
5100	≈ 74
5200	≈ 73
5300	≈ 76
Mean	**72**

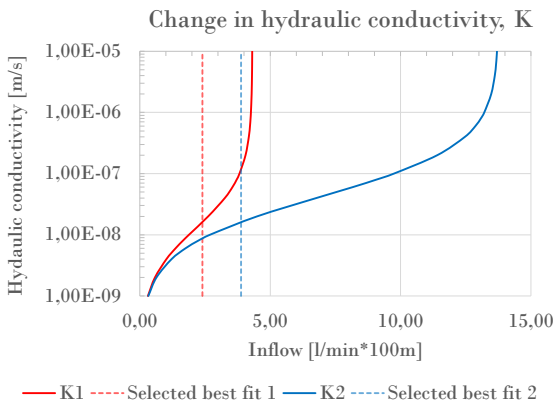

(a) Sensitivity analysis of the hydraulic conductivity.

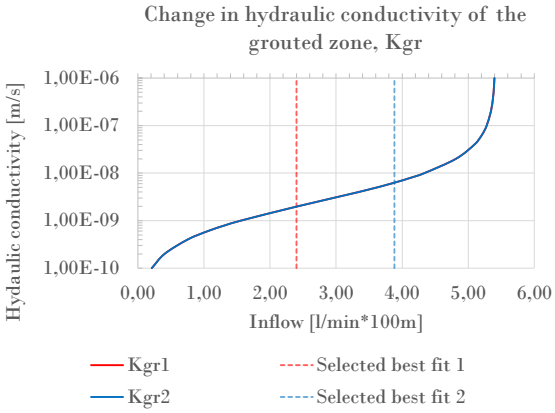

(b) Sensitivity analysis of the hydraulic conductivity of the grouted rock mass.

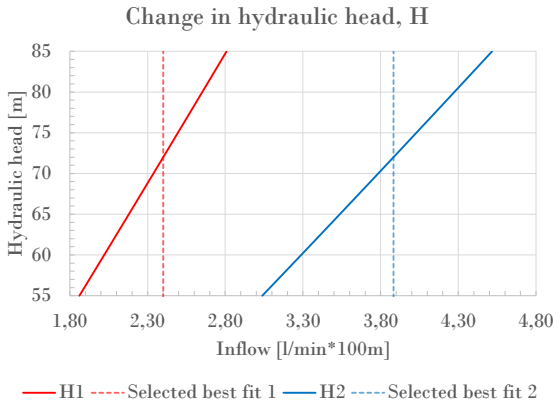

(c) Sensitivity analysis of the hydraulic head.

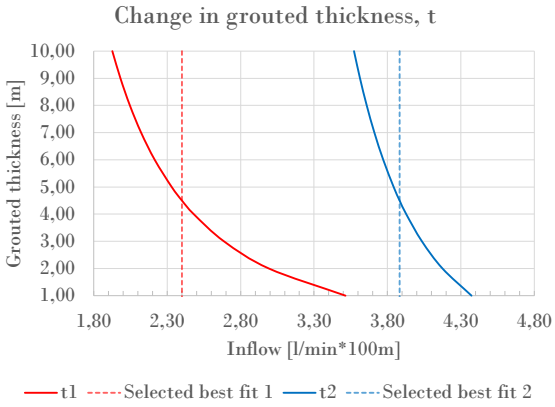

(d) Sensitivity analysis of the thickness of the grouted rock mass.

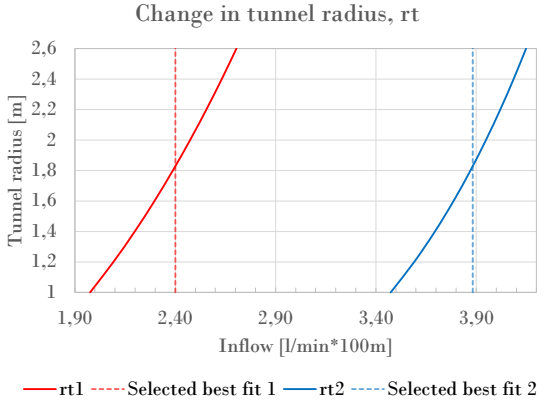

(e) Sensitivity analysis of the tunnel radius.

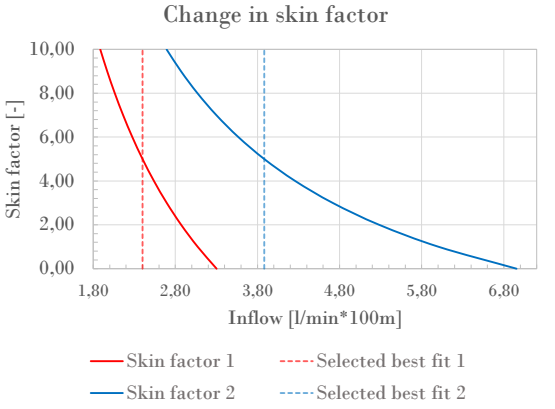

(f) Sensitivity analysis of the skin factor.

Figure C.1: Sensitivity analyses performed for the considered tunnel stretch in the Lerum tunnel.

D

Appendix

The following figures and tables show the results received for the Göta tunnel.

Table D.1: Estimated groundwater head for the considered tunnel stretches in the Göta tunnel.

Section southern tube	**Groundwater head [m]**	**Section northern tube**	**Groundwater head [m]**
2/285 - 2/400	22	21/275 - 21/390	18
2/400 - 2/430	22	21/390 - 21/420	20
2/430 - 2/530	25	21/420 - 21/520	24

Table D.2: Calculated K_{gr} from the corrected inflow taking into account the symmetry on the measured inflow after the tunnel was finished between section 2/285-2/460 and 21/275-21/430 in the Göta tunnel. The measured inflows correspond to the dates given in Table 5.9.

Section 2/285 - 2/460		*Section 21/275 - 21/430*	
Corrected inflow [l/min·100m]	**Calculated K_{gr} [m/s]**	**Corrected inflow [l/min·100m]**	**Calculated K_{gr} [m/s]**
0.07	$7.0 \cdot 10^{-11}$	0.13	$1.3 \cdot 10^{-10}$
0.06	$5.1 \cdot 10^{-11}$	0.09	$8.0 \cdot 10^{-11}$
0.07	$5.9 \cdot 10^{-11}$	0.11	$1.0 \cdot 10^{-10}$
0.09	$7.7 \cdot 10^{-11}$	0.13	$1.3 \cdot 10^{-10}$
0.10	$8.9 \cdot 10^{-11}$	0.13	$1.3 \cdot 10^{-10}$
0.08	$7.0 \cdot 10^{-11}$	0.09	$8.0 \cdot 10^{-11}$
0.08	$7.0 \cdot 10^{-11}$	0.09	$8.0 \cdot 10^{-11}$
0.08	$7.0 \cdot 10^{-11}$	0.13	$1.3 \cdot 10^{-10}$

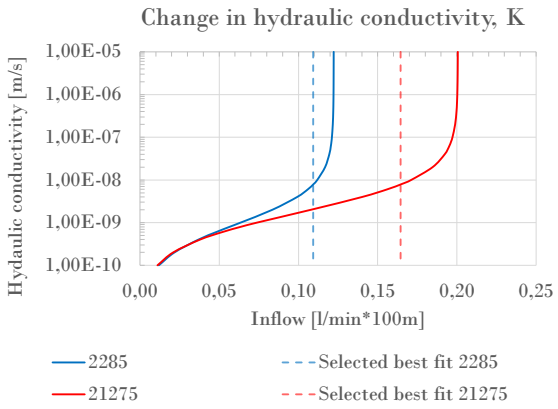

(a) Sensitivity analysis of the hydraulic conductivity for the Göta tunnel.

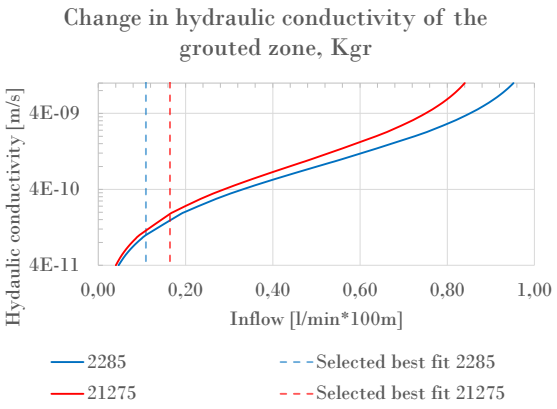

(b) Sensitivity analysis of the hydraulic conductivity of the grouted rock mass.

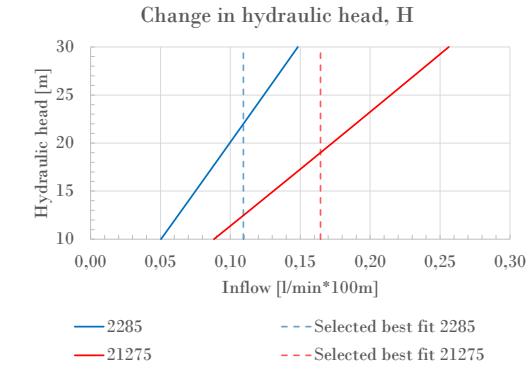

(c) Sensitivity analysis of the hydraulic head.

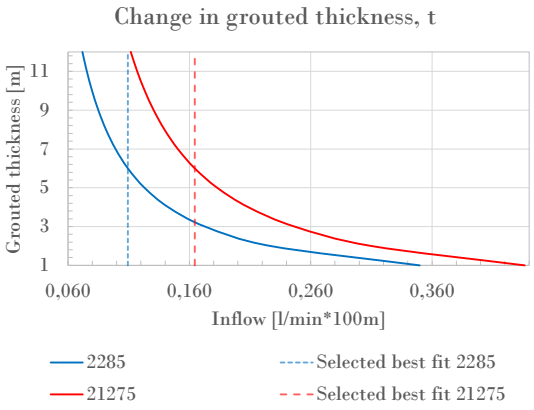

(d) Sensitivity analysis of the thickness of the grouted rock mass.

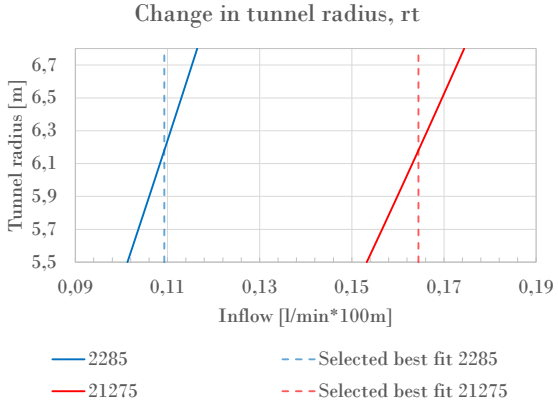

(e) Sensitivity analysis of the tunnel radius.

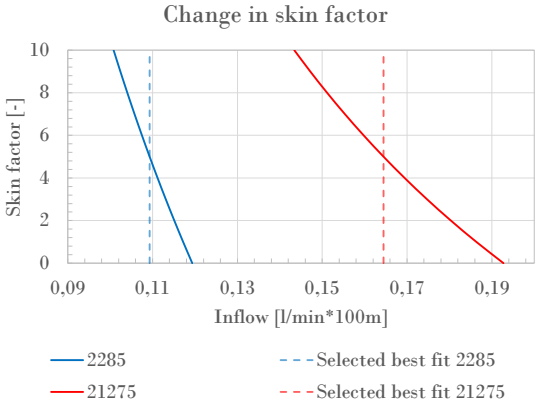

(f) Sensitivity analysis of the skin factor.

Figure D.1: Sensitivity analyses performed for the considered tunnel stretches in the Göta tunnel.

E

Appendix

The following figures and tables show the results received for the Västlänken service tunnels.

Table E.1: The groundwater pressure used in the calculation of inflow for the Västlänken service tunnels. All levels are given in the unit meters.

Tunnel	**Section**	**Groundwater pressure [m]**
ST206	0/052 - 0/072	≈ 10
	0/072 - 0/092	≈ 20
Mean ST206-02: 17m		
ST207	0/000 - 0/018	≈ 5
	0/018 - 0/038	≈ 10
	0/028 - 0/058	≈ 16
	0/058 - 0/078	≈ 23
	0/078 - 0/098	≈ 29
	0/098 - 0/118	≈ 32
	0/118 - 0/138	≈ 34
	0/138 - 0/158	≈ 38
	0/158 - 0/178	≈ 39
	0/178 - 0/198	≈ 40
Mean ST207-01: 9m *Mean ST207-03: 35m*		
ST210	0/000 - 0/100	≈ 25
	0/100 - 0/500	≈ 35
Mean ST210-02: 25m *Mean ST210-03: 34m* *Mean ST210-04: 35m* *Mean ST210-05: 35m*		

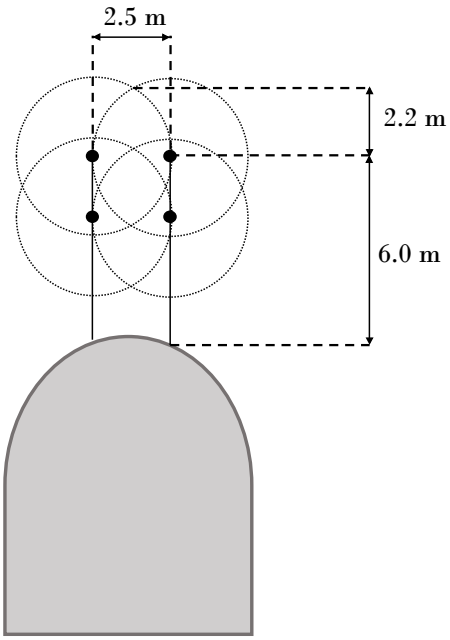

Figure E.1: Estimation of the grouted thickness for the Västlänken service tunnels according to the general grouting design. The two uppermost dots illustrates the end-point of the grouting boreholes of the first grouting round, while the two dots below illustrates the end-point of the grouting boreholes of the second grouting round.

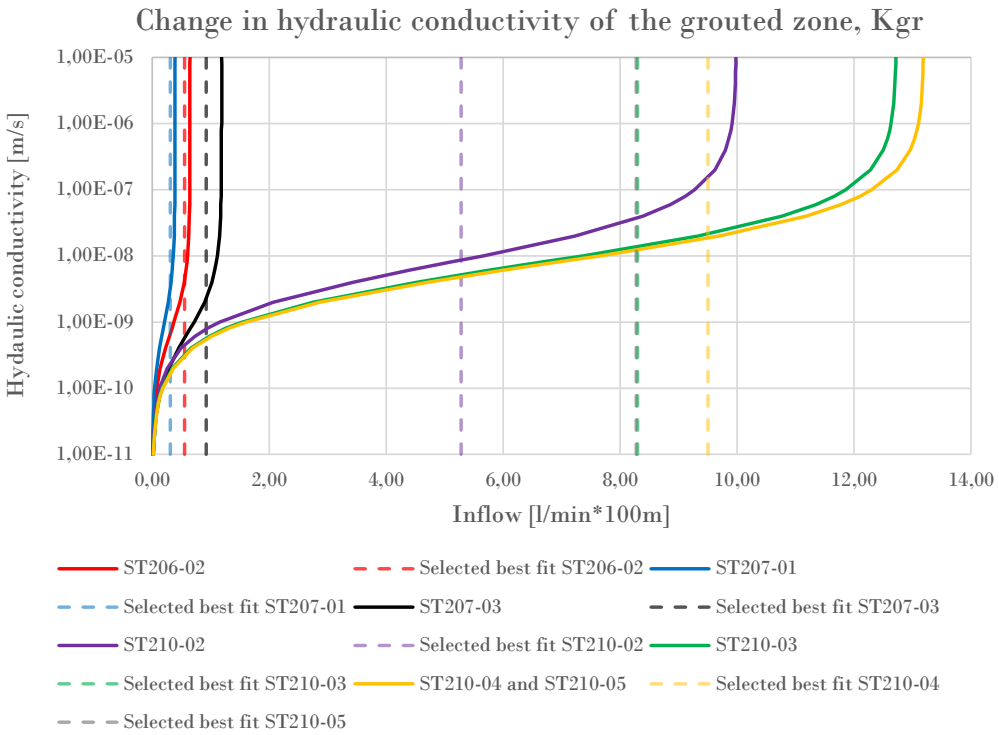

Figure E.2: Sensitivity analysis of the hydraulic conductivity of the grouted rock mass for the Västlänken service tunnels.

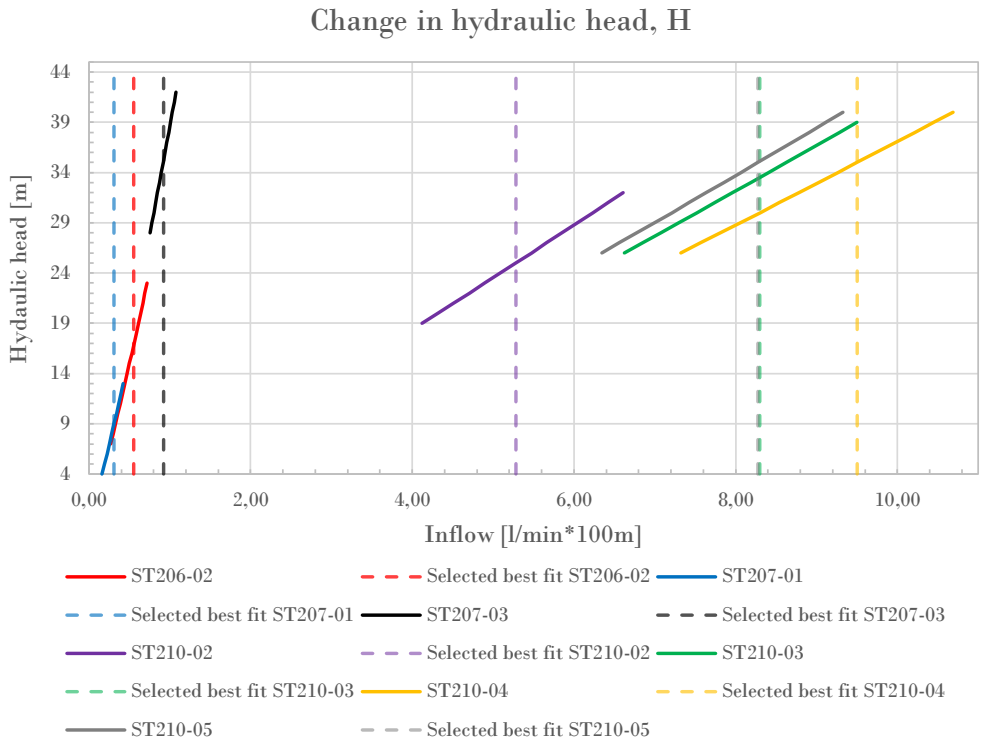

Figure E.3: Sensitivity analysis of the hydraulic head for the Västlänken service tunnels.

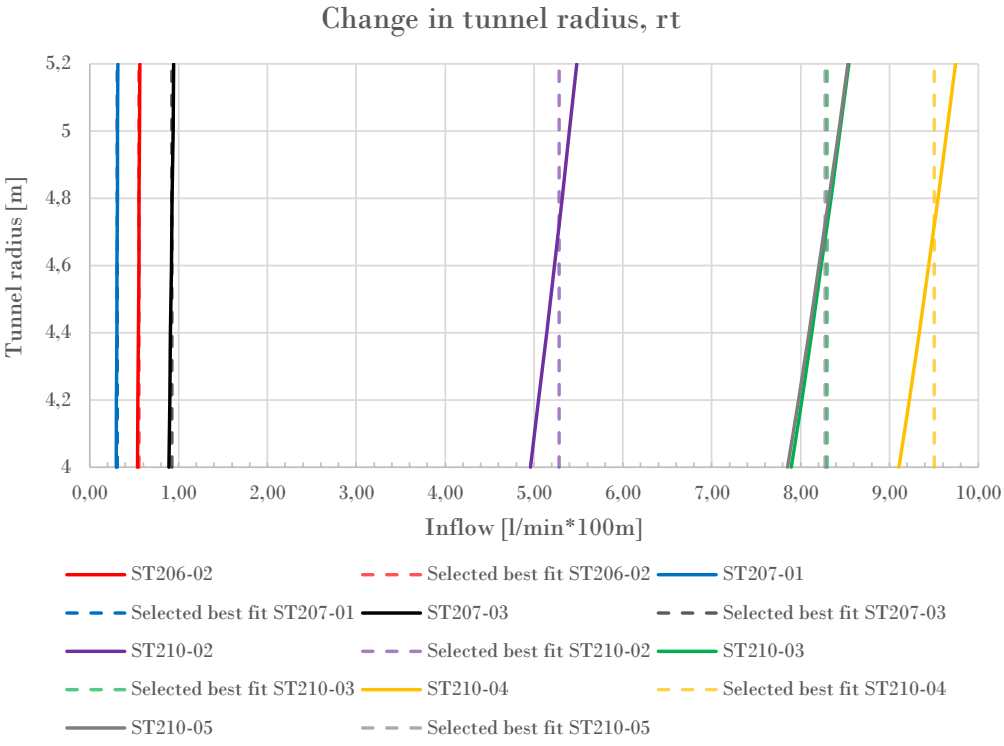

Figure E.4: Sensitivity analysis of the tunnel radius for the Västlänken service tunnels.

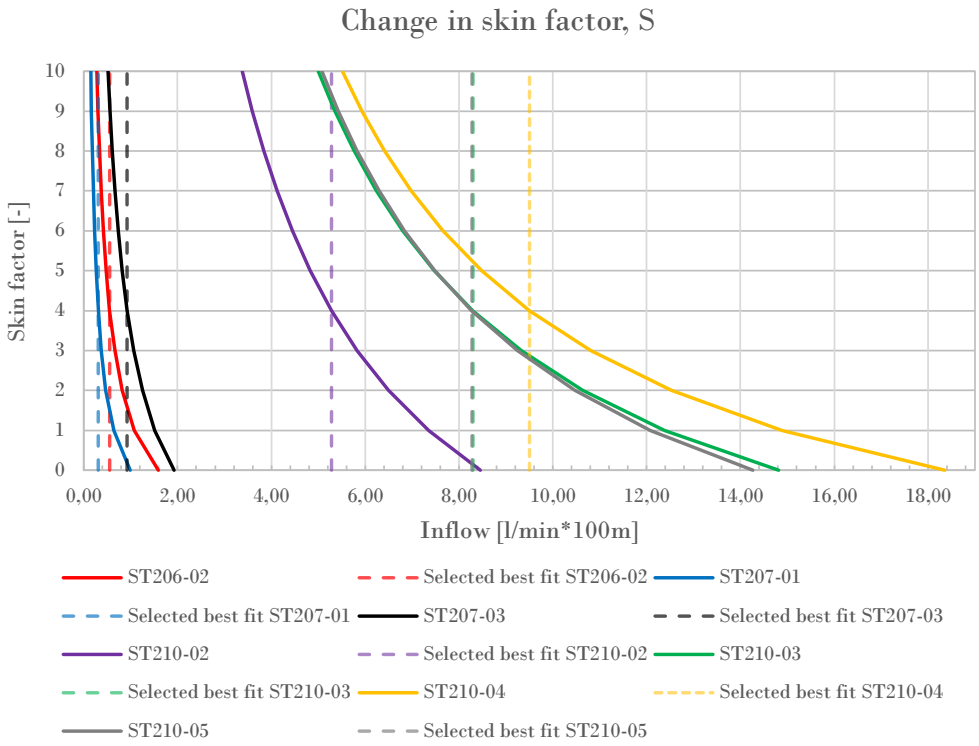

Figure E.5: Sensitivity analysis of the skin factor for the Västlänken service tunnels.

F

Appendix

The following appendix contains a figure used in the discussion of the influence of the skin factor.

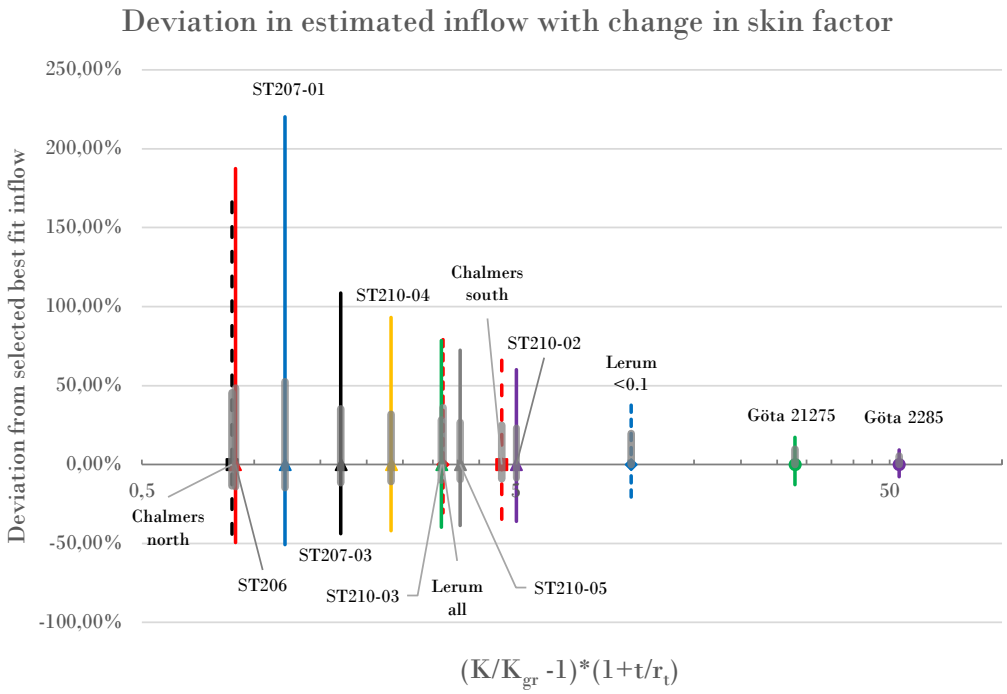

Figure F.1: Deviation from the estimated inflow calculated with the selected best fit parameters when the skin factor is changed between 1-10, and the corresponding value of the multiplication of factor (1) and (2) in Equation 6.1 for the considered tunnel stretches. The grey highlighted thicker lines correspond to a change in skin factor between 2-5.

DEPARTMENT OF ARCHITECTURE
AND CIVIL ENGINEERING
CHALMERS UNIVERSITY OF TECHNOLOGY
Gothenburg, Sweden
www.chalmers.se

CHALMERS
UNIVERSITY OF TECHNOLOGY